UNIVERSITÀ
DEGLI STUDI
DI PADOVA

UNIVERSITÀ DEGLI STUDI DI PADOVA

DIPARTIMENTO DI PSICOLOGIA GENERALE

DOTTORATO DI RICERCA IN SCIENZE PSICOLOGICHE

(curriculum PSICOBIOLOGIA CLINICA E SPERIMENTALE)

CICLO XXVII

Elaborato finale:

THE COMBINED USE OF TRANSCRANIAL MAGNETIC STIMULATION AND ELECTROENCEPHALOGRAPHY IN THE INVESTIGATION OF REACTIVITY, CONNECTIVITY AND PLASTICITY OF THE PRIMARY MOTOR CORTEX

Coordinatore : Ch.ma Prof.ssa Francesca Peressotti

Supervisore : Ch.ma Prof.ssa. Patrizia Silvia Bisiacchi

Dottorando : Elias Paolo Casula

A Michela,

"App'a cantare su numene tuo in tuttue
App'a iscurtare sas paraulas tuas
comente su mare
iscurtat dae sempere
s'istoria 'e sa vida
de custa galana zenìa"

INDEX

CHAPTER III

STUDY 1 – NEUROMODULATORY EFFECTS OF LOW-FREQUENCY RTMS: INSIGHTS FROM TMS-EEG

CHAPTER IV
STUDY 2 – TMS-EEG MARKERS OF INHIBITORY DEFICIT IN HUNTINGTON'S DISEASE

CHAPTER VI

STUDY 3 – TMS-EEG ARTIFACTS: A NEW ADAPTIVE ALGORITHM FOR SIGNAL DETRENDING

SUMMARY

The present thesis comprises two main parts: one theoretical and one experimental. The first part, composed of two chapters, is an in-depth introduction to transcranial magnetic stimulation (TMS) and its simultaneous use with neuroimaging techniques (coregistration). The second part is composed of some of the studies I conducted during my PhD. I chose to include three studies representing the different aspects of my research in the last three years, mainly regarding the study and the application of TMS-EEG coregistration in research (study 1), clinics (study 2) and technical methodology (study 3). The first study (study 1), conducted at the Department of General Psychology of Padova, was aimed to investigate the neuromodulatory effects of an rTMS protocol on healthy volunteers. The second study (study 2) was conducted at the Institute of Neurology of University College London in the context of the international "TrackOnHD" longitudinal project aimed to investigate Huntington disease (HD) in a multimodal approach. The target of this study was to investigate possible TMS-EEG markers of inhibition deficits in Huntington patients. The third study (study 3), conducted in collaboration with the Department of Information Engineering of Padova, was aimed to develop an algorithm of correction to remove an artefact induced by TMS during EEG recordings.

CHAPTER I – TRANSCRANIAL MAGNETIC STIMULATION

In the last twenty years the development of new techniques able to investigate the brain function *in vivo* during cognitive and motor tasks lead to impressive advances in understanding the human brain. Transcranial magnetic stimulation (TMS) is a tool whose popularity has grown progressively thanks to its ability to stimulate the brain in a focal and non-invasive way (Barker et al., 1985), permitting to establish a causal link in the brain-cognition/motor-behaviour relationship (Pascual-Leone et al., 2000).

In the first chapter of this thesis the possible applications of TMS in the field of cognition, physiology and rehabilitation are discussed. Specifically, the first part focuses on the operating mechanisms of TMS and on the different stimulation

parameters that define the effects of the stimulation. In the second part of the first chapter, the three main TMS protocols are discussed: *single-pulse TMS*, which is used in the temporal and spatial characterization of cognitive processes, in the study of motor cortex reactivity, and in the investigation of the cortico-spinal tract functioning; *paired-pulse TMS*, that investigates the connectivity and the interaction of cerebral networks at rest or during a task performance; and *repetitive TMS (rTMS)*, that explores the cerebral plasticity processes both in relation to cognitive processing and for rehabilitation treatments.

CHAPTER II – THE SIMULTANEOUS USE OF TRANSCRANIAL MAGNETIC STIMULATION WITH EEG AND OTHER NEUROIMAGING TECHNIQUES

Despite the widespread use of TMS in current research, its mechanism of action is still poorly understood (Miniussi et al., 2010). This lack in comprehension results from missing a firsthand "visible" marker of cortical response and a need for secondary measures of primary motor and visual cortex stimulation. In the last twenty years, thanks to the progressive improvements in neuroimaging technology, the first attempts to simultaneously use TMS with other neuroimaging techniques have been made possible (e.g. TMS-EEG, Ilmoniemi et al., 1997; TMS-PET, Paus et al., 1997). On one hand, the possibility to actively stimulate the brain with TMS allows to establish "causal" inferences in neuroimaging studies, in which, traditionally, only "correlational" inferences were possible. On the other hand, neuroimaging techniques potentially provide an important contribution through the spatial and temporal information of the neural activation evoked by TMS.

In the second chapter of this thesis, the strong and the weak points of different TMS-neuroimaging coregistration approaches are depicted. Specifically, the middle part of the chapter focuses on the main topic of this thesis, i.e. the TMS-EEG coregistration. TMS-EEG, among the different approaches, is the most successful and widespread, thanks to its promising value in the investigation of brain dynamics. Indeed, EEG is able to record the post-synaptic potentials following the neuronal depolarization evoked by TMS at a high temporal resolution (Ilmoniemi et al., 1997). The analysis of the TMS-evoked EEG activity in terms of time, space, frequency and power, potentially provides important and accurate

information in the local activation induced by the stimulation (cerebral reactivity), in the spread of such activation (cerebral connectivity), and in the long-lasting neuromodulatory effects following rTMS protocols (cerebral plasticity).

On the other hand, the TMS-EEG coregistration, presents several technical difficulties mainly due to the different artefacts that electromagnetic stimulation induces in the EEG signal. These aspects are discussed thoroughly in the second chapter. Finally, the last part of the second chapter is dedicated to the other TMS coregistration approaches with magnetic resonance imaging (MRI), functional magnetic resonance imaging (fMRI), positron emission tomography (PET), single-photon emission computed tomography (SPECT) and near-infrared spectroscopy (NIRS).

CHAPTER III – STUDY 1: NEUROMODULATORY EFFECTS OF LOW-FREQUENCY RTMS: INSIGHTS FROM TMS-EEG

The neuromodulatory effects of rTMS have been mostly investigated by means of peripheral motor-evoked potentials (MEPs). However, MEPs are an indirect measure of cortical excitability, also being affected by spinal excitability. The development of new TMS-compatible EEG systems allowed the direct investigation of the stimulation effects through the cortical responses evoked by TMS (TEPs). In this study, we investigated the effects of a repetitive TMS (rTMS) protocol delivered at low frequency (1 Hz), which is known to produce an inhibitory effect on cortical excitability (Chen et al., 1997). The protocol was applied over the primary motor cortex of 15 healthy volunteers and, as a control, over the primary visual cortex of 15 different healthy volunteers to examine the spatial specificity of the stimulation. The effects of the stimulation were analyzed in both groups through the single-pulse stimulation of the primary motor cortex, before and immediately after the rTMS protocol. Different measures were tested: MEPs, TEPs, local mean field power and scalp maps of the activity distribution.

Results on MEPs amplitude showed a significant reduction following the rTMS over the primary motor cortex. Results on TEPs, showed a well-known TEPs pattern evoked by single-pulse stimulation of the motor cortex: P30, N45, P60 and N100. Following the motor cortex rTMS, we observed a significant increase of P60

and N100 amplitude, whose origin has been linked to the GABAb-mediated inhibitory post-synaptic potentials (Ferreri et al., 2011; Premoli et al, 2014). Results on LMFP, showed an increase of general activity induced by the single-pulse stimulation of the motor cortex, starting from 90 ms after the TMS pulse. This latency actually corresponds to the peak of GABAb inhibition. No significant effects were detected after rTMS of the primary visual cortex.

The results of this study are relevant in three main aspects: (1) we confirmed the inhibitory effect of 1-hz rTMS, also providing a central correlate of such effect (TEPs); (2) we defined the spatial specificity and the origin of the inhibitory effect of 1-Hz rTMS; (3) we confirmed the possible role of the TMS-evoked N100 as a cortical inhibitory marker. The present findings could be of relevance both for therapeutic purposes, especially for pathologies characterized by inhibitory deficits (e.g. Parkinson's disease; Huntington's disease); and for basic research, especially in studies aimed to correlate a behavioral performance to the amount of cerebral excitability.

CHAPTER IV – STUDY 2: TMS-EEG MARKERS OF INHIBITORY DEFICIT IN HUNTINGTON'S DISEASE

Recent studies have shown the potential value of combining TMS and EEG for clinical and diagnostic purposes. Several TMS-EEG measures in terms of evoked potentials (i.e. TEPs), brain sources analysis, oscillatory activity and global power has been used in the assessment of brain dynamics deficits in several pathologies, such as: schizophrenia (Ferrarelli et al., 2008); psychotic disorders (Hoppenbrouwers et al., 2008); depression (Kähkönen et al., 2005); awareness disorders (Massimini et al., 2005); epilepsy (Rotenborg et al., 2008) and autism (Sokhadze et al., 2012). For instance, the potential contribution of TEPs in the investigation of the cerebral facilitatory/inhibitory balance has been demonstrated, given their origin from different GABAergic neuronal populations (Ferreri et al., 2011; Premoli et al., 2014). In particular, the TMS-evoked N100 has been related to the amount of GABAergic inhibition, as shown by pharmacological (e.g. Kähkönen et al., 2003) and behavioral research (e.g. Bender et al., 2005; Bonnard et al., 2009) as well as studies in patients (e.g. Helfrich et al., 2013).

As a part of the multi-site international "TrackOnHD" project, we used TMS-EEG to investigate the electrophysiological markers of motor cortex stimulation in Huntington patients. In Huntington's disease (HD) the progressive degeneration of GABAergic neurons in the striatum lead to a strong reduction of inhibition, resulting in an excessive increase in glutamatergic excitability (i.e. excitoxicity). Our study compared a group of 12 HD patients with a group of 12 healthy volunteers over several different TMS-EEG, EMG, fMRI and clinical measures (in the chapter only the TMS-EEG results are reported).

We found a specific and significant decrease of the N100 as assessed by the time point-by-time point permutation analysis of TEPs and from the analysis of the global activity from 90 to 104 ms after the TMS pulse. Scalp maps of the activity distribution showed a bilateral decrease of negativity, such effect was stronger over the site of stimulation. Event-related spectral perturbation and inter-trial coherence analysis showed a significant difference in the oscillatory activity of the two groups within the GABAb-ergic time window (i.e. 60-110 ms after the TMS pulse). We speculated that the observed results might be produced by the deficit in GABAergic inhibition as a consequence of the striatum neuronal degeneration in HD patients. Although preliminary, these results provided potentially useful TMS-EEG markers for inhibitory deficits in HD patients. Further analyses are needed to correlate the present findings with the other measures collected.

CHAPTER V – STUDY 3: TMS-EEG ARTIFACTS: A NEW ADAPTIVE ALGORITHM FOR SIGNAL DETRENDING

During EEG recording the discharge of the TMS coil may generate an artefact that can last for tens of milliseconds, known as "decay artefact" (Rogasch et al., 2014). This can represent a problem for the analysis of the TMS-evoked potentials (TEPs). So far, two main strategies of correction have been proposed involving the use of a linear detrend or independent component analysis (ICA). However, none of these solutions may be considered optimal: firstly, because in most of the cases the decay artefact shows a non-linear trend; secondly, because the ICA correction (1) might be influenced by individual researcher's choices and (2) might cause the removal of physiological responses.

Our aim is to verify the feasibility of a new adaptive detrend able to discriminate the different trends of the decay (linear or non-linear). Forty healthy volunteers were stimulated with 55 TMS pulses over the left M1. The TMS-EEG responses were compared among five conditions: RAW (no correction of the decay artefact was applied); INFOMAX29 (the decay components were extracted and removed by the INFOMAX ICA algorithm, using 31 electrodes); FASTICA (the decay components were extracted and removed by the fastICA ICA algorithm, using 31 electrodes); INFOMAX15 (the decay components were extracted and removed by the INFOMAX ICA algorithm, using 15 electrodes) and ALG (the decay artefact was corrected through the use of an adaptive algorithm). To assess whether the artefact correction significantly affected the physiological responses to TMS as well, we examined the differences in the -100 + 400 ms time window around the TMS pulse by means of a non-parametric, cluster-based, permutation statistical test. Then we compared the peak-to-peak TEPs amplitude within the detected time windows. The grand-averaged EEG response revealed five main peaks: P30, N45, P60, N100 and P180. Significant differences (i.e. Monte Carlo p-values < 0.05) were detected in a cluster nearby the TMS coil, and specifically over FC1, CP1, C3 and FC2. Repeated-measures ANOVA revealed a significant corruption of the peak-to-peak amplitude after INFOMAX29 (3 TEPs out of 8), FASTICA (4 TEPs out of 12), INFOMAX15 (5 TEPs out of 15) and ALG correction (2 TEPs out of 15), compared to the original signal. Furthermore, abnormal LMFP and TEPs scalp distribution were detected following the INFOMAX29 and FASTICA correction. When our algorithm was used, however, the TEPs amplitude, morphology and distribution was in line with the literature and not significantly different from the original signal. Also the decay artefact was correctly removed.

The main contribution of this study is the proposal of a new adaptive algorithm to correct the decay artefact induced by TMS in the EEG signal. Our results demonstrated that the proposed adaptive detrend is a reliable solution for the correction of this artefact, especially considering that, contrary to ICA, (1) it is not dependent from the number of recording channels; (2) it does not affect the physiological responses and (3) it is completely independent from the experimenter's choices.

RIASSUNTO

La presente tesi si compone di due parti principali: una teorica e una sperimentale. La prima parte, suddivisa in due capitoli, è un approfondimento teorico sullo strumento stimolazione magnetica transcranica (TMS) e sul suo utilizzo simultaneo (ossia, in coregistrazione) con le tecniche di neuroimaging. La seconda parte comprende alcuni degli studi condotti durante il mio dottorato. Nello specifico, si tratta di tre studi che coprono i diversi aspetti applicativi delle ricerche che ho condotto in questi tre anni, ossia lo studio e l'utilizzo della coregistrazione TMS-EEG in ricerca (studio 1), in ambito clinico (studio 2) e per aspetti tecnico-metodologici (studio 3). Il primo studio (studio 1), condotto nel Dipartimento di Psicologia Generale di Padova, era volto all'analisi degli effetti neuromodulatori di un protocollo rTMS su volontari sani. Il secondo studio (study 2) è stato condotto all'Istituto di Neurologia dello University College London (Londra, Regno Unito) all'interno del progetto internazionale "TrackOnHD", uno studio longitudinale avente come obiettivo l'indagine approfondita della Malattia di Huntington (HD) attraverso un approccio multimodale. L'obiettivo di questo studio era la ricerca di potenziali marker TMS-EEG che riflettessero il deficit di inibizione cerebrale che caratterizza questa patologia. Il terzo studio (study 3), svolto in collaborazione col Dipartimento di Ingegneria dell'Informazione di Padova, aveva l'obiettivo di sviluppare un algoritmo di correzione in grado di rimuovere un artefatto indotto dalla TMS durante la registrazione EEG.

CAPITOLO I - LA STIMOLAZIONE MAGNETICA TRANSCRANICA (TMS)

Negli ultimi anni lo sviluppo di nuove tecniche in grado di analizzare l'attivazione cerebrale durante processi cognitivi e motori, ha portato ad un avanzamento progressivo delle conoscenze sul cervello umano. La stimolazione magnetica transcranica (TMS) è stata uno degli strumenti la cui popolarità è cresciuta in questi ultimi anni, grazie alla possibilità di stimolare, in modo focale e non invasivo, il cervello *in vivo* (Barker et al., 1985). Tale capacità ha consentito, per la prima volta,

la straordinaria possibilità di inferire delle relazioni causali tra cervello, processi cognitivi e motori, e comportamento (Pascual-Leone et al., 2000).

Nel primo capitolo della presente tesi vengono passate in rassegna tutte le possibili applicazioni della TMS in campo cognitivo, fisiologico e riabilitativo. Nello specifico, la prima parte è dedicata ai meccanismi di funzionamento della TMS e ai parametri di stimolazione che ne definiscono i diversi effetti sul cervello. Nella seconda parte vengono invece passati in rassegna i tre principali protocolli di stimolazione: la *TMS a singolo impulso*, utilizzata per la caratterizzazione spaziale e temporale dei processi cognitivi, per analizzare la reattività della corteccia motoria primaria, e per verificare l'integrità del tratto cortico-spinale; *la TMS a doppio impulso*, per studiare la connettività e l'interazione di network cerebrali a riposo e durante lo svolgimento di un task; e la *TMS ripetitiva* (rTMS), utilizzata per analizzare i fenomeni di plasticità cerebrale sia durante processi cognitivi, sia in relazione a trattamenti riabilitativi.

CAPITOLO II - L'UTILIZZO SIMULTANEO DELLA TMS CON L'EEG ED ALTRE TECNICHE DI NEUROIMAGING

Nonostante la grande popolarità che la TMS ha conosciuto negli ultimi anni, molti aspetti del suo meccanismo d'azione sono ancora poco chiari (Miniussi et al., 2010). Tale ambiguità è dovuta al fatto che, fatta eccezione per la corteccia motoria e visiva primaria, la stimolazione TMS non fornisce dei marker "visibili" di eccitabilità corticale. Negli ultimi anni, grazie al miglioramento tecnologico degli strumenti di indagine neuroscientifica, si è iniziato a utilizzare simultaneamente (in coregistrazione) la TMS con diverse tecniche di neuroimaging. Ciò ha consentito di trarre delle inferenze di tipo "causale" e non più solo "correlazionale" (come nei tradizionali studi di neuroimaging) grazie alle informazioni spaziali e temporali sull'effetto della TMS che le tecniche di neuroimaging offrono.

Nel secondo capitolo della presente tesi, vengono trattati dettagliatamente le potenzialità e i limiti delle diverse coregistrazioni TMS-neuroimaging. In particolare, nella parte centrale del capitolo è dato ampio spazio all'argomento centrale di questa tesi, ossia la coregistrazione TMS-EEG. L'approccio TMS-EEG, tra i vari metodi di coregistrazione, è stato quelli che negli ultimi anni ha riscontrato

maggiore successo e diffusione, dovuto all'enorme potenzialità che questo metodo garantisce nello studio delle dinamiche cerebrali. L'EEG, infatti, è in grado di registrare, ad altissima risoluzione temporale, i potenziali post-sinaptici indotti dalla depolarizzazione neuronale evocata dalla TMS (Ilmoniemi et al., 1997). L'analisi dell'attività EEG indotta dalla TMS - in termini di tempo, spazio, frequenza e potenza - è in grado di fornire delle preziose informazioni sia sull'attivazione locale indotta dalla stimolazione (reattività cerebrale), sia su quella distale (connettività cerebrale), sia sulle modificazioni a seguito di protocolli di stimolazione ripetitiva (plasticità cerebrale).

D'altra parte, la coregistrazione TMS-EEG presenta numerose difficoltà di tipo tecnico, dovuto ai numerosi artefatti che la stimolazione elettromagnetica induce sul segnale EEG (così come sui segnali delle altre tecniche di neuroimaging), questi aspetti sono trattati in maniera dettagliata all'interno del capitolo. Infine, l'ultima parte del capitolo è dedicata agli altri metodi di coregistrazione TMS con risonanza magnetica (MRI), risonanza magnetica funzionale (fMRI), tomografia a emissione di positroni (PET), tomografia a emissione di fotone singolo (SPECT) e spettroscopia del vicino infrarosso (NIRS).

CAPITOLO III – STUDIO 1: EFFETTI NEUROMODULATORI DELLA RTMS A BASSA FREQUENZA: EVIDENZE DALL'APPROCCIO TMS-EEG

Tradizionalmente gli effetti neuromodulatori della rTMS sono stati studiati attraverso l'analisi dei potenziali motori evocati (MEP). Tuttavia, come noto, i MEP sono una misura indiretta dell'eccitabilità corticale avendo una forte componente anche spinale. Con lo sviluppo di nuovi sistemi EEG compatibili con la TMS, è stato possibile analizzare gli effetti della stimolazione in modo più diretto, tramite l'analisi dei potenziali corticali evocati dalla TMS (TEPs). In questo studio abbiamo analizzato l'effetto di un protocollo di TMS ripetitiva (rTMS) a bassa frequenza (1 Hz) molto noto, soprattutto in ambito riabilitativo, per sortire un effetto di inibizione dell'eccitabilità corticale. Il protocollo è stato applicato sulla corteccia motoria primaria di quindici volontari sani e sulla corteccia visiva primaria di altri quindici volontari sani, assunti come gruppo di controllo per analizzare la specificità spaziale della stimolazione. Gli effetti della stimolazione ripetitiva sono stati testati

su diverse misure elettrofisiologiche evocate da una stimolazione a singolo impulso della corteccia motoria, prima e subito dopo il protocollo rTMS, ossia: MEP, TEPs, local mean field power (LMFP) e distribuzione dell'attività sullo scalpo.

I risultati sui MEP hanno mostrato una diminuzione significativa dell'ampiezza a seguito del protocollo rTMS sulla corteccia motoria. I risultati sui TEP hanno mostrato un pattern noto composto di quattro principali picchi: P30, N45, P60 e N100. A seguito del protocollo rTMS sulla corteccia motoria si è osservato un incremento significato dell'ampiezza dei TEP P60 e N100, la cui origine è legata all'attività dei potenziali post-sinaptici inibitori GABAb (Ferreri et al., 2011; Premoli et al., 2014). I risultati sul LMFP hanno mostrato un incremento di attività generale indotta dalla TMS sulla corteccia motoria a partire da circa 90 ms dalla stimolazione, ossia la latenza del picco massimo di inibizione GABAb. A seguito del protocollo di stimolazione di controllo, applicato sulla corteccia visiva, non si è riscontrato nessun cambiamento significativo.

I risultati di questo studio hanno una rilevanza su tre aspetti: (1) si è confermato l'effetto inibitorio del protocollo rTMS a 1-Hz, offrendo anche un correlato centrale di inibizione (TEPs) oltre che periferico (MEPs); (2) sono state definite la spazialità e l'origine dell'inibizione indotta dalla rTMS a bassa frequenza; (3) la N100 evocata dalla TMS si conferma essere un marker affidabile del grado di inibizione corticale. I risultati di questo studio potrebbero avere una rilevanza sia in campo terapeutico e riabilitativo, specie per i disturbi alla cui base si suppone vi sia un deficit di inibizione corticale (ad es. malattia di Parkinson, malattia di Huntington); sia in campo di ricerca, specie in studi in cui si vogliano correlare performance a task cognitivi o motori con il grado di eccitazione/inibizione corticale.

CAPITOLO IV – STUDIO 2: DEFICIT DI INIBIZIONE NELLA MALATTIA DI HUNTIGTON: EVIDENZE DALLA COREGISTRAZIONE TMS-EEG

Evidenze recenti hanno mostrato le potenzialità dell'utilizzo della coregistrazione TMS-EEG in ambito clinico e diagnostico. Diverse misure TMS-EEG in termini di potenziali evocati (TEPs), analisi di sorgenti, attività oscillatoria e potenza dell'attività globale, sono state utilizzate per lo studio di dinamiche cerebrali

deficitarie in diverse patologie, come: schizofrenia (Ferrarelli et al., 2008); disordini psicotici (Hoppenbrouwers et al., 2008); depressione (Kähkönen et al., 2005); disturbi di coscienza (Massimini et al., 2005); epilessia (Rotenborg et al., 2008) e autismo (Sokhadze et al., 2012). Ad esempio, diverse evidenze hanno mostrato il potenziale contributo dei TEPs nello studio degli equilibri eccitatori/inibitori corticali, data la loro origine GABAergica (Ferreri et al., 2011; Premoli et al., 2014). In particolare, la N100 TMS-evocata sembra essere strettamente correlata al grado di inibizione GABAergica, come mostrato da evidenze a carattere farmacologico (ad es. Kähkönen et al., 2003; Premoli et al., 2014); studi comportamentali (ad es. Bender et al., 2005; Bonnard et al., 2009) e studi in pazienti (ad es. Helfrich et al., 2013).

Nel presente studio, facente parte di un ampio progetto internazionale multicentrico ("TrackOnHD"), abbiamo utilizzato la coregistrazione TMS-EEG per analizzare dei possibili marker elettrofisiologici della malattia di Huntington, tramite stimolazione della corteccia motoria primaria. La malattia di Huntington (HD) è caratterizzata da una progressiva degenerazione dei neuroni striatali di natura GABAergica. Tale degenerazione porta a un eccessivo incremento del tono eccitatorio mediato dal glutammato, un fenomeno noto come eccitossicità. Nel presente studio sono stati analizzati dodici pazienti HD e dodici volontari sani su varie misure TMS-EEG, EMG, fMRI e cliniche (nel capitolo sono riportati solo i risultati relativi alle misure TMS-EEG).

I risultati hanno mostrato una riduzione significativa e specifica della N100, come rilevato dall'analisi dei TEP per permutazioni punto-per-punto e dall'analisi dell'attività media globale da 94 a 104 ms dopo l'impulso TMS. Le mappe dello scalpo della distribuzione dell'attività hanno mostrato una riduzione della negatività su entrambi gli emisferi, con un effetto maggiore sul sito di stimolazione. Le analisi di perturbazione dello spettro evento-relata e della coerenza inter-trial hanno mostrato una differenza significativa nell'attività oscillatoria dei due gruppi all'interno della finestra di interesse GABAb-ergico (60-110 ms dopo l'impulso TMS). I risultati osservati potrebbero essere prodotti dal deficit di inibizione GABAergica nei pazienti HD conseguente alla degenerazione neuronale nello striato. Anche se preliminari, i risultati dello studio hanno rilevato dei marker TMS-EEG potenzialmente d'interesse per la valutazione dei deficit inibitori in pazienti HD.

Ulteriori analisi sono necessarie per correlare i risultati ottenuti con le altre misure raccolte all'interno del progetto.

CAPITOLO V – STUDIO 3: ARTEFATTI TMS-EEG: UN NUOVO ALGORITMO ADATTATIVO PER IL DETREND DEL SEGNALE

Durante un EEG, la stimolazione TMS può generare un artefatto a lunga latenza, noto come artefatto "decay". Tale artefatto rappresenta un problema per l'analisi dei potenziali evocati dalla TMS (TEP). In letteratura, per risolvere il problema, sono comunemente utilizzate due principali strategie: l'utilizzo di un detrend lineare e l'utilizzo dell'independent component analysis (ICA). Tuttavia, nessuna di queste soluzioni può essere considerata ottimale. Per quanto riguarda l'utilizzo di un detrend lineare, dal momento che nella maggior parte dei casi l'artefatto decay non segue un andamento lineare, questo tipo di correzione risulta inefficiente. Per quanto invece riguarda l'ICA, anche questa procedura presenta dei limiti intrinseci: (1) può essere eccessivamente influenzato dalle scelte dello sperimentatore e (2) può causare la rimozione di componenti fisiologiche, oltre che artefattuali.

Il nostro obiettivo è di verificare l'efficienza di un nuovo detrend adattivo, sviluppato su MATLAB, in collaborazione col dipartimento di Ingegneria Informatica di Padova, capace di discriminare i diversi trend dell'artefatto decay (ossia lineare e non-lineare). Quaranta volontari sani sono stati stimolati con 55 impulsi TMS singoli sulla corteccia motoria primaria di sinistra. Le risposte EEG indotte dalla TMS sono state analizzate in cinque condizioni: RAW (in cui non veniva applicata nessuna correzione dell'artefatto decay); INFOMAX29 (in cui l'artefatto decay veniva corretto con un algoritmo ICA-INFOMAX, considerando tutti i 29 canali); FASTICA (in cui l'artefatto decay veniva corretto con un algoritmo fastICA, considerando tutti i 29 canali); INFOMAX15 (in cui l'artefatto decay veniva corretto con un algoritmo ICA-INFOMAX, considerando solo 15 canali) e ALG (in cui l'artefatto decay veniva corretto tramite il nostro algoritmo adattivo). Per verificare se la correzione dell'artefatto avesse influenzato anche i TEP, sono state analizzare le differenze in una finestra temporale da -100 a +400 ms dall'impulso TMS attraverso l'utilizzo di un test per permutazioni, non-parametrico e corretto per cluster. Successivamente, sono state comparate le ampiezze e le latenze picco-picco dei TEP all'interno delle

finestre temporali negli elettrodi risultati significativi. La risposta grand-average ha rilevato cinque picchi principali: P30, N45, P60, N100 e P180. Sono state rilevate delle differenze significative (i.e. Monte Carlo $p < 0.05$) in un cluster di elettrodi vicino alla stimolazione, comprendente i canali FC1, CP1, C3 e FC2. Le analisi sull'ampiezza picco-picco hanno rilevato una significativa modulazione dell'ampiezza dopo la correzione INFOMAX29 (in 3 TEP su 8), FASTICA (in 4 TEP su 12), INFOMAX15 (in 5 TEP su 15) e ALG (in 2 TEP su 15), rispetto al segnale RAW originale. I risultati LMFP e delle mappe di distribuzione sullo scalpo hanno rilevato diverse anomalie a seguito della correzione INFOMAX29 e FASTICA.

I risultati hanno mostrato che la correzione ICA modifica in modo significativo l'ampiezza, la morfologia e la distribuzione di una parte dei TEP analizzati e nello stesso tempo non garantisce una completa rimozione dell'artefatto decay. Al contrario, a seguito della correzione col nostro algoritmo (condizione ALG), l'ampiezza, la morfologia e la distribuzione dei TEP rimanevano fedeli a quella originale, con una rimozione pressoché completa dell'artefatto decay. Il principale contributo di questo studio è stato la proposta di un nuovo algoritmo di correzione per un artefatto a lunga latenza che la TMS induce sul segnale EEG (artefatto decay) rendendo difficoltosa l'analisi. I risultati hanno dimostrato che questo metodo è più efficiente delle strategie attualmente in utilizzo in letteratura, non avendo i limiti intrinseci presentati dall'algoritmo ICA.

GENERAL INTRODUCTION

The development of neuroimaging techniques represents one of the most impressive advancements in neuroscience. The main reason for the widespread use of these instruments lies in their capacity to provide an accurate description of neural activity at rest or during a cognitive and/or a or motor process. However, besides the fascinating perspectives that neuroimaging techniques offer, their correlational nature represents one the main limitations because it does not permit to establish any causal inference among a brain area activation, a cognitive or motor process, and a behavioural response. The development of tools such as transcranial magnetic stimulation (TMS) have compensated for this limit, thanks to the possibility to actively interfere with the ongoing brain activity. Indeed, the active stimulation provided by TMS allows to establish a directional (i.e. causal) link between a brain area, a cognitive or motor process, and a behavioural response. However, despite its widespread usage, the exact mechanism of TMS is still unclear. A number of studies have reported contrasting results on the effects of TMS in cognitive task performances, physiological assessment and neuromodulatory protocols (for a review, Bestmann et al., 2008; Miniussi et al., 2010). Thus, the clarification of the TMS mechanism of action in cognition, physiology and clinics is a topic of central relevance in the current literature.

In the last twenty years, a new methodological approach, consisting in simultaneously use TMS with neuroimaging techniques (i.e. coregistration), is becoming popular. The idea of this approach is to monitor the cerebral activity induced by TMS over space and time in order to provide insights into the brain dynamics of reactivity (i.e. the local response to TMS), connectivity (i.e. the spread of the response to connected networks) and plasticity (i.e. the long-lasting changes following a neuromodulatory protocol).

Five years ago, as an MSc student of Neuroscience and Neuropsychological Rehabilitation, I was fascinated by the new perspectives derived from the simultaneous use of TMS and electroencephalography (EEG). Amazing works, such as the paper by Massimini and colleagues (2005, *Science*), lead me in starting with my TMS-EEG researches, that are partially summarized in the five chapters of this

thesis. The main purpose of my PhD researches was the investigation and the application of the TMS-EEG coregistration over the primary motor cortex in order to characterize the dynamics of this area in terms of reactivity, connectivity and plasticity. The three studies included in this thesis (chapter III, IV and V) covered the three main TMS-EEG applications in which I focused on: research on neuroscience (study 1); clinics (study 2) and technical aspects (study 3).

CHAPTER I
TRANSCRANIAL MAGNETIC STIMULATION (TMS)

1. OPERATING MECHANISMS OF TMS

Transcranial magnetic stimulation (TMS) is a technique able to non-invasively stimulate and modulate the excitability of the brain through the electromagnetic induction of an electric field, namely Faraday's law (Barker et al., 1985). According to this law the exposition of a material to a time-changing magnetic field causes the induction of an electric field. The magnitude of the evoked electric field and the current produced by it are directly proportional to the change rate in time of the magnetic field induced by TMS:

$$E \sim dB/dt \quad (1.1)$$

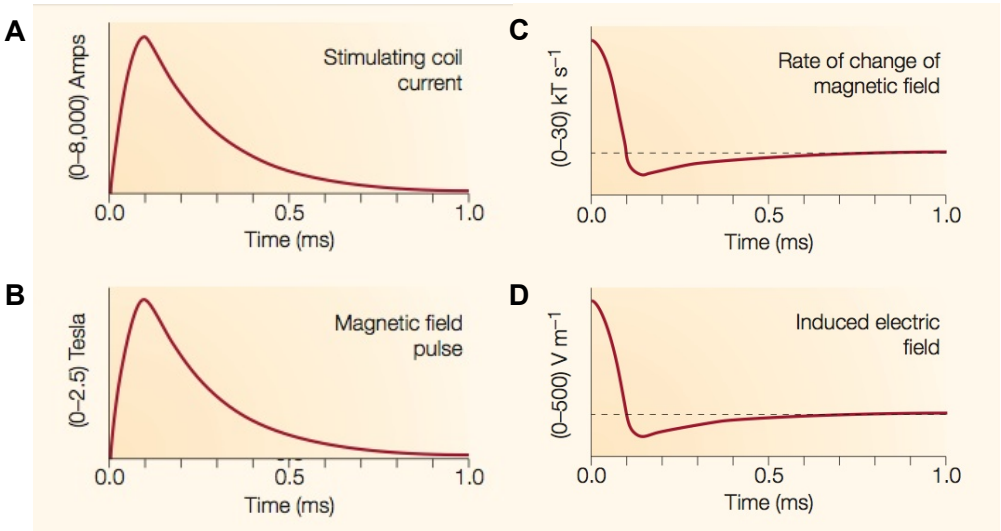

Figure 1.1 (a) electric current generated by TMS (maximum intensity 8kA) **(b)** magnetic field produced by the coil (maximum intensity 2.5 T) **(c)** rate of change of magnetic field (maximum intensity reached at 200μs , duration 1 ms) **(d)** induced electric field (adapted from Walsh e Cowey, 2000)

Where E is the electric field, B is the magnetic field and t is time. In the TMS a strong electrical current (up to 8kA) is generated by a capacitor and subsequently discharged into a solenoid made of 5-20 turns of wire, called coil. The coil produces

a magnetic pulse of up to 2 T with a rise time of 200 μs and duration of 1 ms which in turn induce an electric field directly in the cortex (fig. 1.1). The internal circuitry of a TMS consists of three main elements (fig. 1.2): a power capacitor, the inductor (i.e. the stimulating coil) and the switch that connect the two parts when is closed. This structure is common to all the monophasic TMS devices (see paragraph 2.2).

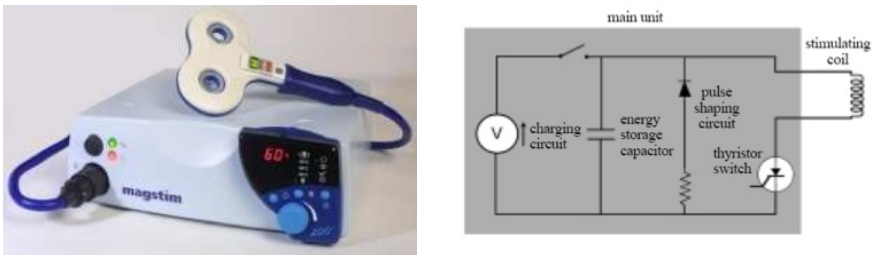

Figure 1.2 A TMS device (left), internal circuit of a standard monophasic TMS device (right) (adapted from Barker, 1991)

When TMS is applied to the brain, the induced electric currents cause a transient and non-invasive depolarisation of cell membranes and thereby neuronal activation in the stimulated area (Barker et al., 1985). Such mechanism, which is still poorly understood, has been mostly inferred from the application of TMS to the primary motor cortex (M1). The application of TMS over this area induces a depolarisation of the neurons of the corticospinal tract, which evokes a response in the controlateral muscle represented in the portion of the stimulated motor cortex, called motor-evoked potential (MEP) (fig. 1.3). MEPs characteristics, such as amplitude and latency, are used both in clinics to assess the correct functioning and efficiency of the corticospinal tract in healthy volunteers and in patients, and in research to investigate the physiology of the motor cortex. The size of the MEP reflects the excitability of the corticospinal system and increases with increasing the stimulus intensity (Barker et al., 1985). MEPs are one of the few "visible effects" that TMS induces when it is applied to the brain and currently most of the knowledge on the physiological mechanisms of the technique is based on the analysis of such peripheral markers.

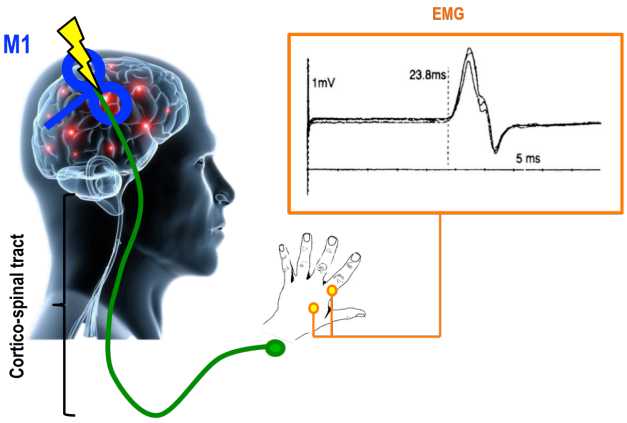

Figure 1.3 Schematic representation of the induction of motor-evoked potentials (MEP) with TMS over M1

2. TMS PARAMETERS OF STIMULATION

The investigation of the physiological and behavioural effects produced by the different parameters of stimulation is still a topic of central relevance, despite 30 years of TMS literature (Pascual-Leone et al., 1998). In fact, an impressive intra- and inter-individual variability in TMS responses is often observed in studies using similar TMS protocols (Maeda et al., 2000). Some subject-dependent factors can partially account for this variability, such as the subjective vigilance state and the scalp dimensions (Kammer et al., 2001; Okamoto et al., 2004; Stokes et al., 2005). However, most of the variability can be explained by some TMS-dependent factors mainly referable to the characteristics of the coil, the pulse shape and the protocol of stimulation. In the following three paragraphs the effect produced by these factors are discussed.

2.1 Characteristics of the coil: shape and orientation

The first TMS coils to be used were the circular coils. These coils are made of 5-20 turns of wire and have an outer diameter of 8-15 cm so that the magnetic field is stronger under the centre of the coil (Cohen et al., 1990). Differently, the induced current is stronger near the outer edge of the coil (fig. 1.4a) making the stimulation not focal. For this reason, circular coils are mainly used in clinics for the assessment of the cortico-spinal conduction time, usually tested by placing the coil over the cranial vertex in order to stimulate both the motor cortices simultaneously. A more

focal, but also less efficient, stimulation can be obtained if the coil is tilted relative to the scalp surface. Currently, most of the research and clinical tests use a more focal coil commonly known as “figure-of-8” coil (fig. 1.4b). Figure-of-8 coils are composed by two round coils placed side by side, such configuration make the electric current flow in the same direction at the junction point, so that the induced electric fields are maximum below this point (Ueno et al., 1988). The area stimulated by the figure-of-8 coils is about 1-2 cm^2 at a threshold intensity depending on the intensity of stimulation (Thielscher and Kammer, 2004), even if recent TMS studies simultaneously using EEG showed that the stimulation trans-sinaptically spreads over connected areas (Ilmoniemi et al., 1997; Massimini et al., 2005). Compared to circular coils the stimulation with figure-of-8 coils is more focused but also limited in terms of penetration of the induced electric field, because the two side loops are usually smaller. Such limit can be to some extent compensated by using a different coil configuration such as the “double-cone” coil. In double-cone configuration the round coils are bent into a spherical “cap” shape, this allows a more focused and deep stimulation usually used for stimulation of deep brain areas such as the cerebellum or the supplementary motor area (Kraus et al., 1993). More complex coil design have also been proposed in order to increase the focality and the penetration of the stimulation, such as the “H-coil”, designed to have a focused and deep stimulation (Roth et al., 2002). Another factor influencing the dimension of the electric field is the size of the coil: smaller coil induce more focal stimulation. On the other hand, the electric field induced by smaller coil is weaker in depth and the stimulation decrease dramatically depending on the distance between the coil and the scalp (Kozel et al., 2000; McConnell et al., 2001). With a standard figure-of-8 design the depth of stimulation is about 2-3 cm below the scalp (Rudiak and Mark, 1994). An additional critical factor is the coil positioning in terms of orientation and direction, defined by the position of the coil handle respect to the focus of stimulation, which indicate the current direction (i.e. posterior-anterior or anterior-posterior).

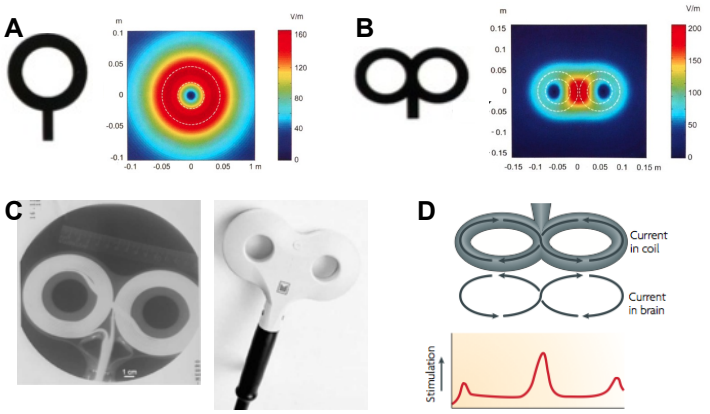

Figure 1.4 (a) magnetic field induced by a circular coil **(b)** by a figure-of-eight coil **(c)** figure-of-eight coil **(d)** current distribution in a figure-of-eight coil

The influence of current direction has been reported by several studies, presumably related by the anatomical orientation of the pyramidal tract neurons and their axons (Brasil-Neto et al., 1992; Porter and Lemon, 1993; Ziemann et al., 1996a). Coil orientation should be adjusted basing on the stimulated area (Pascual-Leone et al., 1994). For MEP evocation from the hand muscles, for example, the optimal orientation is 45 degrees in respect to the midline of the head that corresponds to an orientation perpendicular to the central sulcus (Mills et al., 1992; Brasil-Neto et al., 1992). In particular, current direction seems to be critical in the efficiency of the stimulation between monophasic and biphasic pulse waveform (Niehaus et al., 2000; Kammer et al., 2001; Sommer et al., 2006) discussed in the next paragraph.

2.2 Characteristics of the pulse waveform: monophasic and biphasic

Two pulse waveforms are mainly used in TMS literature: monophasic and biphasic. The monophasic waveform is generated by a switch or a diode in the stimulator that prevents the coil current from flowing in the reverse direction, so after a rise period the current falls to a zero level. Differently, in biphasic stimulators, after the first rise and fall of the current (which is the major component of the electric field) there is a second phase of the current allowed by the inductance and resistance of the circuit (Mills, 1999). The difference between the two pulses has been increasingly investigated in the last years (Kammer et al., 2001; Sommer et al., 2006). Several

studies, for instance, demonstrated a difference efficacy of the two pulses in the motor and visual threshold depending on the direction of the current (see below). Motor threshold, which is defined as the lowest TMS intensity that evokes at least five out of ten MEPs with amplitude of > 50 μV (Rossini et al., 1994), is lower with the current flowing in a posterior-anterior direction with a monophasic stimulator. Differently, when a biphasic stimulator is used, the anterior-posterior direction seems to be more effective (Sommer et al., 2006). MEPs latency is also known to be highly affected by the pulse waveform and current direction: longer latencies are observed with the optimal directions for the two pulse waveforms that are posterior-anterior for the monophasic pulse, and anterior-posterior for the biphasic (Di Lazzaro et al., 2001). Studies on visual phosphene threshold, which is the lowest TMS intensity that evokes phosphenes in approximately 50% of a number of trials (Steward et al., 2001), revealed that also visual cortex is sensitive to current orientation. Phosphene threshold is lower with latero-medial orientation than with the opposite (Kammer et al., 2001). In addition, Corthout and colleagues (2001), comparing two different stimulators, demonstrated that also the later phases of the biphasic pulse (i.e. the third and the fourth quarter cycle) contribute in the stimulation. Finally, a mounting number of studies is investigating the effect of the waveform on the long-lasting effects of the repetitive TMS (rTMS; see paragraph 2.3.3). Specifically, there is an increasing body of evidence that neuromodulatory effects with monophasic rTMS may be more effective and selective than conventional biphasic rTMS pulses (Sommer et al., 2002; Antal et al., 2002; Tings et al., 2005; Arai et al., 2005). However, this hypothesis was difficulty testable since traditional rTMS devices produce biphasic pulse. Recently, advances in TMS technology produced new devices able to deliver high-frequency rTMS pulses with different waveforms. Specifically, with this device, called controllable TMS (cTMS), it is possible to modify the ratio between the two phases of the pulse producing monophasic and different biphasic pulses (Peterchev et al., 2010).

2.3 Characteristics of the stimulation protocol: intensity and frequency

TMS intensity is adjusted basing on the motor or phosphene threshold (defined in paragraph 2.2). The physiological implication of TMS intensity is that stronger

stimuli recruit larger neuronal populations (Amassian et al., 1987). Indeed, at lower intensities only neuronal populations with low threshold are activated, so the stimulation is more focal (Rothwell and Ridding, 2007). On the other hand, previous studies showed that stronger intensities produced stronger inhibition using low-frequency rTMS (Siebner et al., 1999; see paragraph 2.3.3.1) and interhemispheric paired-pulse protocols (Ferbert et al., 1992; see paragraph 2.3.2.1). Depending on the frequency of stimulation, three main TMS protocol can be distinguished which use depends on the goal of the application: "single-pulse" (spTMS), "paired-pulse" (ppTMS), and "repetitive" (rTMS).

2.3.1 Single-pulse TMS

Single-pulse is commonly used in the assessment of motor physiology, for clinical and research purposes, and in the study of cognitive processes.

2.3.1.1 Single-pulse TMS in the assessment of motor physiology

spTMS provides measures of corticospinal excitability, information about the functional integrity of intracortical neuronal structures, conduction along corticospinal, corticonuclear and callosal fibres. The amplitude of the MEP is used to examine the integrity of the corticospinal tract and its excitability. Although very useful, this measure cannot distinguish between the different contributes of cortical, subcortical or spinal excitability. Indeed, patients with dysfunction at any level of the corticospinal tract show abnormalities in MEPs amplitude or latency. However, it must be taken in account that great inter- and intraindividual variability is often observed in healthy volunteers, leading to a large range of normal values (Kiers et al., 1993). The motor threshold, defined in paragraph 1.1, is increased by drugs that block voltage-gated sodium channels (Ziemann et al., 1996a) whereas no effect are observed after the administration of drugs altering γ-aminobutyric acid (GABA) or glutamate neurotransmission (Liepert et al., 1997; Ziemann et al., 1996b), so it is believed that reflects the membrane excitability of corticospinal neurons and motor neurons in the spinal cord. Indeed, motor threshold is strongly affected by disease of the corticospinal tract. Patients with multiple sclerosis, stroke, brain or spinal cord injury usually show an increase in the motor threshold (Davey et al., 1998), whereas

a decrease in the motor threshold is often observed in patients with amyotrophic lateral sclerosis (Mills and Nithi, 1997). Phosphene threshold, even if less commonly used, can also provide information on the visual cortex physiology. Patients with migraine, for instance, showed a lower phosphene threshold compared to control individuals (Aurora et al., 1998). Recruitment curve is generated by the increase in MEP amplitude with increasing the TMS intensity. The slope of the curve reflects the strength of corticospinal projections. For instance, in muscles with a low motor threshold, such as intrinsic hand muscles, they curve is generally steeper (Chen et al., 1998). Previous studies investigated the effects of drugs on the recruitment curve which is increased by drugs enhancing adrenergic transmission, whereas a decrease has been observed after the administration of sodium and calcium channel blockers and after drugs increasing the effects of GABA (Boroojerdi et al., 1999). Another important measure assessed by spTMS is the cortical silent period, which refers to the block of electromyographic (EMG) activity after the evocation of a MEP, usually lasting a few hundred of ms (Chen et al., 2000). The silent period is evoked when a single suprathreshold TMS pulse is applied over the motor cortex during a muscle contraction. It is believed that the origin of the silent period is mostly due to cortical inhibitory mechanism, even if a spinal contribute is likely to play a role at least for the first 50-60 ms (Brasil-Neto et al., 1992; Fuhr et al., 1991) whereas the late part is most likely mediated by cortical $GABA_B$ receptors (Werhahn et al., 1999). Abnormal duration of silent period is often observed in patients with movement disorders. For instance, in patients with amyotrophic lateral sclerosis the duration of silent periods is usually shorter than healthy controls, due to impairment of intracortical inhibition (Caramia et al., 2000). Central motor conduction is another common measure provided by spTMS over the motor cortex and spinal cord (with the coil placed over the back of the neck). This index is calculated as the difference between the peripheral conduction time (obtained by spinal stimulation) and the MEPs latency evoked in the target muscle (Chen et al., 2000). Patients with multiple sclerosis, stroke and amyotrophic lateral sclerosis usually showed a delay in central motor conduction time (Rossini and Rossi, 1998).

2.3.1.2 Single-pulse TMS in the study of cognitive processes

In the last 25 years the use of TMS in cognition has increased progressively in the investigation of a wide range of cognitive processes, such as: perception (Amassian et al., 1989), attention (Walsh et al., 1998; Ashbridge et al., 1997), learning (Pascual-Leone et al., 1994; Steward et al., 1999), language (Pascual-Leone et al., 1991; Epstein et al., 1998), executive functions (Mull and Seyal, 2001; Bisiacchi et al., 2011); memory (Kirschen et al., 2006) and awareness (Cowey and Walsh, 2000). In particular, spTMS has been largely used to transiently "interfere" with the ongoing cognitive processes, providing an accurate description of the cerebral processing timing. In cognitive studies, spTMS is usually applied ad precise time points during a cognitive task in order to investigate the exact timing at which a specific area is critical for the ongoing process, this approach is known as "mental chronometry" (Pascual-Leone et al., 1998). One of the first examples of this approach has been provided by a popular study conducted by Cohen and colleagues (1991). In this study spTMS was used to interfere with the function of different cortical areas in blind patients while they were reading Braille and in healthy volunteers while they were reading embossed Roman letters. When TMS was applied to the primary visual cortex (V1) it induced a distortion of the tactile perception of congenitally and early blind patients, but not in patients that become blind after age 14 and in healthy volunteers (Cohen et al., 1991). This result was one the first that demonstrated the causal role of the visual cortex in tactile spatial processing in early blind subjects. However, the mechanism of how TMS interferes with the information processing is still a matter of debate and different theories have been proposed throughout the years, such as the "virtual lesion theory" (Pascual-Leone et al., 1998) and the "neural noise theory" (Miniussi et al., 2010), this point is discussed in paragraph 1.1 of the second chapter of this thesis. Understanding the mechanism of TMS in cognition is also complicated by the relatively low spatial resolution of the stimulation. Despite the progresses that have been made to make the stimulation focal, such as the developing of focal figure-of-eight coil and neuronavigation systems, it is now clear that the stimulation spreads over brain regions interconnected to stimulated area. This evidence have been provided by a number of studies simultaneously using TMS with neuroimaging techniques (for a review, Casula et al., 2013), a new and interesting topic that is covered in the second chapter of this thesis.

2.3.2 Paired-pulse TMS

2.3.2.1 Paired-pulse TMS in the examination of intracortical inhibitory and excitatory mechanisms

In paired-pulse protocols two stimuli are used: a conditioning stimulus, usually delivered at a subthreshold intensity, and a test stimulus delivered at a suprathreshold intensity. The interstimulus interval (ISI) between the two stimuli is critical in producing different effects on the test MEP and, depending on the ISI length and on the intensity of the stimulation, inhibitory and facilitatory interaction in the cortex can be studied (fig. 1.5). At very short ISI, from 1 to 5 ms, the test MEP is inhibited and this is called short interstimulus interval intracortical inhibition (SICI) whereas an intracortical facilitation (ICF) is usually observed at ISIs ranging from 8 to 30 ms (Kujirai et al., 1993). Such processes are likely to occur within the motor cortex as previously demonstrated by pharmacological studies showing a suppression of ICF and an increase of SICI after the administration of drugs enhancing $GABA_A$ activity and antiglutaminergic drugs (Ziemann et al., 1996a). At longer ISIs, under 200 ms, a long interstimulus interval intracortical inhibition (LICI) of the test MEP is observed which is mediated by $GABA_B$ receptors (Werhahn et al., 1999). Notably, the physiological basis of these mechanisms have been supported by a number of studies using EEG during TMS (e.g. Farzan et al., 2010; Premoli et al., 2014; Casula et al., 2014), this point will be largely discussed in the second chapter of this thesis.

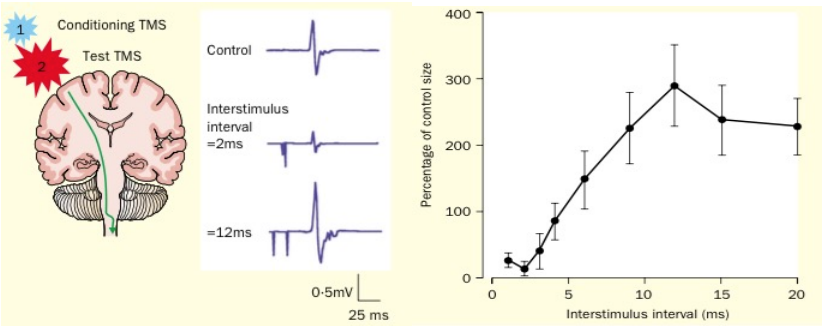

Figure 1.5 Modulation of the MEP sizes induced in the FDI by paired-pulse TMS (adapted from Kobayashi et al., 2003)

2.3.2.1 Paired-pulse TMS in the examination of cortico-cortical interactions

ppTMS can be used to test the connectivity by delivering the conditioning stimulus over an area connected to the motor cortex, this paradigm is known as "twin coil"

(Rothwell, 2010). The assumption is that if the conditioning pulse modulates the test MEP, than there is an interaction between the conditioning area and the motor cortex (Rothwell, 2010). The first and most common example of this protocol is the interhemispheric inhibition paradigm in which one suprathreshold stimulus is delivered to one motor cortex followed by a second test stimulus delivered to the other motor cortex after 4-30 ms, allowing the investigation of interhemispheric interactions and transcallosal conduction times (Ferbert et al., 1992). These authors found a that at ISIs between 7-15 ms the excitability of the motor cortex controlateral to the stimulation is inhibited by the inhibitory connections of the stimulated motor cortex, interestingly the magnitude and the length of the intensity was correlated to the intensity of the conditioning stimulus (Ferbert et al., 1992; fig. 1.6).

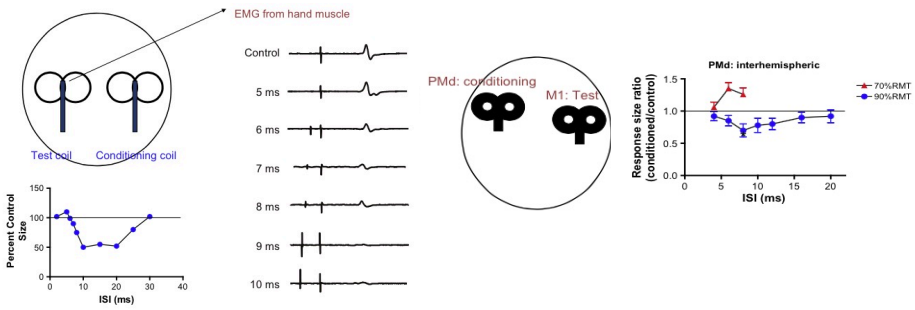

Figure 1.6 Interhemispheric inhibition between the motor cortices investigated with a two coil paradigm (left), on the right the same protocol applied over the premotor cortex and the controlateral motor cortex (adapted from Rothwell, 2010)

Interhemispheric interactions have also been investigated in patients with movement disorders. For instance, patients with affected transcallosal or cortical inhibitory interneurons showed abnormal or absent interactions between the two motor cortices (Hanajima et al., 2001; Shimizu et al., 2002). Twin coil approach has been applied also to detect inputs from other areas. One of the first studies testing this was conducted by Civardi and colleagues (2001) probing the connections between premotor areas and M1 using a smaller TMS coil (fig. 1.6). Other connections have been investigated with the same approach, such has: parietal-motor interactions (Davare et al., 2010); premotor-motor interactions (Münchau et al., 2002); frontal-motor interactions (Hasan et al., 2012). The same approach has been used also to investigate the cerebellar-cortical pathway by delivering a conditioning pulse over the back of the head with a double-cone coil. Ugawa and

colleagues (1995) were the first to find a strong cerebellar inhibition, presumably originating from activation of Purkinje cells, of a test MEP evoked at 5-6 ms after the conditioning pulse over the cerebellum. The twin coil approach have been used also to investigate the role of functional networks activated during a cognitive task, one example have been provided by Hasan and colleagues (2012) finding a muscle and timing-specific connectivity between the dorsolateral prefrontal cortex and the motor cortex during an action selection task, and by Koch and colleagues (2006) finding an activation between dorsal premotor and controlateral motor cortex during a movement selection task.

2.3.3 Repetitive TMS

Repetitive TMS (rTMS) consists of a "train of pulses" delivered in a certain time frequency. Unlike spTMS and ppTMS, rTMS produces an effect on the excitability of a stimulated area for a period that lasts beyond the duration of the TMS application, depending on stimulation parameters, such as: stimulus frequency, stimulus intensity, duration of the application and total number of stimuli delivered (for a review, Thut and Pascual-Leone, 2010). For its capability to induce long-lasting effects rTMS has been largely used in the investigation of plasticity processes, cognitive studies and in clinical applications, these applications are discussed in the following three paragraphs.

2.3.3.1 Repetitive TMS in the investigation of plasticity processes

In literature, stimulation with a frequency higher than 1 Hz is referred to as "high-frequency rTMS", whereas stimulation with a frequency of less than 1 Hz is referred to as "low-frequency rTMS" (Rossi et al., 2009). It has been generally observed that a low-frequency rTMS protocol produces an inhibitory effect on cortical excitability, while a facilitatory effect is often observed after a high-frequency rTMS protocol. The mechanism of rTMS after-effects is still a matter of debate, because of the indirect nature of the evidence from human studies. It has been suggested that short-term effects (i.e. seconds or a few minutes after the stimulation) might be resulting from changes in neural excitability produced by shifts in ionic balance around neural populations (Kuwabara et al., 2002) whereas long-term effects have been related to changes in the effectiveness of synapses between cortical neurons,

similarly to what occurs in long-term depression (LTD) and long-term potentiation (LTP) mechanisms (fig. 1.7; Ridding and Rothwell, 2007). Another reason why the mechanism is still unclear is the large inter- and intraindividual variability, in terms of size, direction (i.e. inhibitory/facilitatory) and duration of the rTMS effects. A possible explanation for this inconsistency is that TMS experiments of plasticity have been limited by the intensity and frequency of the stimulation. In addition, several subject-dependent factors can account, at least partially, for the variability observed, such as: differences in the anatomy (Stokes et al., 2005); level of ongoing cortical activity (Stefan et al., 2004); changes in hormone levels (Inghilleri et al., 2004); genetic factors (Kleim et al., 2006) and interactions with pharmacological treatments (Fregni et al., 2006). Finally, it must be taken in consideration that these effects has been mainly tested over the M1 given that the stimulation of this area produces a visible and well-defined outcome, which is the MEP. Plasticity rTMS-induced of associative areas such as the dorsolateral prefrontal cortex has also been largely explored, especially for therapeutic purposes discussed in paragraph 2.3.3.3.

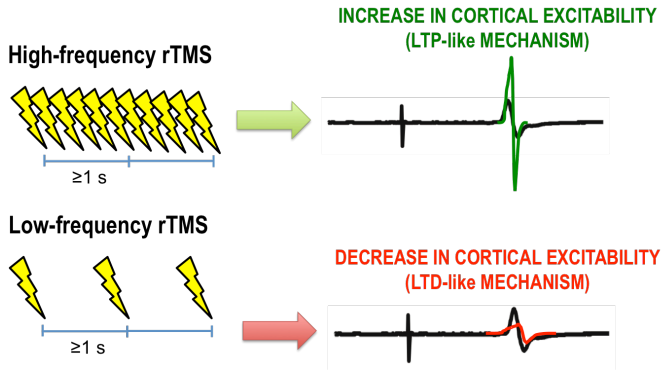

Figure 1.7 Effects of high-frequency (above) and low-frequency (above) rTMS on the excitability of the primary motor cortex

2.3.3.2 Repetitive TMS in the investigation of cognitive processes

rTMS has been largely used in the investigation of a wide range of cognitive processes both in an on-line and in an off-line approach. In on-line studies rTMS is delivered during a task usually in short trains of high-frequencies pulses to interfere with the ongoing cognitive process, such as: picture naming (Mottaghy et al., 1999); analogic reasoning (Boorojardi et al., 2001), action naming (Cappa et al., 2002); episodic memory (Kohler et al., 2004); phonological memory (Kirschen et al., 2006); working memory (Luber et al., 2007) and prospective memory (Bisiacchi et al., 2011). One of the first and well-known example of this approach has been provided by Pascual Leone and colleagues (1991) inducing a speech arrest by applying rTMS over the Broca's area. In off-line rTMS cognitive studies, the stimulation is delivered separately in time from the task, usually following the procedure "task – rTMS – task". Importantly, it must be taken in account that the physiological effects of rTMS over the motor cortex does not have a correlate in behavioural performance, which means that an increase in cortical excitability following high-frequency rTMS does not necessarily lead to a behavioural improvement and *viceversa* (Miniussi et al., 2010). However, in spite of this limitation, most of the cognitive studies using rTMS have been conducted with an off-line approach because this paradigm allow to avoid a number of confounding factors related to a nonspecific effect of the stimulation that can affect the performance, such as: discomfort, noise, muscle twitches, startle response and intersensory facilitation (Sandrini et al., 2011). Although its mechanism is still poorly understood, 1-Hz rTMS is the most frequently used protocol in the investigation of a wide range of cognitive processes, such as: spatial hearing (Lewald et al., 2002) and number processing (Knops et al., 2006) stimulating parietal areas; working memory (Mottaghy et al., 2002), decision making (Knoch et al., 2006) and temporal perception (Correa et al., 2014) stimulating prefrontal areas; motor learning (Perez et al., 2007) stimulating the supplementary motor area and semantic cognition (Pobric et al., 2010) stimulating the anterior temporal lobe.

2.3.3.3 Repetitive TMS in therapeutic applications

As mentioned before, the long-lasting effects of rTMS have been related to LTP/LTD-like changes in synaptic connections between cortical neurons (Ridding and Rothwell, 2007). Following this interpretation there may be a potential for the excitatory or inhibitory effects of rTMS in improving the functioning of an area disrupted after injury or chronic diseases. Indeed, some studies reported an effect of the rTMS-induced LTP over the dorso-lateral prefrontal cortex in a wide range of outcome measures, including: improvements in psychiatric symptoms, long-lasting structural or functional changes (Speer et al., 2000), electrophysiological measures (Esser et al., 2006) and cognitive tasks (Luber et al., 2006). Therapeutic effects of rTMS have been mainly studied in medication-resistant depressive disorders as an adjunctive treatment aimed to potentiate and accelerate the effects of antidepressant drugs via LTP-like mechanisms (Rossini et al., 2005; Rumi et al., 2005). Similarly, rTMS over lateral PFC has been used in the treatment of obsessive-compulsive disorder in an attempt to boost and accelerate the psychotropic effects of tricyclic antidepressant clomipramine, used in the treatment of the disease (Greenberg et al., 1998). Treatment of schizophrenic symptoms is another clinical domain in which rTMS has been used. Specifically, some authors reported a reduction of hallucinations in schizophrenic patients (Lee et al., 2005) and improvements in negative symptoms like apathy, amotivation and attention impairment (Cohen et al., 1999; Nahas et al., 1999). Finally, previous studies report a reduction of substance use disorders after rTMS of the DLPFC (Eichhammer et al., 2003).

2.3.4 Patterned rTMS and other protocols of stimulation

2.3.4.1 Theta-burst stimulation

Besides the variability, one of the main problems of the neuromodulatory effects of rTMS is the limited duration of the effects, which is dependent from the duration of the protocol and the intensity of stimulation. For instance, 20 minutes of 1-Hz rTMS delivered at 80% of MT has been reported to reduce motor cortex excitability for 15-30 minutes after the end of the protocol (Chen et al., 2003). In order to reduce the duration and the intensity of the stimulation, new protocols using short bursts of

TMS delivered at very high frequencies with low intensities have been developed, such protocols are collectively termed as patterned rTMS (Huang et al., 2005; Rossi et al., 2009). Theta-burst stimulation (TBS; Huang et al., 2005) consists in the administration of repetitive three-pulse bursts at 50 Hz, delivered every 200 ms, a frequency based on the physiologic pattern of neuronal firing found in the hippocampus of animal models (Kandel and Spencer, 1961). There are two main TBS protocols: continuous TBS (cTBS) and intermittent TBS (iTBS), originally developed by Huang et al. (2004). CTBS consists of a continuous train of TBS bursts (i.e. three pulses delivered at 50 Hz every 200 ms) without interruption and it induces an LTD-like effect. The two main advantages of this protocol is the relatively shortness of the duration which is delivered for 30 seconds (300 pulses) or 40 seconds (600 pulses) and the low intensity of stimulation, usually 80% of the AMT. ITBS consists of 20 trains of 10 TBS bursts, lasting 2 s, interrupted by 8 or 10 seconds of pause, usually delivered at 80% of AMT. This protocol induces an LTP-like effect, for instance different studies found that 190 seconds of iTBS over M1 facilitates MEPs for 20 minutes (Huang et al., 2005; 2007). Importantly, the results of the protocol are critically dependent from the protocol parameters and from muscle activity that strongly suppress the after-effects of TBS (Huang et al., 2007). Furthermore, it has been generally reported that iTBS is less efficient compared to cTBS and the results obtained show more variability (Huang et al., 2007). Recently, it has been demonstrated that the pulse waveform strongly affects the TBS after-effects (Sommer et al., 2014; Hamada et al., 2014). Specifically, monophasic TBS pulses seem to produce a stronger and more reliable effect compared to traditional biphasic TBS (Sommer et al., 2014; Hannah et al., 2014). Since traditional monophasic TMS are not able to deliver repetitive protocols (see paragraph 2.2) the pulsewave effect has been tested with a new TMS device called controllable shape pulse TMS (cTMS; Peterchev et al., 2010). CTMS induces near-rectangular electric field pulses that are adjustable over a wide continuous range (e.g. pulse width and ratio of positive to negative electric field phase amplitude) enabling the development of more selective and efficient protocols of stimulation (Peterchev et al., 2013). In contrast, standard TMS induces cosine electric field pulses with very limited control over the pulse parameters. The main advantage of cTMS is that the near-rectangular pulse produces a faster change in neuronal membrane potential

resulting in a reduction of the energy necessary to induce a neuronal depolarization (Barker et al., 1991). CTMS can also be used to optimize traditional rTMS protocols. Indeed, it is believed that the neuromodulatory rTMS effects with predominantly unidirectional pulses are more selective and stronger than the neuromodulatory effects of standard biphasic rTMS (Sommer et al., 2002; Antal et al., 2002).

2.3.4.2 Paired associative stimulation

Besides repetitive stimulation, another approach to produce long-term changes in synaptic effectiveness is the paired associative stimulation (PAS). PAS is based on the concept of hebbian spike-timing-dependent plasticity in which two inputs are paired to arrive at a single neuron approximately at the same time; if this pattern is repeated for a certain number of times, a change in the synapses efficiency occurs (fig. 1.8). Usually, when a pre- input arrives just before a post- input, so that the activation (firing) of a presynaptic cell occurs just before the activation of a postsynaptic cell the connection is strengthened. When the contrary occurs, that is when a postsynaptic cell fires an impulse just before the activation of a presynaptic cell the connection is weakened. In humans, PAS usually consists of low-frequency repetitive peripheral nerve stimulation combined with TMS delivered over a controlateral target region of the cortex. It is known that the fastest sensory transmission of an impulse from the median nerve to the sensorimotor cortex takes about 20 ms. When the TMS pulse is repetitively applied just after the peripheral transmission (e.g. 25 ms) than an increase in the excitability of the motor and sensory cortex is observed (PAS25); on the contrary, when the TMS pulse is applied before the peripheral transmission (e.g. 10 ms) a decrease in sensorimotor excitability is observed (PAS10; Stefan et al., 2000). Paired stimuli in PAS are usually delivered for 60-180 times at a very low frequency (0.25 Hz), duration of the after-effects depends on the number of delivered stimuli (e.g. 90 pairs of stimuli can have an effect for more than 30 minutes; Stefan et al., 2000). The influence of different drugs in PAS effects have been investigated: for instance, PAS effects on subjects treated with L-DOPA lasted for more than 24 hours (Kuo et al., 2008); whereas PAS effects are abolished if subjects are treated with dextromethorphan, a blocker of NMDA receptors, proving the critical role of this receptor in PAS-induced plasticity

(Wolters et al., 2003). Recently, some studies used cortico-cortical PAS protocols to induce some hebbian-plasticity of cortical networks (e.g. Koch et al., 2013), such protocols have also been used by concurrent TMS-EEG to provide insights into the plasticity mechanisms induced by PAS (Veniero et al., 2013).

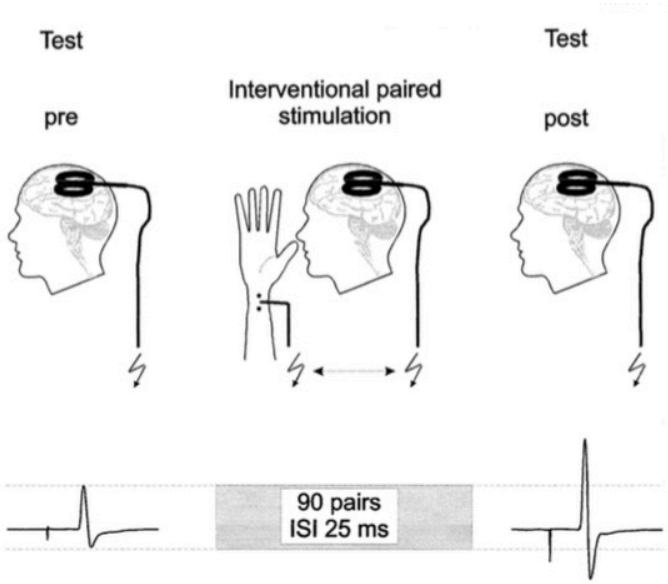

Figure 1.8 Schematic illustration of a paired associative stimulation (PAS) protocol

CHAPTER II
THE SIMULTANEOUS USE OF TMS WITH EEG AND OTHER TECHNIQUES

1. THE NOVELTY VALUE OF TMS-NEUROIMAGING COREGISTRATION

1.1 What can neuroimaging add to TMS?

One of the most controversial aspects of TMS lies in its complex physiological mechanism. In fact, despite the widespread use of TMS in current research, its mechanism of action is still poorly understood. Traditionally, the mechanism of TMS have been mostly investigated over M1 given that the stimulation of this area evokes a twitch in a muscle contralateral to the stimulation, that is the motor-evoked potential (MEP), easily measurable with electromyography (EMG). The modulation of MEPs amplitude, which reflects the degree of excitability of the corticospinal system (Barker et al., 1985), has been used to assess the mechanism of action of TMS, the neuromodulatory effects of rTMS, and the intracortical facilitation/inhibition processes through paired-pulse TMS. However, as already mentioned in the first chapter of this thesis, MEPs origin is far from being fully elucidated because of the complex combination of excitatory and inhibitory events along the motor pathway, which leads to a considerable variability in MEPs amplitude (Fitzgerald et al., 2006). The effects of TMS over cortical areas other than M1 have been mainly inferred through behavioural measures, mainly reaction times and accuracy to a task. At the end of the eighties, the TMS capacity of inducing a non-invasive, transient, and relatively focal depolarisation was used for the first time as a "disruptive" technique, whose effects were interpreted in terms of "virtual brain lesions" (Walsh and Cowey, 2000). This term was proposed considering the TMS effect as inducing a temporary, reversible lesion in the stimulated area. The "virtual lesion" interpretation of the TMS mechanism was widespread for two main reasons: first, it was supported by early studies on cognitive processes (e.g., Amassian et al., 1992); second, it was the most parsimonious and simple explanation of the TMS effect. With the development of neuronavigation systems, the idea of TMS as a "point and shoot" methodology grew further, until several experiments showed that TMS

could also result in the facilitation of cognitive performance (e.g., Cappa et al., 2002; Mottaghy et al., 1999). These "paradoxical" facilitation effects revealed the inadequacy of a "virtual lesion" hypothesis in explaining TMS effects, leading to a reconceptualization of its mechanisms. Recently, new evidence from biophysical and neuroimaging studies (e.g., Allen et al., 2007; Wagner et al., 2009) offered new insights into basic properties of TMS, leading to an interpretation of its effect in terms of a "random-induced neuronal activity" (Miniussi et al., 2010). This activity can be thought of as "neural noise" since is not directly associated with the activity of the stimulated area. For these reasons, its effect can result in interference or facilitation of a cognitive performance depending on the relationship between the "noise" (i.e., TMS-evoked activity) and the "signal" (i.e., target activity) (Miniussi et al., 2010). Nevertheless, besides the credible contribution of these kinds of studies clear evidence of the TMS physiologic mechanisms has not yet been provided.

Neuroimaging techniques offer an important contribution to TMS mechanism comprehension through the description of the neural activation evoked by the electromagnetic pulse. For instance, electroencephalography (EEG) can detect the response of a cortical area to the TMS pulse (i.e., cerebral reactivity) based on the related electric markers of its activity, namely TMS-evoked potentials (TEPs). The analysis of TEP characteristics such as latency, amplitude, polarity, and waveform can offer an insight into the physiological state of the stimulated brain area, allowing researchers to tackle inference with TMS mechanisms. On the other hand, techniques such as fMRI, PET, SPECT, and NIRS, which provide better spatial resolution than EEG, offer a detailed picture of responses to TMS throughout the brain. One of the most direct exemplifications of a neuroimaging contribution is the demonstration of the spread dynamics of TMS-evoked activity from the stimulated area to the connected regions. Ilmoniemi and colleagues (Ilmoniemi et al., 1997) were the first to provide direct evidence of this phenomenon. The authors mapped the ongoing activity evoked by the stimulation of M1 and V1 in the ipsilateral and contralateral homologous regions. This evidence had a high novelty value in the field of TMS research, considering that traditionally its effects were evaluated only in regard to the stimulated area. Besides the elucidations on the general TMS mechanism, neuroimaging techniques can also provide direct evidence on the effect of a single TMS parameter. An example was provided by Käkhönen and colleagues

(2005). The authors investigated reactivity variations of the prefrontal cortex and M1 across different stimulation intensity conditions (Käkhönen et al., 2005). All the different contributions that each neuroimaging technique provides to TMS will be further discussed in the following sections of this chapter.

1.2 What can TMS add to neuroimaging?

The correlational nature of neuroimaging techniques does not allow any conclusion about the causal role of an activated brain region in task performance. Basing on fMRI data, for example, it can be demonstrated that an *X* cerebral area is activated while a *Y* cognitive process is performed. However, from a logical point of view this evidence is not sufficient to establish that if the *X* area is activated, the *Y* process is being performed (Poldrack, 2005). This argument, which has not been legitimated by scientific logic, is known as "reverse inference" (Aguirre, 2003). Furthermore, besides the accurate spatio-temporal information, neuroimaging instruments cannot account for most of the complex variability in neurobiological mechanism modulation. One of the main limitations of these techniques in fact is the poor information about the nature of the brain activation. Basing on PET or fMRI data, for example, it cannot be established whether the observed activity is excitatory or inhibitory (Raichle, 1998). This is a crucial aspect since the activity detected in a certain area might also reflect inhibitory activation aimed to stop or inhibit processes competing with the function of the area. Moreover, a brain area could merely be accidentally activated by a cognitive process (Raichle, 1998). Finally, in the presence of diffuse brain activation during a multi-componential cognitive task, functional neuroimaging cannot discriminate between the different contributions of the activated brain areas within the ongoing cognitive process (Sack and Linden, 2003). These factors pose several problems in demonstrating the role of a certain area within a cognitive process. In summary, since a brain region can be considered crucial in an *"X"* cognitive process only if the modulation of its activity affects cognitive performance (i.e., facilitation/disruption of the performance), the manipulation of brain activation as a variable is a critical factor in establishing its particular causal role. As already reported in the first chapter, this feature is provided in different ways by transcranial magnetic stimulation technique. On one

hand, the active interference induced by single-pulse TMS can be used to make causal inferences regarding the functional contribution of a stimulated brain area. On the other hand, neuromodulatory protocols of rTMS can be used in an offline approach to modulate the excitability of a target area and subsequently investigate its contribute to a task.

1.3 Methodological aspects of TMS-neuroimaging coregistration

Because of the electrical and magnetic principles TMS and neuroimaging are based upon, their simultaneous use (i.e., coregistration) poses several technical problems. The TMS pulse, in fact, induces an electromagnetic artefact that can affect data acquisition when it is performed during neuroimaging (i.e., "on-line" approach), especially when TMS is combined with electroencephalography (EEG) or functional magnetic resonance imaging (fMRI). Such technical problems can mostly be avoided by applying rTMS before or after neuroimaging (i.e., "off-line" approach). Currently, with the exception of MEG, all the other neuroimaging techniques have been successfully used in combination with TMS, both in on-line and off-line approaches. On-line and off-line approaches provide different information and pose different technical and methodological issues. The choice of one approach instead of the other is generally established based on the target of the study, as well as on the setting and the instruments available (fig. 2.1).

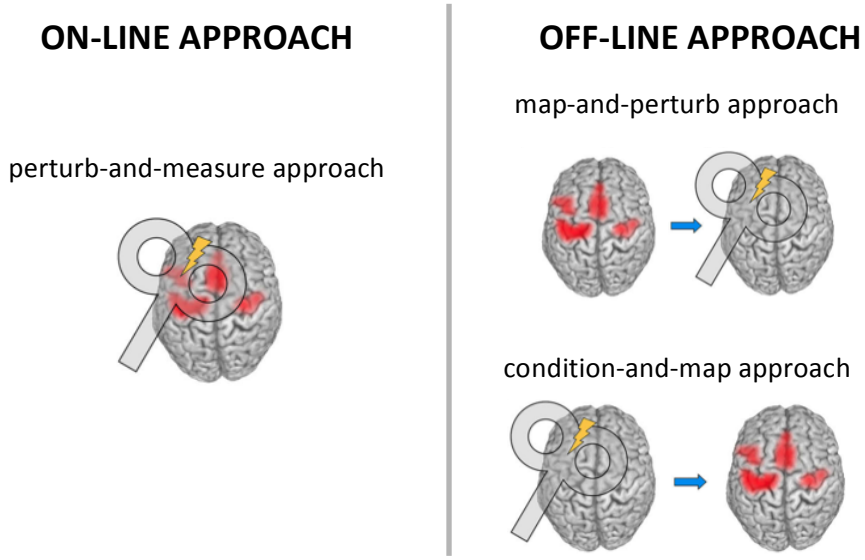

Figure 2.1 Schematic illustration of on-line (left) and off-line (right) approaches in TMS-neuroimaging coregistration (adapted from Siebner et al., 2009)

The on-line approach allows direct evaluation of the instantaneous effect of magnetic stimulation on the brain. More specifically, TMS is used to interfere with the ongoing neuronal activation whose changes are detected by neuroimaging. Besides the information provided on the reactivity of the stimulated area and its connectivity to other areas, this approach also has potential value from a technical point of view since it allows the investigation of the effect of TMS over the brain. One of the first examples of this kind of study was performed by Bohning and coworkers (1997), who aimed to directly measure the exact magnetic field produced by TMS in human subjects. The authors used two TMS coils suitable for concurrent MRI (i.e., constructed with non-magnetic materials) to map the magnetic fields generated by TMS in the human brain. This study was the first one that combined TMS and MRI in an on-line approach.

Off-line coregistration can be performed using neuroimaging before or after TMS. In the first case, neuroimaging can be used to guide the exact coil positioning in a localised brain area. This procedure is particularly used in cognitive neuroscience studies since neuroimaging techniques can reliably identify one or more brain areas that are activated during a cognitive task. Subsequent TMS can be applied over the identified area to interfere with ongoing neuronal processing while participants are performing a task that is supposed to involve the stimulated area. This procedure potentially provides important elucidation regarding the possible contribution to a cognitive process of a certain brain region or its interconnected areas. A famous study by Cohen and colleagues (1997) provides a direct example of this approach. The authors based their work on previous neuroimaging studies on people who were blind from an early age, which showed prominent activation of the occipital visual areas during Braille reading (Sadato et al., 1996). Starting from this evidence, they applied short trains of 10-Hz rTMS to different cortical areas in subjects who were blind from an early age while they were involved in the identification of Braille or embossed Roman letters. When TMS was delivered over the occipital visual cortex tactile perception was distorted, resulting in a large number of errors in both tasks. In contrast, the same stimulation in healthy volunteers affected their visual performance, but not their tactile performance. These data confirmed that blindness from an early age generates a cross-modal cerebral plasticity that causes the recruitment of the visual cortex in somatosensory processing. Neuroimaging

techniques such as MRI can also be used to define specific anatomical targets based on individual brain images for subsequent TMS. With MRI-guided frameless stereotactic neuronavigation, precise coil placement can be obtained with a high degree of reproducibility across different sessions (e.g., Komssi et al., 2002). This application will be further discussed in the section related to TMS-MRI coregistration.

A different application of the off-line approach consists of using neuroimaging after rTMS to investigate and map the long-term effects of the stimulation. This application offers important insights into the cortical plasticity mechanisms and into the TMS after-effects. Since spTMS and ppTMS effects are instantaneous, the only protocol suitable for this approach is rTMS, whose after-effects may last beyond of its application. For this reason, neuroimaging is usually applied immediately after the rTMS protocol to ensure that even short-duration after-effects are detected (Siebner et al., 2009). An example of this application is provided by Lee and colleagues (Lee et al., 2003). The authors explored the effects on regional excitability caused by low-frequency rTMS over M1. The authors applied 1 Hz rTMS for 30 minutes, and then activation was mapped through PET at rest and during freely selected finger movements. The results showed an effect of rTMS both locally, with a major activation in the stimulated motor area, and throughout the brain regions engaged in the task. In summary, on-line and off-line approaches provide different insights into the TMS effects on brain activity and imply different methodological and technical precautions. However, the use of one approach does not exclude the other one; conversely, the utilisation of neuroimaging both before and after TMS is an optimal method to detect the effects of the stimulation on neuronal activity.

2. TMS-EEG COREGISTRATION

Neural activity generates electric as well as chemical signals. The electric signals generated from the simultaneous activity of large neuronal populations can be detected and measured by electrodes applied on the scalp (usually placed according to the 10-20 system) since brain, skull, and scalp tissues passively conduct the electric (as well as magnetic) currents generated by the neurons' activity. Such activity is the summation of thousands or millions of neurons that have similar

spatial orientations, especially pyramidal neurons that are thought to produce the most of the EEG signal because they are well aligned over the cortex and synchronised in the firing activity. The recording of tension variations between different electrodes placed over the scalp is referred to as electroencephalography (EEG) and it is mainly produced by post-synaptic potentials. One of the main EEG applications in clinical and in research studies is the detection of electric responses evoked by cognitive, motor or sensorial processes. These responses are referred to as event-related potentials (ERPs) and they can be analysed over four domains: time, space, power and frequency of oscillation. When TMS is applied during EEG, its time-varying magnetic field induces electric currents in the cortical layers of the brain that generate a flow of ions, whose direction depends on the direction of the induced electric field. After the ion channels are opened, causing a depolarisation of cell membranes, the subsequent post-synaptic potentials are recorded by means of the EEG (Ilmoniemi et al., 1997). The EEG activity induced by TMS is known as TMS-evoked potentials (TEPs) and its made of a sequence of positive and negative deflections lasting around 280-300 ms after the TMS pulse (fig. 2.2), namely: P30, N45, P55, N100 and P180 (Paus et al., 2001; Komssi et al., 2002; Bender et al., 2005; Bonato et al., 2006; Van der Werf et al., 2006; Lioumis et al., 2009; Ferreri et al., 2011; Casula et al., 2014; Premoli et al., 2014).

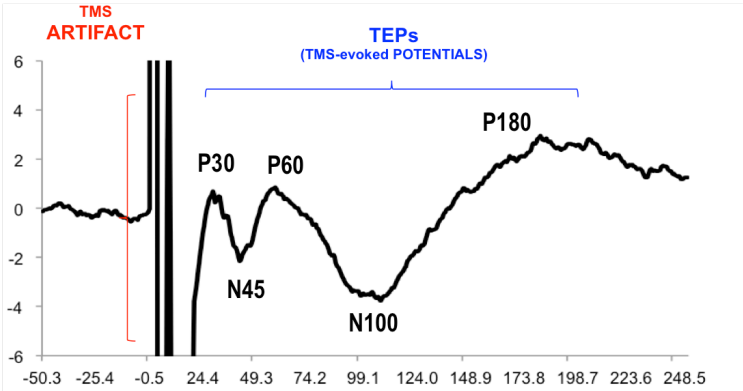

Figure 2.2 TEPs waveform evoked from the stimulation of the primary motor cortex

The origin of TEPs is still a matter of debate even if there is a growing consensus in literature about their GABAergic origin. Specifically, early TEPs (before 50 ms after the TMS pulse) seem to be produced by the GABAa inhibitory post-synaptic potentials, whereas later TEPs are likely to have a GABAb-ergic origin. Recently, the

GABAergic origin of TEPs has been strongly supported by pharmacological studies (Premoli et al., 2014a, b; discussed in paragraph 2.1.1 of this section) and by rTMS studies (e.g. Casula et al., 2014; discussed in the second part of this thesis). Among the five peaks, the N100 is the most pronounced and reproducible, this potential is also the most studied and its origin seem to be strongly linked to inhibitory processes from a series of evidence: (1) the amplitude of the TMS-evoked N100 is strongly enhanced after ethanol consumption (Käkhönen and Wilenius, 2007); (2) its latency coincides with the inhibition peak of GABAb receptors (Davies et al., 1990; Deisz et al., 1999); (3) the N100 amplitude correlates with EMG GABAb-ergic inhibition measures such as CSP and LICI (Daskalakis et al., 2008; Fitzgerald et al., 2008); (4) its amplitude is selectively enhanced/reduced during a movement preparation/inhibition as revealed by study using motor tasks (Nikulin et al., 2003; Bender et al., 2005; Bonnard et al., 2009). The P30, N45, P60, N100 and P180 TEP pattern is strongly reproducible in the primary motor cortex, whereas in other areas it may vary in amplitude, latency and waveform (Kähkönen et al., 2005; Lioumis et al., 2009). The analysis of the TEPs over time, space, power and frequency gives several information on different cerebral dynamics: (1) reactivity, which is revealed by the response of a target area to a stimulus; (2) connectivity, which is revealed by the spread of the TMS-induced activity from the target area over connected regions; (3) plasticity, which is assessed by means of neuromodulatory effects of rTMS. The first published attempt to measure TMS-evoked brain responses was performed by Cracco and coworkers (Cracco et al., 1989). The authors recorded responses to TMS from the homologous area contralateral to the stimulation site with an onset latency of 9-12 ms. This study was the first attempt to examine cerebral connectivity by combining TMS and EEG. Three years later, the same research group used a cerebellar stimulation and recorded responses from the interaural line (Amassian et al., 1992). However, these early attempts were not replicated immediately, probably because of the various technical limitations. Indeed, voltage changes induced by the TMS pulse between scalp electrodes are several orders of magnitude larger than microvolt-level EEG signals (Virtanen et al., 1999). Such high voltage levels can lead to the saturation of a standard EEG amplifier, which can last for hundreds of milliseconds. The subsequent development of TMS-compatible multi-channel EEG recording systems allowed the measurement of instant and direct neuronal effects

of TMS from multiple scalp locations, which was impossible with previous technologies. The first study that used these systems was conducted by Ilmoniemi's group (1997). Technical and methodological aspects relative to these systems will be discussed in paragraph 2.3.

The potential of the concurrent use of TMS-EEG lies in the TMS capacity to non-invasively interfere with brain activity by modulating the voltage over the membranes of the cortical neurons, and in the EEG ability to measure the instantaneous cortical activation induced by TMS with a millisecond time scale, which is currently not possible with any other brain imaging method. Techniques such as PET, SPECT, and fMRI, in fact, are unable to detect the temporal sequence of increased cerebral activity with a sampling frequency similar to that of neural signal transmission because changes in blood flow and oxygenation take several seconds after changes in neuronal activity. On the other hand, EEG does not provide as accurate a spatial resolution as the other techniques do. The next section will address the nuts and the bolts of TMS-EEG coregistration, providing a detailed view of its characteristics and methodology.

2.1 Advantages of TMS-EEG coregistration

This section discusses the main advantages provided by the combined use of TMS and EEG regarding (1) the investigation of brain dynamics in terms of reactivity, connectivity and plasticity; and (2) the clarification of methodological aspects of transcranial stimulation.

2.1.1 TMS-EEG in the assessment of cerebral reactivity

Cerebral reactivity is the response of a brain area to a stimulation. Traditionally, TMS has been used to assess the reactivity of areas that produce a peripheral marker of central excitability when stimulated, namely the primary motor cortex and the primary visual cortex. When TMS is applied to the primary motor cortex, a muscle twitch is elicited, measurable with EMG. Similarly, when the primary visual cortex is stimulated, the subject may perceive a moving/flashing phosphene. Excluding these two regions, the other areas of the cortex are behaviourally silent

and their reactivity can be investigated only through the combined use of TMS and EEG or other neuroimaging techniques. In TMS-EEG studies, cortical reactivity is examined through the analysis of TEPs, in terms of latency, amplitude, scalp distribution, and waveform. These indices represent quantifiable markers of the neurophysiological state of the stimulated area (Miniussi and Thut, 2010). In particular, the study of how cortical response varies across different physiological states and/or cognitive conditions is a topic of central interest in literature. For example, different modulation of reactivity can be generated in comparing responses during a cognitive task and at rest (e.g., Thut et al., 2003) or in comparing different physiological states after a pharmacological treatment (e.g., Premoli et al., 2014a,b). One of the first reactivity studies has been provided by Komssi and colleagues (2004). The authors aimed to directly evaluate the TMS-evoked cortical responses progressively increasing the stimulation intensity. TMS was applied over the primary motor cortices of seven healthy volunteers at four intensities (60%, 80%, 100%, and 120% of MT). The results showed a similar distribution of the potentials for the four intensities, whereas an increment in response amplitude was observed with higher intensities. The evidence provided by the study offered interesting elucidations on the reactivity of motor cortex. First, TMS can evoke measurable brain activity even at subthreshold intensities (60% of motor threshold); second, the analysis of the relationship between the stimulus and response potentially offered insights into the state of activation of the brain. Another recent example of a reactivity study, using a pharmacological approach, has been provided by Premoli and coworkers (2014). These authors investigated the origin of the TEPs which are supposed to be produced by different GABAergic interneurons (Ferreri et al., 2011; Rogasch and Fitzgerald, 2013; Casula et al., 2014). Specifically, the authors tested the effect of different GABAa and GABAb agonist such as alprazolam, zolpidem (GABAa), diazepam and baclofen (GABAb) founding that alprazolam, zolpidem and diazepam produced an increase of the N45 potential (which is supposed to have a GABAa origin) whereas the baclofen had a strong effect on the N100 (which is supposed to have a GABAb origin) (fig. 2.3). The results provided by the authors supported the different GABAergic origin of the TEPs (Premoli et al., 2014).

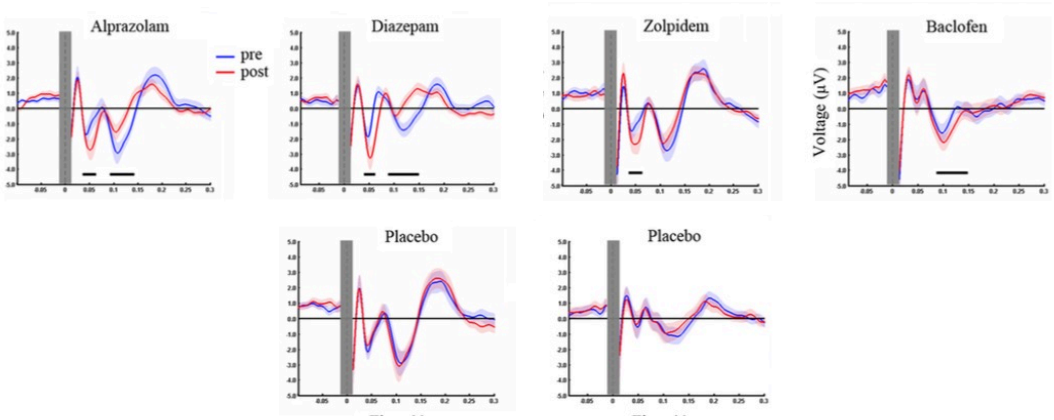

Figure 2.3 Modulation of TEPs induced by alprazolam, diazepam, zolpidem, baclofen (above) and by placebo drugs (below). TEPs were recorded before (pre, blue) and after the drug intake (post, red). Whereas alprazolam increased the N45 and reduced the N100 amplitude, zolpidem increased the N45 only. Diazepam increased the N45 and decreased the N100 similarly to alprazolam, whereas baclofen increased the N100. Black bars underneath represent significant drug-induced changes in TEPs.

From a technical point of view, another interesting example has been provided by Lioumis and coworkers (2009). In this study, the authors aimed to investigate the responses to TMS of the left primary motor cortex and the prefrontal cortex in a test-retest design. TMS was applied at three intensities in two sessions with a 1-week interval between them. Accurate repositioning of the coil was guaranteed by a neuronavigation system. The results showed high reproducibility in cortical responses after the two TMS sessions, providing evidence of the reliability of TMS-EEG investigation of cortical excitability changes in test-retest designs.

2.1.2 TMS-EEG in the assessment of cerebral connectivity

Connectivity studies with traditional TMS-EMG setup were limited to the investigation of motor-associated area interaction (i.e., with "twin-coil" stimulation – see paragraph 2.3.2.1). With the development of TMS-compatible multi-channel EEG, the study of connectivity in non-motor areas has become possible. In TMS-EEG coregistration studies, cerebral connectivity is evaluated by tracing the spread of TMS-evoked activity by reconstructing the activity-sources and/or based on the latency of EEG deflections. The first procedure is realised through a brain source analysis, which localises the source of the electric signals. The first study that successfully applied this procedure was performed by Ilmoniemi's group (Ilmoniemi

et al., 1997). These authors applied TMS at a 0.8 Hz frequency over the primary motor and the visual cortex of healthy volunteers. The spread of the TMS-evoked activity was traced using inversion algorithms that localised an immediate response locally to the stimulation. They observed that 5-10 ms after the magnetic pulse, the activation spread to the adjacent ipsilateral motor areas; furthermore, after 20 ms, activation reached the homologous regions in the opposite hemisphere (fig. 2.4).

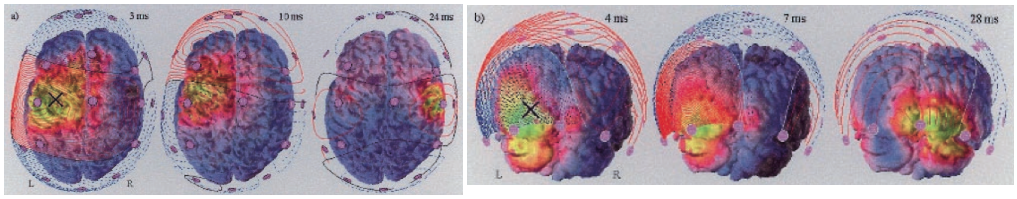

Figure 2.4 Spreading of TMS-induced cerebral activity after primary motor cortex stimulation (left) at 3, 13 and 24 ms; and after primary visual cortex stimulation at 4, 7 and 28 ms (adapted from Ilmoniemi et al., 1997)

This activation pattern was observed stimulating both areas. The study by Ilmoniemi and colleagues was the first that provided direct information about cortico-cortical connections through the use of TMS-EEG coregistration. In recent years, many other research studies have confirmed the results obtained by these authors, also providing important insights into the study of the spread dynamics of TMS-induced activity (e.g., Kähkönen et al., 2001; Massimini et al., 2005).

The analysis of the latencies of scalp-recorded EEG deflections offered a different approach in the investigation of cortico-cortical connectivity. The high temporal resolution of EEG allows the reliable identification of the temporal progress of TMS-evoked activity spread. This permits researchers to infer the causal relations of the TMS-evoked activation. An example of this procedure was provided by Iramina and colleagues (Iramina et al., 2003). The authors applied TMS at three different intensities (90%, 100%, and 110% of MT) over the cerebellum (20 mm above the inion) and recorded frontal positive potential deflections at Cz with a latency of 9 ms and at Fz with a latency of 10 ms. The results obtained by the authors offered a possible demonstration of occipito-frontal connectivity and, on the other hand, provided evidence of the reliability of TMS-EEG coregistration as a precise methodology in connectivity studies. To this end, a further demonstration of TMS-EEG feasibility has been obtained by examining changes in the spread of TMS-

evoked activity while placing the coil over different sites. Komssi and coworkers stimulated five sites in the left sensorimotor cortex of six healthy volunteers while they monitored responses throughout the brain (Komssi et al., 2002). To ensure the precise localisation of the anatomic locus of stimulation the authors used a frameless stereotactic method. A consistent pattern of response both ipsilaterally and contralaterally was recorded with a latency of 17-28 ms. More important, contralateral responses showed consistent changes when different loci were stimulated. Two conclusions may be drawn from these data. First, the importance of coil positioning is critical since even a small shift in its position caused a different response. Second, the precise recording of ipsi- and contralateral responses revealed a corresponding high spatiotemporal resolution of TMS-EEG methodology in detecting the spread dynamics of TMS-evoked activity.

2.1.3 TMS-EEG in the assessment of cerebral plasticity

As described in paragraph 2.3.3 of the first chapter of this thesis, when TMS is applied in train of pulses (i.e. rTMS), it is able to induce long-term changes in brain excitability. The mechanism through which rTMS produces cerebral plasticity is thought to be an LTP/LTD-like mechanism (Ridding and Rothwell, 2007) even if direct evidence has not been provided yet, given that MEPs are an indirect measure of cortical excitability which is also affected by the spinal cord. It must be also taken in consideration that with traditional TMS-EMG setups, the investigation of cerebral plasticity processes is limited to the primary motor cortex. This is a critical point since most of the clinical protocols of rTMS have been applied to the dorso-lateral prefrontal cortex (e.g. psychiatric disorders). In this regard, the concurrent use of EEG and TMS have a potential in clarifying the plasticity mechanism of rTMS by analysing the EEG response to TMS before, after and during a plasticity protocol with low-frequency rTMS (e.g. Van der Werf et al., 2006); high-frequency rTMS (e.g. Esser et al., 2006); TBS (e.g. Vernet et al., 2013); PAS (Veniero et al., 2013); transcranial direct current stimulation (tDCS; e.g. Pellicciari et al., 2013) or transcranial alternating current stimulation (tACS; e.g. Helfrich et al., 2014). As mentioned before, one of the main advantages in investigating the plasticity effects of transcranial stimulation by means of concurrent TMS-EEG is the direct evaluation

of the LTP/LTD-like mechanisms that are supposed to produce the long-term effects of the stimulation. In this regard, Esser and coworkers (2006) tried to obtain a direct measure of LTP in healthy volunteers induced by 5-Hz rTMS applied for 5 minutes over the primary motor cortex during high-definition EEG (60 channels). The authors found a significant potentiation of specific TMS-evoked EEG responses, as assessed by the global mean field power (GMFP). The topographic and the brain source analysis showed that this potentiation was located over the premotor cortex, bilaterally. Along the same lines, Veniero and colleagues (2013) investigated the plasticity mechanism of a cortico-cortical PAS protocol. The authors applied a PAS protocol to the primary motor cortex and the posterior parietal cortex with an ISI of 5 ms. They found a change in TEPs amplitude accordingly to the occurrence of LTD or LTP, assessed by MEPs modulation. In addition, a strong increase in oscillatory coherence between the two stimulated areas has been found: when an LTD was observed, the coherence was increased in the alpha band; when an LTP was observed, the coherence increased within the beta band. In another recent study of Vernet and colleagues (2013) the plasticity mechanism induced by cTBS has been studied over the primary motor cortex. The authors found specific effects of cTBS on cerebral oscillations, specifically cTBS increased the power in the theta band of eyes-closed resting EEG, whereas it decreased the power of theta and alpha bands induced by single pulse TMS. Basing on these results, the authors proposed an explanation of the plasticity mechanism of cTBS in terms of modulation of the phase alignment between active oscillators (Vernet et al., 2013). The neuromodulatory mechanism of tDCS has been also investigated. In a study by Pellicciari and colleagues (2013) concurrent TMS-EEG was applied before and after different stimulation protocols. The authors found a reduction of motor cortex excitability after cathodal stimulation, as assessed by a MEPs reduction, which was also confirmed by a reduction of the local cortical activity TMS-induced, assessed by LMFP. On the other hand, following anodal stimulation an increase in motor excitability was observed (i.e. enhancement of MEPs amplitude) as well as an increase in the local cortical activity TMS-induced (Pellicciari et al., 2013). This study is one of the first direct examples of the effect of tDCS on cortical excitability.

2.2 Methodological approaches

As suggested by Miniussi and Thut (2010), TMS-EEG applications can be grouped into three approaches: inductive, interactive, and rhythmic. Within the "inductive approach" TMS-EEG coregistration is used to provide insights into the neurophysiological state of the brain through TEP analysis across different conditions. The "interactive approach" aimed to investigate the temporal course and the spatial spread of TMS-induced activity during a cognitive performance. Finally, in the "rhythmic approach", TMS is used as a technique to interact with oscillatory brain activity.

2.2.1 TMS-EEG: the inductive approach

From an inductive approach perspective, TEPs are considered an index of the cerebral neurophysiological state in areas that does not produce a peripheral marker in response to a TMS pulse. TEP analysis has useful application in clinical and research studies as well as in technical studies. As discussed above, cortical responses evoked by TMS potentially offer important insights into brain activity both locally, in the stimulated area, and in connected regions. More specifically, the inductive approach aims to infer brain activity dynamics focusing on TEP characteristics and distribution (e.g., Ilmoniemi et al., 1997; Komssi et al., 2002) without considering behavioural outcomes (which are more relevant in interactive approach studies). Indeed, inductive studies are more interested in comparing conditions generated from different neurophysiological states of the brain (e.g., Käkhönen et al., 2001; Massimini et al., 2005). An interesting example of this approach has been provided by Massimini and colleagues, who aimed to investigate connectivity changes across different states of consciousness (Massimini et al., 2005). The authors applied TMS at a subthreshold intensity (90% of MT) over the rostral portion of the right premotor cortex of six healthy volunteers. The results revealed a critical difference in the spread of TMS-evoked activity between the state of wakefulness and non-REM sleep (fig. 2.5). A prominent spread of the activity from the stimulation site to ipsi- and contralateral areas was observed during quiet wakefulness. In contrast, during non-REM sleep, the authors observed a rapid decrease in the initial response that did not spread beyond the stimulation site.

Thus, the authors concluded that states of consciousness are strictly related to cerebral connectivity efficiency.

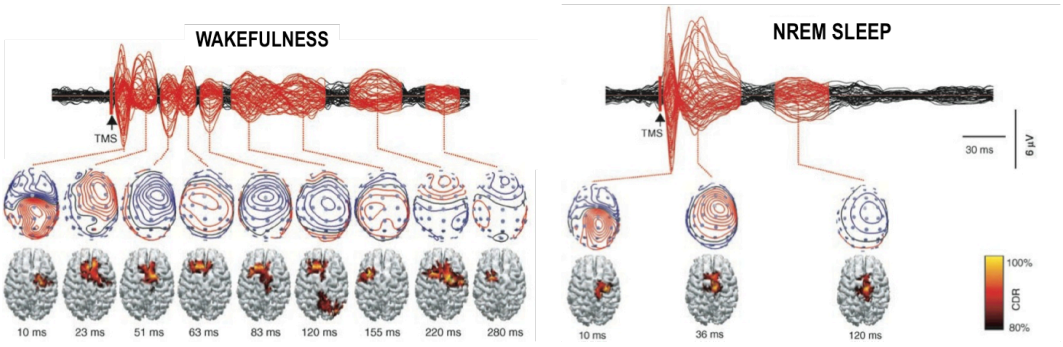

Figure 2.5 Spreading of TMS-induced cerebral activity after premotor cortex stimulation during wakefulness (left) and during non-REM sleep (adapted from Massimini et al., 2005)

The data provided by this study are a direct exemplification of TEP's potential in revealing important information on the local and distant spread dynamics of cerebral activity. Regarding technical applications, TEP analysis in combination with a systematic and methodical manipulation of TMS parameters can potentially provide important information on which parameters (e.g., stimulation intensity, coil orientation) are the most effective in producing a certain neuronal modulation. As seen previously in this chapter, the studies by Komssi and colleagues (2002; 2004) provided direct evaluation of the effects of stimulation intensity and coil positioning. Another example of this approach has been provided by Bonato and colleagues (2006). The authors applied TMS over the left primary motor cortex of six healthy volunteers, varying the coil orientation. Two orientations were compared: one at 45 degrees with respect to the sagittal plane (which was found to be optimal by previous studies – Mills et al., 1992; Brasil-Neto et al., 1992) and one at 135 degrees with respect to the sagittal plane. The authors found that the two orientations evoked a similar pattern of electric potentials but with different amplitudes. From a technical point of view, TMS-EEG can thus provide useful insights into the comprehension of the unclear neurophysiological correlates of the TMS parameters. Future research studies investigating the effects of other TMS parameters might provide important contributions regarding the real outcomes of TMS on brain tissue.

2.2.2 TMS-EEG: the interactive approach

The TMS-EEG interactive approach aims to investigate "where, when and how TMS interacts with task performance" (Miniussi and Thut, 2010, p. 252). Therefore, interactive approach studies are particularly relevant in cognitive neuroscience research since they aim to study how the effects of TMS correlate with behaviour. More specifically, this approach focuses on the precise determination of which areas are affected by the pulse (i.e., "where") during cognitive performance; the definition of the cognitive process timing course, which is the critical temporal interval in which TMS affects cognition (i.e., "when"); and, finally, the clarification of the TMS effect in terms of the facilitation or inhibition of task performance (i.e., "how"). One example of this approach was offered by a study from Taylor and coworkers (Taylor et al., 2006). The authors aimed to investigate a frontal-parietal network interaction during a spatial attention task. TMS was applied in short trains of 5 pulses at a frequency of 10 Hz over the right frontal eye field (FEF). When rTMS was delivered during the cueing period, the authors found that the neural activity evoked by visual stimuli was significantly affected (fig. 2.6).

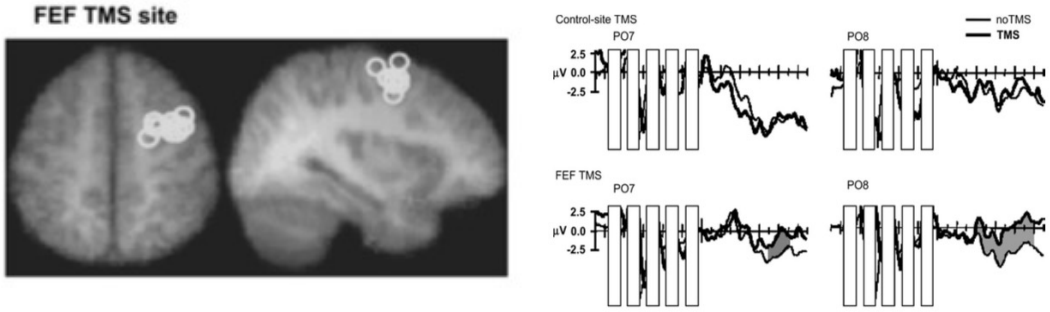

Figure 2.6 Effects of TMS over frontal eye fields (left). When TMS was delivered over the frontal eye fields is shown to affect the normal attentional modulation of the ERP recorded from the visual cortex (left, panel below) (adapted from Taylor et al., 2006)

In another study, the same group of research (Taylor et al., 2007) applied a similar rTMS protocol (3 pulses at 10Hz) over the dorso-medial frontal cortex to test its role in conflict resolution through an Eriksen flanker task (Eriksen and Eriksen, 1974). The results show that when contralateral (right-hand) incongruent trials occurred, TMS disrupted performance by increasing error rates. Both the results of these studies offered clear anatomo-functional contributions to FEF (Taylor et al., 2006) and to dorso-medial frontal cortex (Taylor et al., 2007). Moreover, they provided

interesting data on TMS focality since in both studies no effects were observed after the stimulation of a control site that was physically closer to the target areas. In summary, this evidence offers a demonstration of the value of TMS-EEG coregistration as a reliable technique in the study of TMS effects during cognitive tasks with high temporal and spatial resolution. Another study applying concurrent TMS-EEG in cognition has been conducted by Mattavelli and colleagues (2013). These authors used concurrent TMS-EEG to investigate the global and local cortical excitability at rest and during two different face processing behavioural tasks. TMS was delivered over the medial prefrontal cortex during the processing of face expressions or identities. The authors found that TMS reduced the P1-N1 component recorded from occipital electrodes and a modulation of early TEPs (< 30 ms) of temporal and occipital electrodes after prefrontal stimulation. This study provided a direct evidence of the early influence of the prefrontal cortex to the occipital cortex in face processing, during which the excitability of right fronto-temporal regions is significantly modulated (Mattavelli et al., 2013).

2.2.3 TMS-EEG: the rhythmic approach

In the last years magnetic and electric transcranial stimulation has been used to interact and to induce an entrainment of brain oscillations in a frequency-specific manner (Brignani et al., 2008; Thut and Miniussi, 2009). This approach, known as rhythmic approach, represents one of the most promising avenues for studying the impact of oscillatory activity in cognition (e.g. Romei et al., 2008), corticospinal excitability (e.g. Sauseng et al., 2009), cortical connectivity (e.g. Veniero et al., 2013) and in clarifying the neuromodulatory mechanism of TMS (e.g. Vernet et al., 2013) and tACS (e.g. Helfrich et al., 2014). An example of this approach has been offered by Sauseng and colleagues (2009). The authors of the study aimed to investigate the relation between 10 Hz oscillatory activity and cortical excitability. To address this question they applied TMS to the primary motor cortex of six healthy volunteers. Their results showed that when the pre-stimulation level of alpha power was low, an MEP was evoked more easily, and vice versa. Moreover, this effect occurred only at the stimulation site. The results of the study offered insight into the relation between motor cortex excitability and local alpha oscillations (Sauseng et al., 2009).

Differently, other studies have focused on the capacity of rTMS to induce a pattern of oscillatory activity. Brignani and colleagues, for example, investigated the effects of low-frequency rTMS on the EEG oscillatory activity (Brignani et al., 2008). The authors applied rTMS at a 1 Hz frequency over the primary motor cortex of six healthy volunteers. The results showed an increase in the alpha band related to the period of the stimulation. These data confirm the TMS capacity to induce a synchronisation of the background oscillatory activity locally to the stimulation site. The possibility to interact with brain oscillations trough TMS have also a value in the cognitive domain. Specifically, the effects of a TMS-induced entrainment in a specific frequency of oscillation during the performance of a cognitive task, open the possibility to establish a direct link between brain rhythms and cognition. Some studies have explored this possibility. In a study by Klimesch and coworkers (2003), for example, the authors applied rTMS at individual alpha frequency (IAF) to influence the dynamics of alpha desynchronisation leading to an improvement of cognitive performance. Repetitive TMS was delivered over the mesial frontal cortex (Fz) and the right parietal cortex (P6) while subjects performed a mental rotation task. The results confirmed the authors' hypothesis: rTMS improved task performance by enhancing the extent of alpha desynchronisation (fig. 2.7). This study, besides providing evidence of the rTMS capacity to interact with cerebral rhythms, also demonstrated the functional relevance of oscillatory neuronal activity in the alpha band during cognitive processing.

Recently, more studies have investigated a possible relation between alpha oscillations and cognition. In particular, recent research studies using visual tasks identified a relation between the occipito-parietal alpha amplitude and the perception of visual stimuli (e.g., Romei et al., 2008). TMS effects on cerebral oscillations have also been used to investigate connectivity and plasticity dynamics. In a study by Veniero and colleagues (2013), for example, it has been found a strong increase of oscillations coherence between the primary motor cortex and posterior parietal cortex, after these areas were stimulated with PAS. The results proved that PAS effects are associated with an increase in connectivity between two connected areas (Veniero et al., 2013).

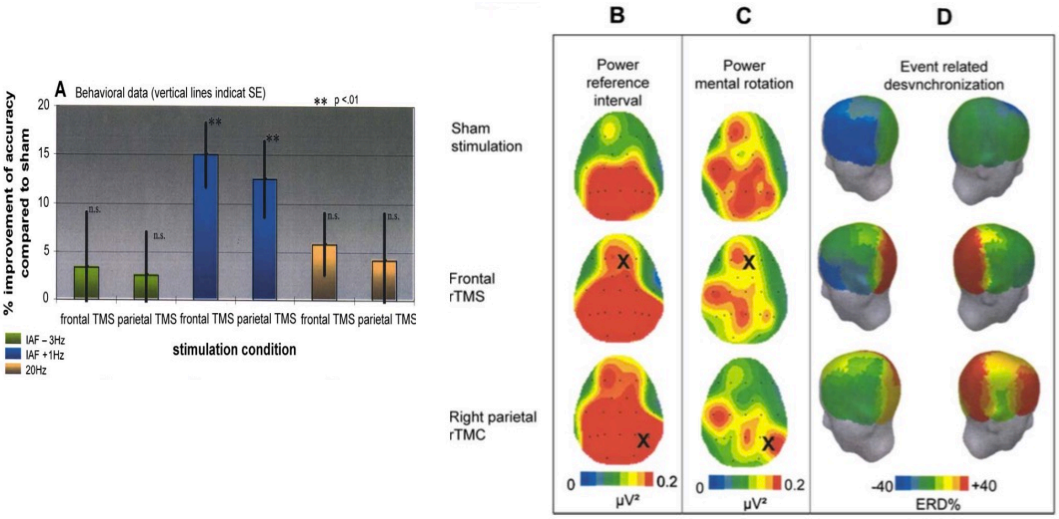

Figure 2.7 the rTMS induced improvement of accuracy of mental rotation is significant for individual alpha frequency (IAF) 1 Hz only (left, blue bars). The influence of rTMS at individual upper alpha frequency (right). An increase in power during reference interval is observable, whereas a decrease is observable during the mental rotation task (adapted from Klimesch et al., 2003)

Along the same lines, rhythmic effects of TMS have been recently used to hypothesize the mechanisms underlying the plasticity effects of TBS. For example, Vernet and colleagues (2013), basing on the effects of cTBS on cerebral oscillations, proposed two possible mechanisms of cTBS: the first one implies that cTBS modulates the number of active oscillators without modifying the percentage of synchronization between active oscillators, the second mechanism implies that cTBS modulates the percentage of synchronization between active oscillators without modifying the number of active oscillators (Vernet et al., 2013; fig. 2.8).

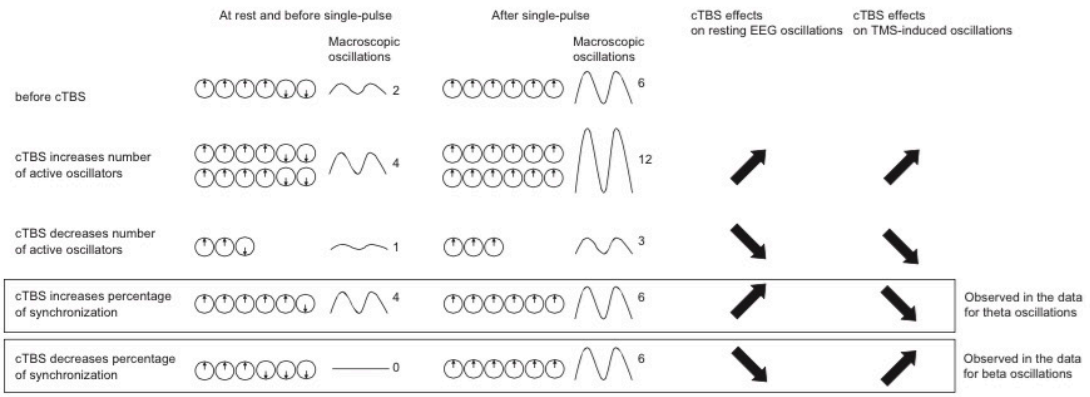

Figure 2.8 Schematic representation of the hypothetical effects of cTBS on neural oscillators (adapted from Vernet et al., 2013)

Finally, new fascinating perspectives are rising about the possibility to induce neuronal entrainment with transcranial electric stimulation. In particular tACS seems an effective method to non-invasively modulate the cortical oscillation in specific band of frequencies (Herrmann et al., 2013). In a recent study conducted by Helfrich and colleagues (2014), simultaneously 10-Hz tACS and EEG have been applied to the parieto-occipital cortex to study neuronal entrainment during stimulation. Results showed an increase of parieto-occipital alpha activity and a synchronization of cortical oscillators with similar intrinsic frequencies to the entrainment frequency after 10-Hz tACS. Additionally, the authors showed a tACS specific modulation of the target detection performance in a phase-dependent fashion highlighting the causal role of alpha oscillations for visual perception.

2.3 Technical issues in TMS-EEG coregistration

The simultaneous use of TMS and EEG, like the other TMS-neuroimaging combinations, poses several technical issues due to artefacts of different nature. In this part of the chapter, the technical problems concerning the combined use of TMS and EEG will be discussed. The aim is to review the strategies developed so far to obtain a reliable EEG recording during TMS. As mentioned above, the main problem of this approach is caused by the high TMS-induced electrical field, which can saturate recording EEG amplifiers.

A great portion of the studies that have analysed the EEG response to TMS have focused on the cortical response evoked by a single pulse on the primary motor cortex at rest (e.g., Komssi et al., 2002; Lioumis et al., 2009; Massimini et al., 2005; Bonato et al., 2006; Paus et al., 2001; Bender et al., 2005; Ferreri et al., 2011). The TEPs detected in most of these studies are: N15, P30, N45, N100, P180, and N280. The large number of studies that observed this pattern of TEPs demonstrated the high reproducibility of TMS-evoked deflections, contrary to motor-evoked potentials, whose amplitude is highly variable (Kiers et al., 1993). The N100 is the most evident, pronounced, and reproducible component evoked by TMS over the motor cortex (e.g., Lioumis et al., 2009; Massimini et al., 2005; Paus et al., 2001; Bender et al., 2005; Nikulin et al., 2003;]). On the other hand, the occurrence of the other components can vary depending on TMS-related factors (e.g., coil positioning

or orientation – Komssi et al., 2002; Bonato et al., 2006) as well as subjective-related factors (e.g., state of the cortex and state of consciousness – Nikulin et al., 2003; Massimini et al., 2005). Different TMS parameters, for example, can determine a temporal shift in the potentials, even of a few milliseconds (e.g., Bonato et al., 2006; Ferreri et al., 2011). Currently, the origin of TEPs is still unknown with the exception of the N45 component, which has been localised in the central sulcus (ipsilateral to the stimulation) and whose amplitude is directly related to the stimulus intensity (Paus et al., 2001). Interestingly, most of the studies mentioned above were unable to detect cortical responses before 10-15 ms from the TMS pulse onset or even later. This latency period that precedes TEP recording is due to the high voltages induced by the TMS pulse between scalp electrodes. These currents can cause saturation of the amplifier, which might last hundreds of milliseconds before the system resumes working appropriately. Thus, all attempts to apply TMS during an EEG recording have faced these technical issues. In recent years, the development of new technologies and solutions has gradually led to an improvement of the temporal resolution of EEG recording during TMS. Such strategies can be divided in two types: on-line strategies, which consists of the creation of technologies that are able to avoid saturating the EEG amplifiers during TMS (e.g., Virtanen et al., 1999) and off-line strategies, which aim to remove artefacts once the recording is completed (e.g., Thut et al., 2003; Litvak et al., 2007).

2.3.1 TMS-EEG artefacts: on-line solutions

In 1997, TMS-compatible multi-channel EEG systems were introduced, allowing the instantaneous measurement of TMS effect on brain activity from multiple scalp locations. The 60-channel EEG system developed by Virtanen and colleagues (1999), guaranteed the simultaneous recording with TMS through the use of gain-control and sample-and-hold circuits, which permits the locking of EEG signals for several milliseconds (i.e., "gating period") immediately after the TMS pulse (fig. 2.9). This technology avoids the saturation of the recording by preventing the passage of the strong electromagnetic field along the amplifier circuits. This blocking system is controlled by an external trigger, which is activated about 50 μs before the TMS pulse and is released 2.5 ms after the pulse.

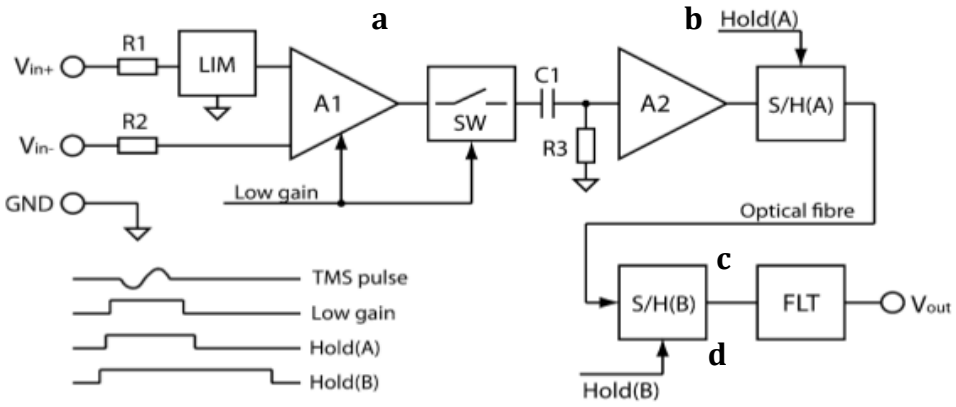

Figure 2.9 Schematic representation of the TMS-compatible EEG system developed by Virtanen et al., 1999 capable of recording the EEG responses to single TMS pulses after just a few milliseconds

In the study performed by Virtanen group in 1999, the authors successfully recorded EEG responses while TMS was applied over FCz with an intensity of 100% and 120% of MT and a frequency of 1 Hz. In spite of the novelty value of this system, some problems remained unsolved. For instance, the gating period lasts much longer than the TMS pulse itself, which lasts only about 300 μs. This did not allow the recording of the signal immediately after the stimulation. Other TMS-compatible EEG amplifiers have been developed recently. In 2003, Iramina and colleagues (2003) developed a 64-channel system based on a sample-and-hold circuit and were able to measure EEG activities 5 ms after the TMS pulse onset. Another system developed by Thut and coworkers (2003) was based on a slew-rate limiter: this technology allowed continuous recording and prevented saturation during TMS. Nowadays, new TMS-compatible EEG systems are able to avoid saturation due to TMS pulse, which results in a very short-duration artefact. This feature permits continuous EEG recording during TMS, allowing researchers to see what happens in the EEG signal around the TMS pulse. Bonato and colleagues (2006), for example, used TMS-compatible DC amplifiers that were able to tolerate the high time-varying magnetic field induced by TMS. This characteristic allowed the recording of cortical response to TMS with high temporal and spatial resolution. In spite of the high temporal resolution recording provided by these new systems, some technical questions remain unsolved. For instance, it is still difficult to distinguish between the cortical and non-cortical (i.e., magnetic) currents that characterise at least the

early part of the response after TMS (Veniero et al., 2009). All these considerations reflect the relevance that artefact investigation still has in the literature in order to discriminate artefactual activity from physiological responses.

2.3.2 TMS-EEG artifacts: off-line solutions

Off-line strategies, unlike on-line ones, aim at removing the artefact only after the complete acquisition of the TMS-EEG recordings. This aim is achieved through the use of software solutions (i.e., algorithms, off-line filters) or experimental procedures. Off-line strategies have been developed recently: the first work that used a similar approach was performed by Thut and colleagues (2003 - see below). Two main approaches can be distinguished: a subtractive approach and a correctional approach. Both procedures although based on different logics aim to correct, reduce, or remove the TMS-induced electromagnetic artefact. In the subtractive approach, a template artefact is generated by delivering stimulation in a control condition (e.g., Thut et al., 2003) or applying TMS over a phantom (e.g., Bender et al., 2005). The subtraction of the template artefact from experimental data permits the isolation of the target response. The studies of Thut and colleagues (2003; 2005), as mentioned above, were the first to use a subtractive approach that aimed to isolate cortical responses related to a visual task (VEPs). To this end, they created a control condition in which TMS pulses were delivered at rest. This procedure permits the isolation of the only artefact without task-related responses. This condition was then subtracted from the visual task condition to isolate only the task-related TEPs. A similar procedure was followed by Bender and coworkers (2005), who aimed to investigate the influences of cerebral maturation on TMS-evoked N100. The authors used a glass head dummy covered by a cloth soaked with water (simulating the impedances of skull and scalp) to generate a template artefact. The study of only the N100 component was permitted by subtracting phantom artefacts from human-evoked potentials.

The correctional approach comprises all procedures aimed at reducing or removing artefacts through the use of algorithms and off-line filters. These procedures are more common in technical studies, often performed by biomedical and computer engineers. Morbidi and colleagues (2007), for example, proposed an

off-line Kalman filter as a new effective and low-cost strategy for artefact reduction. The solution proposed by the author allowed the modelling of the dynamic components of TMS-EEG signal through the use of time-varying covariance matrices. The authors compared the dynamic Kalman filter with stationary filters such as the Wiener filter, concluding that the first one guarantees a more efficient deletion of TMS-induced artefacts while preserving the integrity of EEG signals around TMS pulses. Another example of artefact correction via software was performed by Litvak and colleagues (2007). The authors used a method developed by Berg and Scherg (1994), originally applied for ocular artefact correction, based on a multiple-source approach (fig. 2.10).

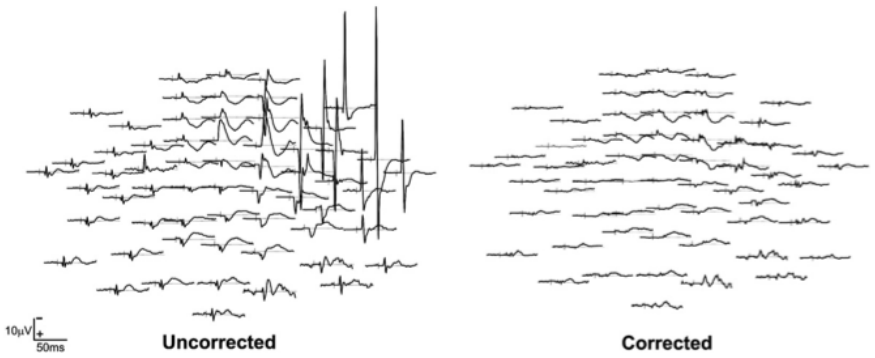

Figure 2.10 TEPs waveform before (left) and after (right) artifact off-line correction (adapted from Litvak et al., 2007)

Using a set of artefact topographies, the authors constructed a source model and a set of brain topographies that consisted of multiple dipoles that model brain activity. From this source model a linear inverse operator was computed that decomposed the data into a linear combination of brain and artefact activities, which were subtracted from the data. The results showed that the modelled brain activity was not altered after the correction process. In summary, off-line procedures also potentially offer a wide range of possible solutions to clean EEG recordings from TMS artefacts. Nevertheless, since this approach is still in an early stage, other research studies are needed to develop and improve new ad hoc strategies that provide an optimal dissociation between cortical and artefactual TMS-related activity.

2.3.3 TMS-EEG artifacts: equipment-related aspects

Besides the relevance of the aspects just discussed, many other factors play an important role in providing a reliable signal-to-noise EEG with concurrent TMS. These aspects are mainly referable to TMS (e.g., parameters of stimulation, stimulator devices) and to EEG setup (e.g., electrodes, wires, cap). Recently, several research studies have investigated the effect of specific TMS parameters, such as TMS frequency, intensity, waveform (e.g., Veniero et al., 2009), ISI (e.g., Ferreri et al., 2011), or coil orientation (e.g., Bonato et al., 2006) on the TMS-induced artefact. In their study, Veniero and colleagues (2009) manipulated several TMS parameters to observe their effect in the electromagnetic artefact amplitude and latency. The authors compared three TMS devices (two biphasic and one monophasic), four types of figure-of-eight coils, ten intensities (from 10% to 100% of the maximum output), three frequencies (spTMS; rTMS at 5 Hz; rTMS at 20 Hz), and two sham conditions (i.e., performed with a placebo coil and with a real coil turned over). Furthermore, EEG artefact generated by TMS delivered over the scalp was compared to the EEG artefact generated by TMS over two phantoms (i.e., a melon and a human knee). The authors found that the artefact produced by the magnetic pulse lasted approximately 5 ms after TMS onset in all conditions. Its duration, therefore, was not affected by different parameters of stimulation. In contrast, the artefact amplitude was higher when evoked by a monophasic pulse compared to a biphasic one (fig. 2.11).

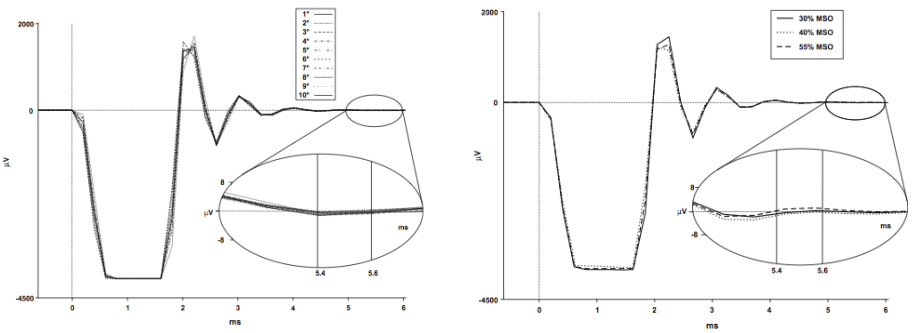

Figure 2.11 TMS-induced artifact amplitude: effect of the frequency (left) and of the intensity of stimulation (right) (adapted from Veniero et al., 2009)

Other studies that manipulated the TMS ISI and coil orientation did not find a prominent effect of these parameters on cortical response except for minor

variations in the latency of some components (Bonato et al., 2006; Ferreri et al., 2011).

Regarding EEG-related factors, the electrode type is one of the most influential variables in performing an efficient TMS-EEG coregistration. Because of the strong electric field generated by TMS, an electrode suitable for TMS-EEG coregistration should satisfy numerous physical requirements to work appropriately. Small dimensions are necessary, first to prevent the forces caused by the induced currents from affecting the electrode too much, and second to avoid overheating. Moreover, to provide the best interface with the skin, it should be coated with a suitable surface material. For these reasons, traditional electrodes (made of silver or tin and with a diameter of ~1 cm) are not suitable for concurrent TMS since they are more affected by the induced currents. This can result in both a larger artefact and a higher risk of skin burns (Roth et al., 1992; Wassermann et al., 1998; Tallgreen et al., 2005). Additional problems can result from electrode polarisation, caused by electric currents between the electrolyte and the electrode. When an electrode is polarised, the artefact might cause an EEG baseline shift that can last for hundreds of milliseconds. Currently, the most frequently used electrodes in TMS-EEG systems are small Ag/AgCl pellet electrodes. These characteristics, other than reducing temperature by more than 50%, permit excellent recording during TMS (Ives et al., 2006). Another technical aspect that influences the artefact amplitude is electrode impedance which has to be kept at low values (generally below 5 kΩ). High values of impedance in fact can lead to greater artefacts (Ilmoniemi and Kičić, 2010). Generally, low values of electrode impedance are reached with skin scrubbing and cleaning with alcohol or ad-hoc products, and several strategies may be implemented to achieve this result. A study conducted by Julkunen and colleagues (2008), for example, found a significant reduction of TMS-induced artefacts after puncturing the epithelium under the electrode contacts with custom-made needles. Finally, recent studies have observed that the electrode wire arrangement can also play an important role in reducing TMS-evoked artefacts (e.g., Veniero et al., 2009; Sekiguchi et al., 2011). Sekiguchi and coworkers (2012), in particular, tested the effect of coil direction relative to the orientation of the stimulated electrode wire. The authors observed a great reduction in the artefact amplitude when the coil was placed perpendicularly to the wire direction of the

stimulated electrode. Their results suggested that the rearrangement of the lead wires relative to the fixed coil orientation can significantly reduce TMS artefacts from EEG recordings.

Besides the electric effect on the brain, TMS application can affect EEG recording also as a result of multimodal sensory stimulation. A TMS pulse, in fact, has multiple "indirect" effects; for instance, it produces a "click" of 100-120 dB (Starcks et al., 1996) that elicits an auditory response which, in turn, might produce a startle reflex that can affect behavioural data, especially in reaction time detection (Terao et al., 1997). Furthermore, there is evidence of auditory and sensorial-evoked potentials related to the TMS click that should be considered and controlled for, especially in the electrophysiological analysis of TMS evoked-potentials. A solution to avoid this problem is using earplugs or masking the coil click with white noise (Nikouline et al., 1999; Tiitinen et al., 1999) or a sound with a similar spectral content (Massimini et al., 2005). Alternatively, if the experimental design does not allow the use of earplugs, some authors have created a control condition to isolate and exclude the auditory artefacts (e.g., Bender et al., 2005). Finally, TMS-elicited muscle activity (e.g., involuntary stimulation of a facial nerve; Korhonen et al., 2011), eye blinks (Bruckmann et al., 2012) or electrode movement that can also be source of artefacts during EEG recording. In these cases only slight modifications of the setting can improve the record, for instance by reorienting the coil, reducing the intensity, or trying to avoid direct contact of the coil with the recording electrodes (Mutanen et al., 2013; Rogasch et al., 2014).

3. SIMULTANEOUS USE OF TMS AND OTHER NEUROIMAGING TECHNIQUES

3.1 TMS-MRI coregistration

Magnetic resonance imaging (MRI) is an imaging technique based on the properties of the atomic nuclei of biological tissues. This technique measures their spin precession within a strong magnetic field induced by the MRI scanner. More specifically, the MRI-induced magnetic field causes an alignment of some atomic nuclei in the body parallel to the magnetic field itself. The radio frequency fields subsequently applied systematically perturb the alignment of the magnetised nuclei in a predictable direction. The rotating magnetic field produced by the nuclei is

detectable by the MRI scanner, which records this information to construct an image of the scanned area. The images generated by an MRI scanner have a high spatial resolution of a few millimetres and provide detailed structural information on brain anatomy. However, since this method provides only static information, only a few research studies have focused on the simultaneous use of TMS and MRI. Most of the studies acquired TMS and structural data separately in time (i.e., by the off-line approach), avoiding most of the technical problems that characterise on-line coregistration.

The main technical problem in performing simultaneous TMS-MRI coregistration lies in the presence of the coil within the MRI scanner since it is made of ferromagnetic material. New MRI-compatible coils are suitable for concurrent MRI and fMRI since they are not made of magnetic material. The first study that used this kind of coil was performed by Bohning and colleagues (1997). The authors measured the magnetic field generated by TMS in healthy human brains using a standard 1.5 T MRI scanner. Specifically, they obtained 3D maps of the magnetic field created by two TMS coils.

The combined use of TMS and MRI can have useful applications for both research and clinical purposes. Since TMS, as stated above, provides precious insights into the physiological state of brain regions, such information, if appropriately combined with detailed images provided by an MRI scanner, might reveal important correlations between physiological indices (e.g., cortical reactivity and connectivity) and structural measures. An example of this kind of study was provided by Boorman and coworkers (2007). The authors investigated the relationship between a physiological measure of functional connectivity and a measure of structural connectivity during the execution of a decision-making test. Functional connectivity was investigated (i.e., through a twin-coil approach – see paragraph 2.3.2.1 of chapter I) by applying TMS over the dorsal premotor cortex and the primary motor cortex. The structural anatomic network, linking the brain regions involved in the task, was reconstructed using diffusion-weighted imaging (DWI). The results of the study revealed a relationship between individual differences in functional and structural connectivity in action choice-related brain networks. The potential contribution of TMS-MRI combined use in revealing possible correlations between physiological data (i.e., provided by TMS) and

structural data (i.e., provided by MRI) is also evident in clinical studies. A study by Sach and colleagues, for example, used TMS capacity to non-invasively investigate the central-motor conduction in relation to changes in tissue structure due to the degeneration of corticospinal fibres, detected by MRI (Sach et al., 2003). The authors applied single-pulse TMS over the primary motor cortex of fifteen patients with amyotrophic lateral sclerosis (ASL), six of whom had no clinical signs. The results showed a negative correlation between central-motor conduction time and fractional anisotropy. This evidence offered insights into the diagnosis of motor neuron disease before clinical symptoms become apparent.

Regarding off-line TMS-MRI combined applications, these might not be strictly considered as coregistration approaches. However, the use of MRI imaging before TMS is highly popular especially in cognitive neuroscience research to perform neuronavigated TMS (for a recent review, see Sparing et al., 2010). This procedure consists, first, of the acquisition of high-resolution structural images. Then, the subject's head outside the scanner is co-registered to MR images based on anatomical landmarks that are easily identifiable such as nasion, inion, and auricular deflexions. This permits precise guidance for the placement of the TMS coil over a particular brain region based on the subject's anatomy. Moreover, such a system allows on-line control of the TMS position, which can be monitored and fixed during a session of stimulation. Therefore, the highly reproducibility of TMS positioning and orientation across different sessions is guaranteed. In current cognitive neuroscience studies that use TMS, as stated before, the use of neuronavigation systems is now very common, even with the use of an MRI template, in case subjects do not have personal MRI scans.

3.2 TMS-fMRI coregistration

Functional magnetic resonance imaging (fMRI) is a functional imaging technique that uses magnetic resonance imaging to detect and measure the activation of a brain area. This procedure consists of the image of variations in regional blood flow, measured by changes in endogenous oxy- and deoxyhemoglobin concentration, which reflect the energy use of brain cells. The detection of such variations is based on the magnetic properties of deoxyhemoglobin and oxyhemoglobin, which are

paramagnetic and diamagnetic, respectively. The local magnetic field variations caused by the quantity of oxygen in haemoglobin are detected by fMRI, offering a measure of the activation of a certain brain area. As mentioned above, fMRI is able to detect the activation of certain brain regions with high spatial resolution (i.e., with millimetre precision) and poor temporal resolution since changes in blood flow last longer than the underlying neural responses (i.e., a few seconds).

The combined use of TMS and fMRI is a promising methodology in determining the limitations of both techniques, as stated in section 1 of this chapter. However, the simultaneous use of the two techniques is technically challenging because of the high magnetic field strength of MRI scanners, which can vary from 1.5 to 7 T. The mere presence of TMS coils within the scanner can affect the homogeneity of the fMRI static magnetic field. This problem can lead to a signal loss in echo-planar images as well as spatial distortions. A recent study by Bungert and coworkers used some shims made of thin patches of austenitic stainless steel to reduce the effect of the TMS coil on the magnetic field (Bungert et al., 2012). The results showed a reduction of about 80% of the effect of the coil, which permitted the elimination of the associated artefact. Many technical problems arise from the simultaneous functioning of TMS and fMRI. A TMS stimulator, for example, may generate radiofrequency noise that can affect the MRI signal. This problem is generally managed through the use of radiofrequency filters (Siebner et al., 2009). Recently, another type of image artefact generated by leakage currents in a TMS system was investigated by Weiskopf and his group (Weiskopf et al., 2009). The authors characterised the image artefacts through the use of numerical simulations and the application of different coil geometries in phantom studies. The problem was solved by devising a relay-diode combination that was inserted in the TMS circuit, reducing the leakage current. Furthermore, as in TMS-EEG coregistration, the TMS pulse itself can be a source of different artefacts during fMRI. Distortions caused by the TMS pulse were investigated at 2.0 T by Bestmann and colleagues (Bestmann et al., 2003). The authors found that both the echo-planar imaging section orientation (EPI) relative to the plane of TMS coil and the temporal gaps between TMS and image acquisition play a crucial role in artefact generation. Based on the results of the study, the authors concluded that TMS should be applied at least 100 ms before EPI to avoid stimulation during imaging. To our knowledge, the

first study that demonstrated the feasibility of TMS application during fMRI acquisition was performed by Bohning and co-workers. The authors used non-ferromagnetic TMS coil to stimulate the primary motor cortex of three healthy volunteers inside a 1.5 T MR scanner. They observed significant responses in the motor cortex during the TMS condition compared to a rest condition, proving that the combined use of the two techniques is possible.

Besides the technical issues posed by the simultaneous use of TMS and fMRI, this methodology has potential value for different purposes. The on-line coregistration of the two techniques might reveal the effect of TMS in neural circuits with respect to its spatial resolution, which is provided by MRI with high precision. This procedure can be performed at rest with the aim of investigating the basic mechanism of TMS-brain interaction and measuring the reactivity and connectivity of stimulated areas for neurophysiological applications. One example of these applications was provided by Bestmann and collaborators (2004). The authors applied high-frequency rTMS (3.12 Hz) over the left sensorimotor cortex of healthy volunteers. They compared stimulations with intensities above and below the active motor threshold of the subjects. The two intensities produced different results: suprathreshold rTMS produced high activation in the stimulated area (sensorimotor cortex) and in its connected regions, both cortical (supplementary motor area, dorsal premotor cortex, cingulate motor area) and subcortical (putamen, thalamus), whereas subthreshold rTMS elicited a similar pattern of activation but no MRI-detectable activity in the stimulated sensorimotor cortex. These results, on one hand, offered insight into the cerebral motor system's connectivity and reactivity; on the other hand, they showed interesting evidence regarding the TMS mechanisms of action regarding its different dynamics depending on the stimulation. Interestingly, its effects spread not only in cortical areas but also in subcortical structures.

Concurrent TMS-fMRI studies also potentially provide contributions to cognitive neuroscience research. TMS applied during a task permits establishment of the causal role of an area within a cognitive process. This inference can be reinforced by mapping with high spatial resolution the TMS-induced activity through concurrent fMRI. Sack and coworkers (2007), for example, investigated the role of the parietal cortex in visuospatial judgements. The authors applied TMS to the left and right parietal cortices during fMRI while the participants performed a

visuospatial task. The behavioural results revealed impaired performance when TMS was applied over the right parietal cortex, whereas left stimulation produced no effect. Furthermore, fMRI detected a change in the activity of a specific fronto-parietal network in the right hemisphere, which had a significant correlation with the impaired cognitive performance. This result revealed a specific right fronto-parietal activation during the task, corroborating the previous hypothesis of a distributed fronto-parietal network underlying visuospatial processes (Sack et al., 2007).

Useful applications can also be obtained using rTMS and fMRI separately in time (i.e., off-line approach). In a study performed by Tegenthoff and colleagues (2005), for example, the authors aimed to investigate the effects of high-frequency rTMS in tactile perception as well as in cortical plasticity. rTMS was applied at a frequency of 5 Hz over the cortical representation of the right index finger of the primary somatosensory cortex. Stimulation of this area caused a lowering of the discrimination threshold of the right index finger. This data was corroborated by subsequent fMRI, which detected an enlargement of the right index finger's somatotopic representation. The results obtained by the authors provided evidence of the effects of rTMS on perceptual as well as on cortical plasticity (Tegenthoff et al., 2005). Concurrent TMS-fMRI can, thus, have potential in establishing causal links between cognition, perception, and motor processes and their cortical correlates.

Clinical applications of TMS-fMRI coregistration have mainly focused on the long-term effects of either a cerebral dysfunction or a rehabilitation program. The residual cortical activity was considered to be a variable indicating cerebral plasticity. Several studies conducted by Li and colleagues (e.g. 2004; 2011) were devoted to evaluating the cortico-cortical network in depressant patients and the influence of medications on this network. In their first study Li and colleagues (2004), administered cycles of 1 Hz rTMS on the prefrontal cortex, interleaving fMRI measurements of the regional changes in BOLD response. Through principal component analysis (PCA), they were able to describe the network of brain areas that increased activity, which included the stimulated area as well as deep limbic regions, critical in the treatment of depression. Later, these authors applied the stimulation in a temporal window after administering lamotrigine and valproic acids and demonstrated that "interleaved TMS/fMRI can assess region- and circuit-

specific effects of medications or interventions" (Li et al., 2011, p. 141). Hamzei and coworkers (2006) assessed the effects of rehabilitative therapy after a stroke (of either the middle cerebral artery or internal capsule) that involved the motor functions of the hand area. Paired pulse was applied to investigate intracortical inhibition and intracortical facilitation; BOLD response was measured following passive and active movements of either the affected or the non-affected hand. Their study was important since it was the first one to investigate the efficacy of a treatment using a multiple-view perspective obtained from several techniques. Although appealing, this kind of study is really rare, perhaps because of the several challenges posed by the combination of these methods.

3.3 TMS-PET and TMS-SPECT coregistration

The functioning of PET is based on the detection of pairs of gamma rays generated by the collision of positrons (emitted by an isotope that is introduced into the body as a tracer) with electrons. Through the detection of the exact points where gamma rays are generated, PET allows the reconstruction of three-dimensional images of tracer concentration within the body. Different radioactive tracers (e.g., carbon-11, oxygen-15) provide different indices, such as the regional cerebral blood flow (rCBF), which are strictly related to neuronal activity. Thus, PET images are able to detect selective activations of the brain both at rest and during a task with a spatial resolution of about 5 mm. Like PET, SPECT is a nuclear medicine tomographic imaging technique whose functioning is based on gamma ray detection. Since the two techniques are very similar, their combined use will be discussed together.

The first study, as far as we know, that applied TMS during PET was performed by Paus' group (Paus et al., 1997). In this study, the authors tested previous evidence of anatomical fronto-occipital connectivity provided by studies on monkeys (Schall et a., 1995). Transcranial magnetic stimulation was delivered over the left frontal eye fields (FEF) in different trains of pulses (5, 10, 15, 20, 25, and 30 trains) at a frequency of 10 Hz with an intensity at 70% of the maximum output of the stimulator. The authors found a significant positive correlation between the number of TMS pulses and cerebral blood flow. More specifically, prominent activation was found in the stimulation site in the left medial parieto-occipital cortex

and in the left and right superior parietal cortices. The results corroborated previous studies that investigated FEF connectivity on macaque monkeys and provided clear evidence of the reliability of the combined TMS-PET technique in the study of cerebral connectivity. As demonstrated by the above-mentioned study, the use of TMS during PET poses fewer technical problems compared to other neuroimaging coregistration approaches. Moreover, TMS-PET combined use guarantees distinctive advantages. First, during PET acquisition, it is possible to monitor the coil positioning since it is clearly visible; this is not possible during fMRI acquisition. Furthermore, during PET, even long rTMS sessions can be delivered without temporal limits, allowing researchers to see the effect of the stimulation both in the stimulated area and in the connected regions. On the other hand, this also represents a limitation since PET is unable to detect the effects of a single-pulse TMS or even of a short sequence of pulses. Therefore, because of its poor temporal resolution, only cumulative rTMS effects on brain activity can be detected by a PET scan (Siebner et al., 2009).

Simultaneous TMS-PET coregistration has also been used in the study of cognitive processes. Motthaghy and colleagues (2000), for example, tested the effect of rTMS on a working memory task and on regional blood flow changes. Repetitive TMS was applied in 30 s trains at a frequency of 4 Hz over the dorsolateral prefrontal cortices and over the midline frontal cortex as a control site. In the same time, subjects were required to perform a verbal working memory task. The results showed worse performance on the task when the stimulation was applied over the left and right dorsolateral prefrontal cortex. Concurrently, significant reductions in regional blood flow changes were detected both locally and in connected regions. The results obtained by the authors represent some of the first direct evidence showing the disruptive effects of rTMS in a cerebral region within a network involved in a cognitive task. Other studies have focused on rTMS effects on motor cortical excitability, offering interesting elucidation regarding its neurophysiological mechanisms; an example of this approach was provided by Lee's group (2003).

Regarding therapeutic applications, few studies have used TMS-PET coregistration for clinical purposes. The PET and SPECT techniques are suitable for detecting changes in plasticity due to the TMS therapy, especially given that repetitive TMS has mostly been used with patients resistant to pharmacological

treatments. As a consequence, a relatively large body of literature on mood disorders, such as depression, has allowed the mapping of long-lasting activity changes and cortical reorganisation (Speer et al., 2000; 2009; Nadeau et al., 2002). Frontal-lobe rTMS was also proposed as a treatment for Parkinson's dementia: studies conducted by Strafella and colleagues (2005) tried to determine the modification caused by rTMS in the cortical functioning and in the neurotransmitters tied to the development of this kind of dementia. Apart from these examples, the situation clearly suggests that TMS combined with these techniques for clinical purposes is limited to the study of the long-lasting effects of the TMS technique itself. Therefore, in the future, there will probably be no attempts to apply the simultaneous recording of PET/SPECT with TMS.

3.4 TMS-NIRS coregistration

Near-infrared spectroscopy (NIRS) is a spectroscopic method of detecting changes in haemoglobin concentrations through the measurement of the absorption of near-infrared light by neural tissue. This permits the detection of changes in brain activity with good spatial resolution, limited to the cortical regions. Since this method does not make use of magnetic fields, it is suitable to be combined with TMS without particular technical precautions. However, compared to other TMS-neuroimaging coregistration approaches, a smaller number of studies have used NIRS during TMS; therefore, technical details regarding this coregistration are still lacking.

One of the first studies that successfully applied TMS during NIRS was performed by Oliviero and colleagues (1999). The authors compared cerebral variations in oxyhemoglobin, deoxyhemoglobin, and cytochrome oxidase-induced magnetic and electrical stimulation. Stimulation was delivered at a frequency of 0.25 Hz over the NIRS probe on the anterior right frontal region. Repetitive TMS immediately induced a significant increase in oxyhemoglobin and a decrease in cytochrome oxidase, whereas this effect was not observed after electrical stimulation. The results of the study underlined the different effects provided by magnetic and electric stimulation, suggesting that rTMS induced higher regional cerebral blood flow rate and, consequently, an increase in the activation of the stimulated area. Interestingly, some studies have also evaluated the effect on

metabolic activity after single-pulse TMS (e.g., Noguchi et al., 2003; Mochizuki et al., 2006), which is otherwise impossible with other neuroimaging techniques such as PET and SPECT (see paragraph 3.5). In a study by Mochizuki and coworkers (2006), for example, the authors applied single-pulse TMS over the left primary motor cortex at different intensities (100%, 120%, or 140% of the AMT) both at rest and during contraction of the right first dorsal interosseous muscle. The results showed an increase in oxyhemoglobin in the active condition when TMS was delivered at 100% intensity. In contrast, significant decreases in deoxyhemoglobin and total haemoglobin were observed under the resting condition with TMS at 120% and 140% intensity. The authors interpreted the decrease as a lasting inhibition induced by higher-intensity TMS that results in a reduction in the baseline firing of corticospinal tract neurons. Moreover, combined TMS-NIRS studies have also evaluated the effect of high-frequency rTMS such as 1-Hz (e.g., Chiang et al., 2007) and TBS (e.g. Mochizuki et al., 2007), on the regional cerebral haemoglobin rate. However, compared to the other techniques NIRS is a very new methodology. Therefore, more studies are needed in this field. Clinical research, for example, is lacking at the moment, but all indications suggest that this combination would be a worthwhile field of application for several pathological conditions (e.g., executive functions, learning disabilities).

CHAPTER III
STUDY 1 – NEUROMODULATORY EFFECTS OF LOW-FREQUENCY RTMS: INSIGHTS FROM TMS-EEG

1. INTRODUCTION

Repetitive transcranial magnetic stimulation is a non-invasive technique able to produce long-term modulations of cortical excitability (Ridding and Rothwell, 2000). Over the years, its use for research and therapeutic purposes has increased even if a clear explanation of its mechanisms of action is still lacking (Pascual-Leone et al., 1998; Ridding and Rothwell, 2000; Rossi et al., 2009). In traditional TMS/EMG literature, the neuromodulatory effects of rTMS have been investigated through the analysis of MEPs, which reflect the degree of corticospinal excitability and represent an indirect measure of cortical excitability (Barker et al., 1985). However, although reliable, MEP origin is far from being fully elucidated because of the complex combination of excitatory and inhibitory events along the motor pathway, which leads to a considerable variability in their amplitude (Fitzgerald et al., 2006). Nowadays, with the current development of TMS-compatible EEG systems, it is possible to record the cerebral activity evoked by TMS from the entire scalp (Ilmoniemi et al., 1997). The electrical potentials evoked by TMS represent a purely central index through which it is possible to directly investigate the effects of TMS not only at the site of stimulation but throughout the cortex (Ilmoniemi and Kičić, 2010). Compared to MEPs, some studies demonstrated the higher reproducibility and sensibility of TEPs over time and in different conditions of stimulation (Lioumis et al., 2009; Casarotto et al., 2009). Given these advantages, there is a growing interest in using EEG measures during TMS, in order to clarify the effects of stimulation protocols, such as: rTMS (Van der Werf et al., 2006; Helfrich et al., 2013), ppTMS (Daskalakis et al., 2008; Ferreri et al., 2011), tDCS (Pellicciari et al., 2013) and PAS (Veniero et al., 2013; Bikmullina et al., 2009).

A large part of the TMS/EEG studies in literature, focused on the time-locked EEG response evoked by the primary motor cortex (M1) stimulation, which consist in a sequence of positive and negative components, usually reported as: P30, N45, P60, N100 and P180 (Paus et al., 2001; Komssi et al., 2002; Bender et al., 2005; Bonato et al., 2006; Van der Werf et al., 2006; Lioumis et al., 2009; Ferreri et al., 2011; Ter Braack et al., 2013). Up to date, a consensus is developing about a possible relevance of the N100 peak, whereas there is not clear evidence on the functional origin of the other TEPs (Kähkönen et al., 2006). Specifically, some studies hypothesized an inhibitory nature of N100 based on the amplitude modulations of this potential in different conditions of motor cortical excitability (Nikulin et al., 2003; Bender et al., 2005; Bonnard et al., 2009). In their study, Nikulin and colleagues (2003) instructed participants to make a movement in response to a checkerboard displayed on a screen or to merely watch the visual stimulus. These authors found a significant decrease of N100 amplitude in the movement condition, associated to an increase of MEP amplitude. Such N100 attenuation was explained by the authors as a consequence of the increased firing rate of motor cortex neurons, which suggested that N100 amplitude could reflect the degree of (motor) cortical excitability (fig. 3.1, Nikulin et al., 2003). Along the same lines, Bender and colleagues (2005) used a forewarned reaction time task to test the effects of response preparation on N100 amplitude. These authors found that when participants were preparing to make a movement (i.e. a condition of higher cortical excitability) N100 was significantly reduced (fig. 3.1). Additional converging evidence has been provided by Bonnard and colleagues (2009), which instructed participants to be mentally prepared to "resist" or to "assist" a wrist movement evoked by a single-pulse TMS over M1. Interestingly, the authors found a higher N100 and a lower contingent negative variation waveform (a well-known marker of anticipatory increase in cortical excitability, Bastiaansen et al., 1999) in the resist condition, which suggested a decrease in cortical excitability associated (or due to) an increase in inhibitory processes (fig. 3.1; Bonnard et al., 2009). This hypothesis was further supported by the prolongation of the cortical silent period (CSP) in the resist condition, which is known to reflect the degree of cortical inhibition (Chen et al., 1999).

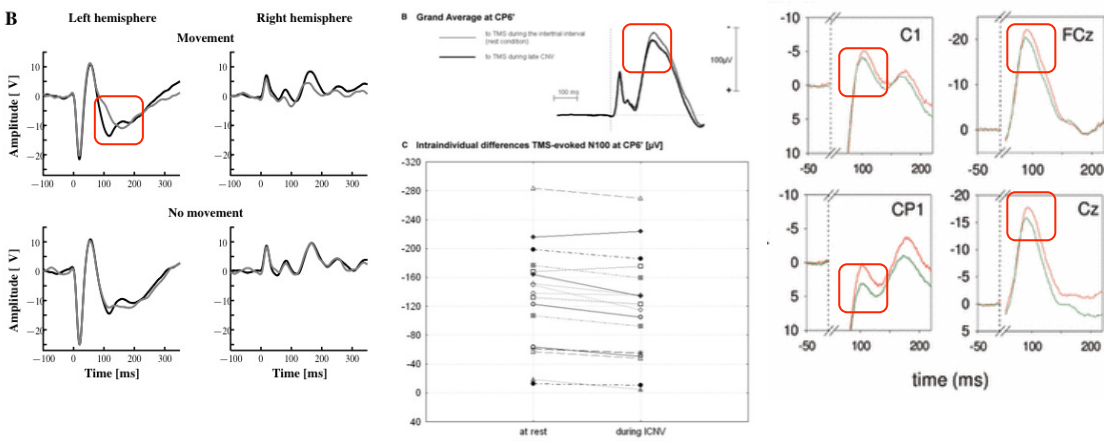

Figure 3.1 TMS-evoked N100 modulation following "movement" or "no-movement" conditions. During movement preparation the N100 was significantly reduced in amplitude (left and center panels), during the preparation to resist to a movement the N100 was significantly increased (right panel) (adapted from Nikouline et al., 2003; Bender et al., 2005; Bonnard et al., 2009)

We aimed this study at investigating the effect of a low-frequency rTMS protocol (1 Hz) in a group of healthy volunteers, by examining the TEPs following single-pulse TMS over M1. To date, this protocol has shown to produce inhibitory effect based on peripheral indexes (MEPs; e.g. Chen et al., 1997; Maeda et al., 2000), even if literature often reports contrasting outcomes in this regard (Pascual-Leone et al., 1998; Fitzegerald et al., 2006; Thut and Pascual-Leone et al., 2010). In the present study, we overcome such limitation examining the amplitude, latency and distribution of early and later TEPs, before and immediately after the rTMS protocol. Given previous findings, we expected that low-frequency rTMS should result in a modulation of N100, because of its supposed inhibitory origin. Moreover, in order to test the specificity of the rTMS effects over M1, we performed a second experiment in which rTMS was delivered over V1. Since there are not direct anatomical connections between M1 and V1 areas (Guye et al., 2003), we should expect no effects on MEPs and TEPs: this result will provide a direct confirmation of the rTMS effects produced over M1.

2. METHODS

2.1 Participants and procedure

Fifteen right-handed healthy volunteers (seven females, mean age 25±5 years) were enrolled for this experiment (experiment 1) after giving written informed consent. All participants were tested for TMS exclusion criteria (Rossi et al., 2009) and had normal or corrected-to-normal vision. The experimental procedure was approved by the Institutional Review Board of the University of Padua, and was in accordance with the Declaration of Helsinki (Sixth revision, 2008). Each participant underwent an experimental session consisting of three blocks of TMS during multichannel EEG and EMG recordings. The first and the third block of stimulation ("pre-rTMS" and "post-rTMS" respectively) consisted of 50 single-pulses delivered before and immediately after a 1-Hz rTMS block (figure 3.2). During the entire session participants were seated on a comfortable armchair in front of a monitor at 80 cm of distance. They were asked to fixate a white cross (6×6 cm) in the middle of a black screen and to keep their right arm in a relaxed position. During TMS participants wore in-ear plugs which continuously played a white noise that reproduced the specific time-varying frequencies of the TMS click, in order to mask the click and avoid possible auditory ERP responses (Massimini et al., 2005). The intensity of the white noise was adjusted for each subject by increasing the volume (always below 90 dB) until the participant was sure that s/he could no longer hear the click (Paus et al., 2001). To reduce the bone-conducted sound we used an EEG cap with a 4 mm plastic sheet that reduced the transmission of mechanical vibration produced by the coil (Nikouline et al., 1999; Esser et al., 2006).

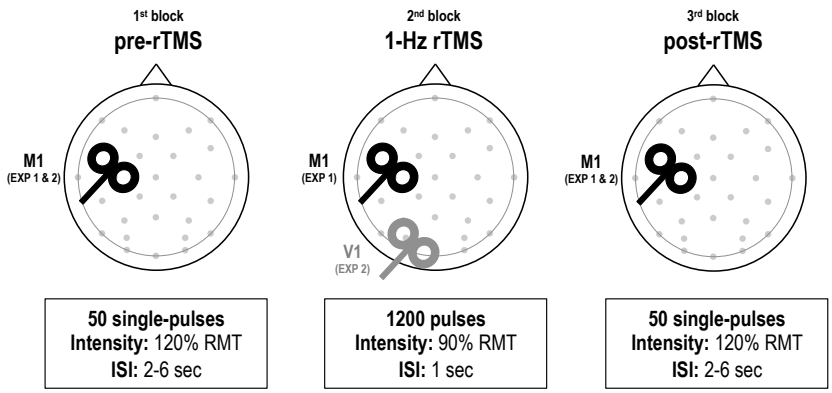

Figure 3.2 Schematic representation of the experimental procedure

2.2 Transcranial Magnetic Stimulation (TMS)

TMS was carried out using a Magstim R^2 stimulator with a 70mm figure-of-eight coil (Magstim Company Limited, Whitland, UK), which produced a biphasic waveform with a pulse width of about 0.1 ms. The position of the coil on the scalp was functionally defined as the M1 site in which TMS evoked the largest MEPs in the relaxed first dorsal interosseous (FDI) muscle of the right hand. The coil was placed tangentially to the scalp at about 45° angle away from the midline, so that the direction of current flow in the most effective (second) phase was posterolateral-anteromedial. To ensure the same stimulation conditions during the entire experiment, coil positioning and orientation on the optimal hotspot were constantly monitored by means of the Brainsight neuronavigation system (using the ICBM152 template), coupled with a Polaris Vicra infrared camera (NDI, Waterloo, Canada). Stimulation intensity varied across the blocks of stimulation (see below) and was determined relative to the resting motor threshold (RMT), defined as the lowest TMS intensity which evoked at least five out of ten MEPs with an amplitude > 50 μV peak-to-peak in the contralateral FDI at rest (Rossini et al., 1994). Single-pulses were delivered with an inter-stimulus interval (ISI) of 4-6 seconds, intensity was set at 120% RMT to obtain reliable MEPs. The rTMS block consisted of 1200 pulses delivered at 1 Hz using an intensity of 90% RMT.

2.3 Electromyographic recordings (EMG)

Surface EMG was recorded from the right FDI muscle via Ag/AgCl electrodes in a belly-tendon montage (Myohandy Matrix Line – Micromed Srl, Mogliano Veneto, Italy); raw signals were sampled at 2.5 kHz and band-pass filtered at 50-1000 Hz. EMG signal was on-line monitored and off-line analyzed by software Brain-Quick System Plus using epochs of 50 ms. MEP amplitudes were measured peak-to-peak.

2.4 Electroencephalographic recordings (EEG)

EEG was recorded using a TMS-compatible AC amplifier (Micromed SD MRI, Micromed Srl., Mogliano Veneto, Italy) designed to work in presence of high external magnetic fields as used in TMS or MRI (Morbidi et al., 2007). The amplifier was

optically connected to a PC with software Brain-Quick System Plus through which EEG was on-line monitored, and to a 64-channels customized EEG cap (EasyCap Inc., Herrsching, Germany). EEG was continuously recorded from 31 TMS-compatible Ag/AgCl pellet electrodes mounted on the cap according to the 10-20 international system including: Fp1, Fpz, Fp2, F7, F3, Fz, F4, F8, FC5, FC1, FC2, FC6, T3, C3, Cz, C4, T4, CP5, CP1, CP2, CP6, T5, P3, Pz, P4, T6, PO3, PO4, O1, Oz, O2. Skin impedance was kept below 5 kΩ. Recordings were referenced to AFz electrode; the ground electrode was placed on POz. EEG signal was bandpass filtered at 0.1-500 Hz and the sampling frequency was 2048 Hz. Off-line analysis was performed with EEGLAB 10.2.2.4b (Delorme and Makeig, 2004), running in a MATLAB environment (Version 7.9.0, MathWorks Inc., Natick, USA). The continuous EEG signal was segmented into epochs starting 50 ms before the TMS pulse and ending 250 ms after it. After this, data from 5 ms before the TMS pulse to 22 ms after were removed from each trial to exclude the TMS artifact through the cubic interpolation function of MATLAB (Thut et al., 2011). The identification of artifacts unrelated to TMS (e.g. eye blinks, muscle activity, electric current, alpha activity) was made using the independent component analysis (ICA) function on EEGLAB. Identified components were then visually inspected in terms of scalp distribution, frequency, timing and amplitude and removed with ICA (Johnson et al., 2010; Mattavelli et al., 2013). Afterwards, all the epochs were visually inspected and those with excessively noisy EEG were excluded from the analysis (resulting less than 5% for each participant). A baseline correction, taken as the interval starting 500 ms before the TMS pulse, was applied on all the epochs. For the TEP analysis, all the epochs of each participant were averaged separately for the pre-rTMS and the post-rTMS conditions. Based on the recent literature (for a review, Ilmoniemi and Kičić, 2010), we chose five time windows to determine the TEPs amplitudes and latencies, computed as the highest peaks in the following intervals: 23-45 ms (positive peak); 30-60 ms (negative peak); 45-70 ms (positive peak); 70-130 ms (negative peak); 130-230 ms (positive peak). To assess the total brain activation induced by TMS over M1, we performed a local mean field power analysis (LMFP), computed as the square root of the signal across the electrodes surrounding the two motor cortices (Pellicciari et al., 2013; Lehmann and Skrandies, 1980).

2.5 Control experiment

A control experiment (experiment 2) was conducted to examine the spatial specificity of the effects observed in experiment 1. Fifteen right-handed healthy volunteers (different from those who participated in experiment 1) were enrolled and underwent the same experimental procedure as experiment 1, except that the rTMS stimulation was delivered over V1 (3 cm anterior and 1 cm lateral from the inion (Silvanto et al., 2007)). The coil was held with the handle pointing towards the left side, so that the current flow direction of the second, most effective, phase wave was latero-medial.

2.6 Statistical Analyses

All data were analyzed using SPSS version 19 (SPSS Inc., Chicago, USA). Prior to undergoing ANOVA procedures, normal distribution of EEG and EMG data was assessed by means of Shapiro-Wilks' test. Level of significance was set at $\alpha = .05$. Extreme outliers (i.e. 3 standard deviations or more) within individual trials were identified and excluded from the analysis (resulting less than 4% for each participant). MEP amplitudes were first log-transformed to limit the effect of outliers and then analysed with a 2 (group: experiment 1, experiment 2) × 2 (rTMS: pre-rTMS, post-rTMS) mixed ANOVA. TEP analysis was performed considering ten electrodes: FC1, C3, T3, CP1 and CP5 for the left stimulated side; FC2, C4, T5, CP2 and CP6 for the right one. TEP amplitudes and latencies were analysed with a 2 (group: experiment 1, experiment 2) × 2 (rTMS: pre-rTMS, post-rTMS) × 2 (laterality: left, right) × 5 (electrode: FC1/FC2, C3/C4, T3/T4, CP1/CP2, CP5/CP6) × 5 (peak: P30, N45, P60, N100, P180) mixed ANOVA. The same electrodes were considered for the LMFP analysis that was performed comparing the LMFP differences of the two conditions (post-pre) between the two groups with paired t-tests, separately for each hemisphere. Sphericity of data was tested with Mauchly's test; when sphericity was violated (i.e. Mauchly's test < 0.05) the Greenhouse-Geisser correction was used. Pairwise comparisons were correct by the Bonferroni method.

3. RESULTS

3.1 Motor-evoked potentials (MEPs)

There was no difference in the baseline MEP amplitudes (i.e. pre-rTMS blocks) in the two groups of experiment 1 and 2 ($p = 0.38$). However, there was a significant group × rTMS interaction [$F(1,28) = 4.247$; $p = 0.049$] that post-hoc analysis revealed was caused by a significant reduction in the post-rTMS MEP amplitude in experiment 1 (1.37±0.14 *vs.* 1.66±0.09 mV; $p = 0.001$) but not in experiment 2 (1.67±0.06 *vs.* 1.72±0.03; $p = 0.47$; fig. 3.4a).

3.2 TMS-evoked potentials (TEPs)

Single-pulse TMS over M1 evoked a sequence of positive and negative deflections lasting up to 180-200 ms. The grand-average waveform clearly shows four main peaks at approximately 30 ms (P30), 45 ms (N45), 60 ms (P60),100 ms (N100) after the TMS pulse (fig. 3.5).

The mixed ANOVA including all factors revealed that there was a significant group × rTMS × peak interaction [$F(4,112) = 6.891$; $p = 0.001$] as well as a significant group × rTMS × electrode × peak interaction [$F(16,448) = 1.738$; $p = 0.037$].

The post-hoc analysis of the first interaction did not reveal any differences between the pre-rTMS blocks of any of the peaks of the two experiments (all ps > 0.15). On the other hand, significant differences between post- and pre-rTMS blocks were detected for the N100 (2.99±0.67 μV; $p < 0.001$) and for the P60 (1.47±0.59 μV; $p = 0.02$) of the experiment 1, which appeared to be larger in the post-rTMS condition. No differences were detected in the experiment 2 (all ps > 0.25). The post-hoc analysis of the second interaction showed that the N100 was larger in the post-rTMS block compared to the pre-rTMS one at the following sites: C3/C4 (3.27±0.86 μV; $p = 0.001$), FC1/FC2 (1.88±0.66 μV; $p = 0.009$), CP1/CP2 (2.95±0.60 μV; $p < 0.001$), CP5/CP6 (3.52±0.83 μV; $p < 0.001$) and T3/T4 (3.35±1.02 μV; $p = 0.003$). The P60 was larger in the post-rTMS block compared to the pre-rTMS at the following sites: C3/C4 (1.56±0.69 μV; $p = 0.033$), CP1/CP2 1.80±0.63 μV; $p = 0.008$), CP5/CP6 (3.52±0.83 μV; $p = 0.005$) and T3/T4 (3.35±1.02 μV; $p = 0.047$). The P60 and N100 amplitudes are reported in figures 3.4b and 3.4c Finally, there were no significant differences in the P30, N45 and P180 amplitudes for experiment 1 (all ps

> 0.15), and no effects on any component for experiment 2 (all ps > 0.07). Figure 3.3 depicts the individual data of the N100 amplitude in experiment 1 and experiment 2. The analysis of TEP latencies failed to reveal any significant effects (all ps > 0.05). Following these results, we tested for possible correlation between the rTMS-induced modulations in MEP and in N100/P60 amplitudes using the Pearson correlation coefficient. No significant correlations were revealed (all ps > 0.05).

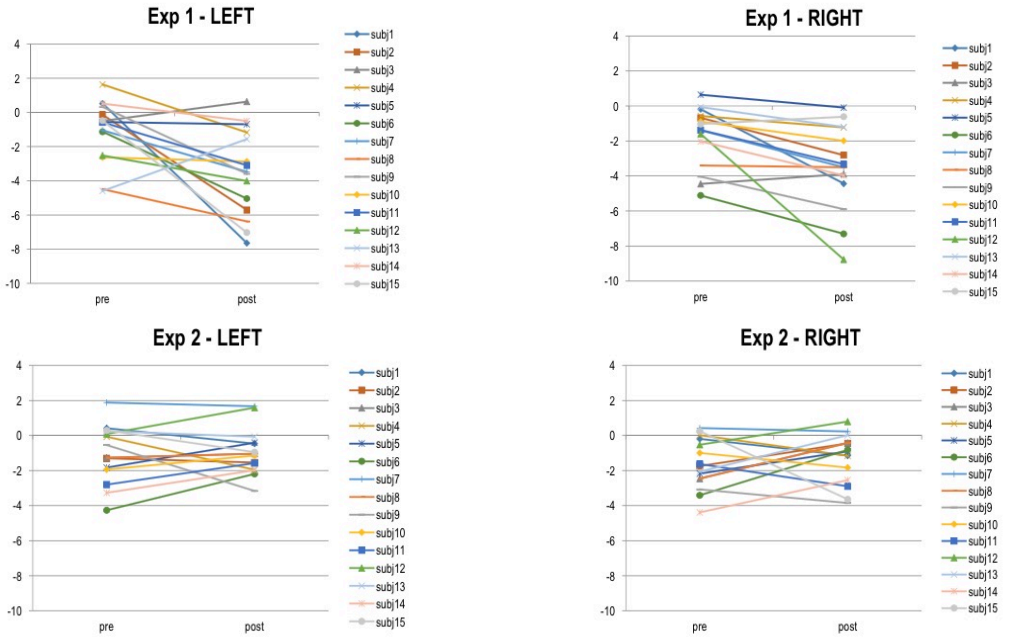

Figure 3.3 Individual subject data of the N100 amplitude for the two hemispheres (left and right) in experiment 1 (above) and experiment 2 (below)

3.3 Local mean field power (LMFP)

No differences were detected in the LMFP of the two groups from 50 ms before the TMS pulse to 72 ms after (all ps > 0.05). Paired sample t-tests revealed a significantly higher LMFP for the experiment 1, compared to experiment 2, in the following temporal windows: 96-231 ms in the left hemisphere (figure 3.4d); 86-90 ms, 132-146 ms and 196-216 ms in the right hemisphere (figure 3.4e).

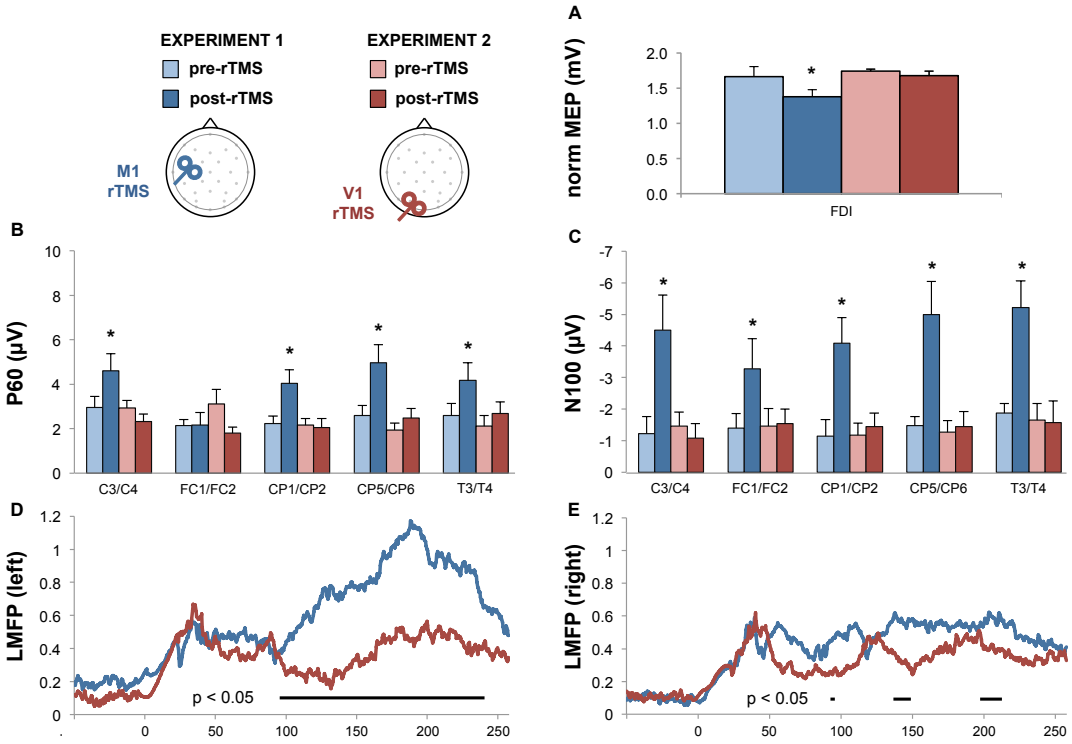

Figure 3.4 (a) MEPs amplitudes before an after rTMS in the experiment 1 (pre-rTMS: light blue; post-rTMS: dark blue) and in the experiment 2 (pre-rTMS: light red; post-rTMS: dark red); (b, c) P60 and N100 amplitude before and after rTMS for the experiment 1 (pre-rTMS: light blue; post-rTMS: dark blue) and for the experiment 2 (pre-rTMS: light red; post-rTMS: dark red). Error bars indicate standard error; (c, d) Local mean field power in the left and in the right hemisphere of the difference post-rTMS – pre-rTMS in the two experiments (experiment 1: blue; experiment 2: red). Black line in the bottom indicates when the difference between the two experiments was significant.

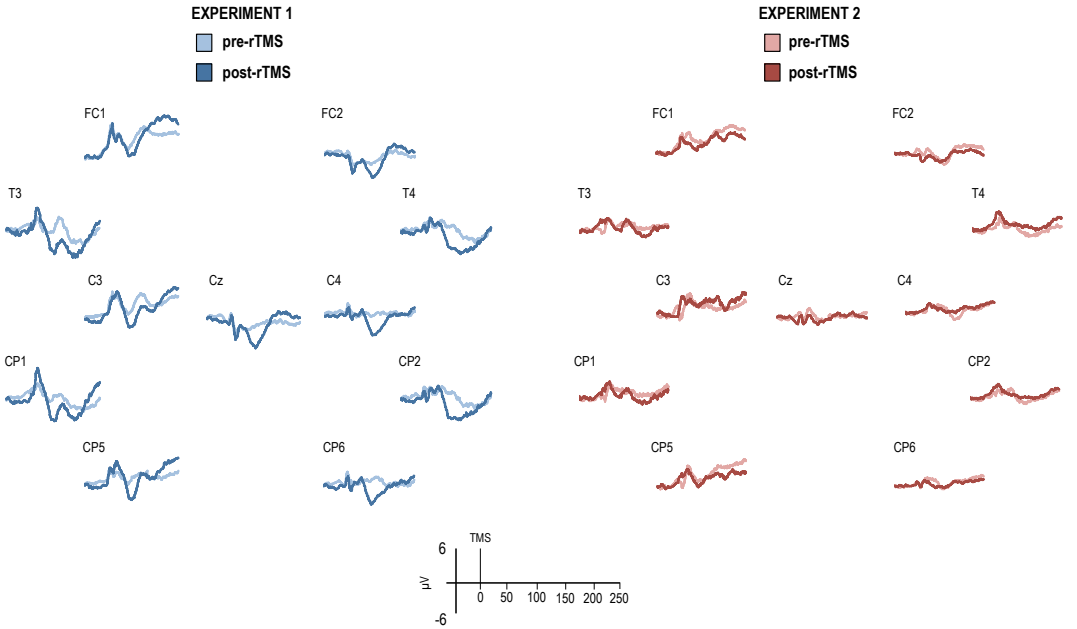

Figure 3.5 a) Grand average waveform recorded before and after rTMS in the experiment 1 (pre-rTMS: light blue; post-rTMS: dark blue). (b) Grand average waveform recorded before and after rTMS the experiment 2 (pre-rTMS: light red; post-rTMS: dark red).

3.4 Scalp maps of activity distribution

Figure 3.6 shows the scalp distribution maps of the difference before and after rTMS in the two experiments. In experiment 1, starting from 50 ms after the TMS pulse, a positivity, representing higher post-rTMS P60, was visible over the site of stimulation which tended to return to baseline levels at 75-80 ms. From 85-90 ms, the higher post-rTMS N100 was evident over the site of stimulation. From 105-110 ms, the negativity amplitude was prominent and tended to gradually spread over the adjacent regions and, interestingly, to the opposite hemisphere at 115-130 ms before returning to baseline levels at 145-150 ms. Starting from 160 ms, a sustained positivity is evident over the site of stimulation before returning to baseline levels at 240-250 ms. No differences were appreciable in the experiment 2.

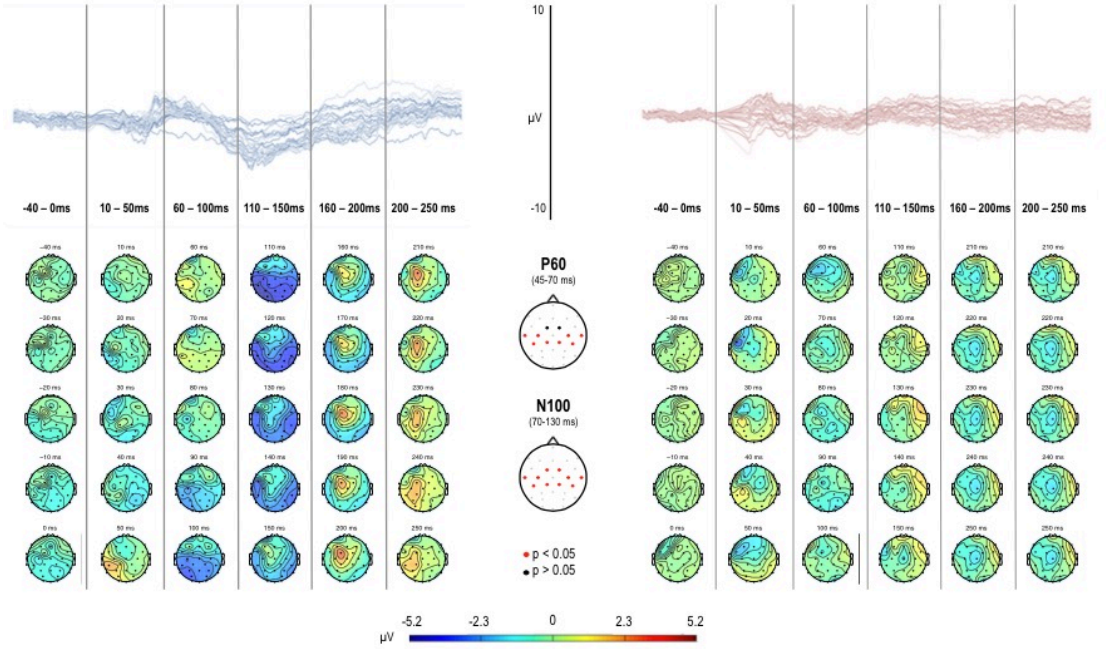

Figure 3.6 Scalp distribution maps of the difference (post-rTMS – pre-rTMS) in the activity changes induced by rTMS in experiment 1 (left) and in experiment 2 (right).

4. DISCUSSION

The present results show that 1-Hz rTMS over M1, but not V1, (a) reduces the amplitude of MEPs, (b) increases the amplitude of the N100 and P60 TEPs evoked by single pulse TMS over M1 and (c) induces a sustained increase in the late LMFP, especially in the stimulated hemisphere. The effect on the MEP has been reported in a number of previous studies (e.g. Chen et al., 1997; Siebner et al., 1999; Maeda et al., 2000), whereas the effect on the TEP has not been described previously in healthy volunteers. Interestingly, the largest changes were seen on the side of stimulation (left scalp), as clearly visible in the LMFP, indicating that their modulation was strictly related to TMS and not to other confounding factors. On the other hand, our TEP analysis failed to reveal a significant effect of laterality. This might be due to the interhemispheric spread of the N100 component from the left hemisphere (85-90 ms) to the right hemisphere (115-120 ms). It has been suggested that early TEPs, such as P30 and N45, originate or are modulated from fast $GABA_A$ (gamma-aminobutyric acid)-mediated inhibitory post synaptic potentials (IPSPs), whereas later TEPs, such as P60 and N100, are produced or modulated by slow $GABA_B$-mediated IPSPs (Tamás et al., 2003; McDonnell et al., 2006; Ferreri et al., 2011; Rogasch et al., 2013). This latter hypothesis is supported by the fact that the N100 increases after consumption of alcohol, which is known to increase GABAergic transmission (Kähkönen and Wilenius, 2007). Moreover, the latencies of the P60 and N100 peaks coincide with the start of the inhibition (around 50-55 ms) and peak of inhibition (around 100-150 ms) produced by activation of $GABA_B$ receptors in both human and animal studies (Davies et al., 1990; Deisz et al., 1999). Finally, some recent work using paired-pulse TMS found a significant correlation between EMG measures of the depth of long-interval cortical inhibition (LICI), a GABAb-ergic effect whose timing coincides with the P60/N100 peaks, and the total amount of EEG activity evoked by the TMS pulses (Daskalakis et al., 2008; Fitzgerald et al., 2008; Farzan et al., 2010). This is strictly in line with what we observed in the LMFP, which became significantly higher after the administration of 1-Hz rTMS from about 75 ms to 230 ms after the TMS single pulse. On the other hand, our TEPs analysis did not reveal any significant change on the P180 component, and this might be explained by the absence of a real peak of activity in that temporal window. Given this reasoning, the increase in P60 and N100 may indicate that 1-Hz rTMS increases

the amount of GABAb-ergic inhibition evoked by a TMS test pulse. The fact that P30 and N45 are unaffected would be compatible with a smaller or absent effect on GABAa-ergic activity. This conclusion would be compatible with the effect of 1-Hz rTMS on two EMG measures of GABAergic excitability in M1. These are (1) short interval intracortical inhibition (SICI) between a pair of TMS pulses, and (2) the cortical silent period (CSP) which describes the reduction in ongoing EMG activity that follows the MEP. The former depends on GABAa activity whereas the latter depends on GABAb. Previous work has shown that when 1-Hz rTMS suppresses MEPs, it is usually accompanied by no change in the GABAa-ergic SICI (e.g. Daskalakis et al., 2006) whereas there may be an increase in duration of the GABAb-ergic CSP (Daskalakis et al., 2006 and Lang et al., 2006). Thus the tentative conclusion would be that 1-Hz rTMS over M1 increases the depth and/or duration of the GABAb-ergic IPSP that follows a single pulse of TMS.

It is important to remember that MEPs are an indirect measure of pyramidal tract excitability, since they are affected by a combination of cortical, subcortical and spinal mechanisms, whereas TEPs are the direct result of activating excitatory and inhibitory postsynaptic potentials (Ilmoniemi et al., 1997). This could explain the absence of a significant correlation between changes in MEP and N100/P60 amplitudes in our data. Indeed, it has been found that reliable TEP patterns are evoked even at subthreshold intensities at which MEPs are not elicited, indicating that TEPs and MEPs reflect two separate indices of the neurophysiological state of a stimulated area (Komssi et al., 2004; Van der Werf et al., 2006). One possible confound to the present explanation is that since we used suprathreshold TMS pulses to evoked the TEP, changes in afferent input from the induced muscle twitch following rTMS could contribute to changes in P60/N100 amplitude. However, this seems unlikely, since MEPs were smaller after rTMS so that the contribution of afferent input should if anything decrease whereas the P60/N100 increased in size. Another possible confound are changes in general arousal or to an expectancy effect that can change EEG alpha and/or slower activity, and secondarily affect TEP amplitudes. As demonstrated by previous studies, low-frequency rTMS increases ipsilateral cortico-cortical and interhemispheric alpha coherence but not its amplitude (e.g. Strens et al., 2002). The effect was also spatially specific, and therefore unrelated to general arousal. Finally, if rTMS were having any general

effects on expectation or arousal we might have expected to observe them equally well after V1 stimulation, but this was not the case. Van der Werf and colleagues (2006) found that 0.6-Hz rTMS over M1 reduced the amplitude of the N45 potential without affecting MEPs. This effect was postulated to be due to activation of inhibitory interneurons that synapse on pyramidal neurons, an interpretation which is in line with the present study. They did not report any modulation of N100 although they interpreted it as being an auditory neural response to the TMS coil click. However, there are several reasons for excluding this hypothesis: (1) some studies found a TMS-evoked N100 in deaf participants (Kimiskidis et al., 2008; Ter Braack et al., 2013); (2) Bonato et al. (2006) did not find an N100 component with a placebo coil nor with a suboptimal orientation of a normal coil (135 degrees); (3) several studies found no difference in the amplitude of TEPs with or without auditory masking, suggesting that the amplitude of the auditory response is negligible compared to the N100 TMS-evoked response (e.g. Nikulin et al., 2003; Komssi et al., 2004; Kähkönen et al., 2005); (4) Lioumis et al. (2009) demonstrated that the amplitude of the N100 evoked over the motor cortex was five times larger than the potential evoked in the prefrontal cortex using the same intensity of stimulation (i.e. the same coil click), and such difference cannot be explained in terms of auditory potentials; (5) the distribution of the N100 is not compatible with an auditory potential distribution (Näätänen and Picton, 1987; Ponton et al., 2001). Finally, a very recent study by Helfrich and colleagues (2013) reported a decrease in the TMS-evoked N100 after 15 minutes of 1-Hz rTMS in a group of ADHD children. This result was attributed to reduced inhibition following 1-Hz rTMS. At first glance, this result seems to be in contrast with our findings. However, Moll and colleagues (2000, 2003), testing LICI with paired-pulse TMS, had demonstrated that ADHD children a) show a significant reduction in intracortical inhibition and b) report an opposite effect of methylphenidate on the balance of intracortical facilitation/inhibition compared to healthy controls. It may therefore be that rTMS has a different effect on cortical inhibition in ADHD than in healthy adults and this could explain the discrepancy with the present results.

5. CONCLUSIONS

In conclusion, we have shown that application of 1-Hz rTMS in healthy volunteers reduced MEPs whilst increasing the P60 and N100 components of the TEP. Previous work suggests that these EEG components may be caused by or modulated by GABAb-ergic activity evoked by the TMS pulse. We propose that 1-Hz rTMS over M1 increases the amplitude or duration of the GABAb IPSP evoked by single pulse TMS over the same area. The present findings could be of relevance for diagnostic and therapeutic purposes, particularly for pathologies characterized by disorders in cortical excitatory/inhibitory processes.

CHAPTER IV
STUDY 2 –TMS-EEG MARKERS OF INHIBITORY DEFICIT IN HUNTINGTON'S DISEASE

1. INTRODUCTION

Combining electroencephalography (EEG) and transcranial magnetic stimulation (TMS) investigates the functional response of the brain to a standardised input. In the last years this approach has provided insights into brain dynamics dysfunctions in several pathologies such as: schizophrenia (Ferrarelli et al., 2008; Frantseva et al., 2012); psychotic disorders (Hoppenbrouwers et al., 2008); depression (Kähkönen et al., 2005); alcohol consumption (Kähkönen et al., 2001; 2003); awareness disorders (Massimini et al., 2005; Huber et al., 2007); epilepsy (Rotenborg et al., 2008) and autism (Sokhadze et al., 2012; Helfrich et al., 2013). The analysis of the EEG activity evoked by TMS in terms of evoked-potentials (i.e. TEPs; e.g. Helfrich et al., 2013); brain sources reconstruction (e.g. Massimini et al., 2005); oscillatory activity (e.g. Ferrarelli et al., 2008) and global power (e.g. Hoppenbrouwers et al., 2008) revealed abnormalities in the local response of a stimulated area (i.e. reactivity; Kahkonen et al., 2002) and in the spreading of such activity over interconnected areas (i.e. connectivity; Massimini et al., 2005). TEPs origin, for instance, have been related to the activity of specific interneurons (Ferreri et al., 2011; Premoli et al., 2014). Specifically, early TEPs (< 50 ms from the TMS pulse) have been related to the activity of GABAa-ergic interneurons, whereas late TEPs (> 50 ms from the TMS pulse) have been related to the activity of GABAb-ergic interneurons. Furthermore, from a growing body of evidence, the TMS-evoked N100 seems to be a reliable marker of the amount of cortical inhibition (e.g. Bender et al., 2005; Bonnard et al., 2009; Ferreri et al., 2011; Casula et al., 2014; Premoli et al., 2014).

In a preview study of our group (Casula et al., 2014) we demonstrated that N100 is linked to the activity of the inhibitory post-synaptic potentials mediated by GABAb receptors, a result that may have interesting clinical and therapeutic

implications, especially for pathologies characterized by hyper- o ipo-excitability of the motor cortex. Huntington's disease (HD) is an autosomal dominant neurodegenerative disorder with complete penetrance (Tabrizi et al., 2009). In HD there is good evidence for cortical and striatal pathology directly contributing to core symptoms of the disease, as shown by numerous studies in animals and humans. Specifically, one of the first alteration HD-related is the progressive degeneration of cannabinoid receptors type 1 (CB1) in basal ganglia, which are highly expressed in GABAergic neurons of the striatum.

Given the GABAergic nature of the TMS-evoked EEG activity, we tested whether GABAergic deficits in HD patients produce any significant change in different TMS-EEG measures compared with a group of healthy volunteers.

The present study was conducted in the context of the international TrackOnHD project. Several EMG, EEG (see paragraph 2.1) as well as functional and neuropsychological measures were taken. In this chapter I reported only the preliminary results on TMS-EEG measures.

2. METHODS

2.1 Participants and procedures

12 participants with early HD and 12 healthy control subjects were examined at the Institute of Neurology (University College London) in the context of the TRACK-ON study, after giving written informed consent. Each participant underwent an experimental session consisting of two blocks of TMS delivered over the primary motor cortex and over the premotor cortex (see paragraph 2.2) during multichannel EEG (see paragraph 2.4) and EMG recordings (see paragraph 2.3). The following measures were taken during the entire experiment:

- Input/Output curves at rest and during muscular activation
- Cortical silent period
- Resting EEG during eyes closed and eyes open
- TEPs from the primary motor cortex and from the premotor cortex
- Somatosensory-evoked potentials
- Visual-evoked potentials
- Long-latency reflexes

During the entire session participants were seated on a comfortable armchair in front of a monitor showing their muscular activity, at 80 cm of distance. They were asked to keep their right arm in a relaxed position for the entire experiment. During TMS participants wore disposable earplugs to mask the TMS click and avoid possible auditory ERP responses.

2.2 Transcranial Magnetic Stimulation (TMS)

TMS was carried out using a Magstim 200 stimulator with a 70mm figure-of-eight coil (Magstim Company Limited, Whitland, UK), which produced a monophasic waveform with a pulse width of about 0.1 ms. The position of the coil on the scalp was functionally defined: as the M1 site in which TMS evoked the largest MEPs in the relaxed abductor pollicis brevis (APB) muscle of the right hand. The coil was placed tangentially to the scalp at about 45° angle away from the midline, so that the direction of current flow was posterolateral-anteromedial. Stimulation intensity was 95% of resting motor threshold (RMT), defined as the lowest TMS intensity which evoked at least five out of ten MEPs with an amplitude > 50 μV peak-to-peak in the

contralateral APB at rest (Rossini et al., 1994). Single-pulses were delivered with an inter-stimulus interval (ISI) of 4-6 seconds.

2.3 Electromyographic recordings (EMG)

Surface EMG was recorded from the right abductor pollicis brevis (APB), right first dorsal interosseous (FDI) and right abductor digiti minimi (ADM) muscle using Ag/AgCl disc surface electrodes (1 cm of diameter) in a belly-tendon montage. Sweep length run in was 100 ms before and 200 ms after the stimulus. The EMG signal was and analogue filtered at 30-1000 Hz with a Digitimer D150 amplifier (Digitimer Ltd., Welwyn Garden City, UK). Data (sampling rate 4 kHz) was digitized for off-line analysis using Signal software (Cambridge Electronic Devices, Cambridge, UK).

2.4 Electroencephalographic recordings (EEG)

EEG was recorded using a TMS-compatible EEG DC amplifier (Advanced Neuro Technology, Enschede, Netherlands). The amplifier was connected to a PC with Visor software through which EEG was on-line monitored, and to a 64-electrode cap ('Wave-Guard', ANT). EEG was continuously recorded from 31 TMS-compatible Ag/AgCl pellet electrodes mounted on the cap according to the 10-20 international system including: Fp1, Fpz, Fp2, F7, F3, Fz, F4, F8, FC5, FC1, FC2, FC6, T3, C3, Cz, C4, T4, CP5, CP1, CP2, CP6, T5, P3, Pz, P4, T6, PO3, PO4, O1, Oz, O2. Skin impedance was kept below 5 kΩ. Recordings were referenced to left mastoid electrode; the ground electrode was placed on the forehead. Sampling frequency of the EEG signal was 2048 Hz. Off-line analysis was performed with EEGLAB 13.3.2 (Delorme and Makeig, 2004) and Fieldtrip toolbox (Oostenveld et al., 2011), running in a MATLAB environment (Version 7.9.0, MathWorks Inc., Natick, USA). The continuous EEG signal was segmented into epochs starting 500 ms before the TMS pulse and ending 500 ms after it. After this, data from 5 ms before the TMS pulse to 22 ms after were removed from each trial to exclude the TMS artifact through the cubic interpolation function of MATLAB (Thut et al., 2011). The identification of artifacts unrelated to TMS (e.g. eye blinks, muscle activity, electric current) was made using the

independent component analysis (ICA) function on EEGLAB. Identified components were then visually inspected in terms of scalp distribution, frequency, timing and amplitude and removed with ICA (Johnson et al., 2010; Mattavelli et al., 2013). Afterwards, all the epochs were visually inspected and those with excessively noisy EEG were excluded from the analysis (resulting less than 5% for each participant). A baseline correction, taken as the interval starting 100 ms before the TMS pulse, was applied on all the epochs. For the TEP analysis all the epochs of each participant, divided between healthy volunteers and HD patients, were averaged. Data analysis was conducted on different TMS-EEG measures:

- TEPs waveform
- Spectral power
- Scalp maps of voltage distribution
- Time/frequency analysis

2.5 Statistical Analyses

All data were analyzed using SPSS version 19 (SPSS Inc., Chicago, USA). Prior to undergoing ANOVA procedures, normal distribution of EEG data was assessed by means of Shapiro-Wilks' test. Level of significance was set at $\alpha = .05$. Extreme outliers (i.e. 3 standard deviations or more) within individual trials were identified and excluded from the analysis (resulting less than 4% for each participant). EEG analysis was conducted time point-by-time point with a permutation analysis (3000 permutations) within each electrode in order to investigate possible differences in specific time windows among the two groups (healthy volunteers *vs.* patients). For TEPs analysis we considered a time window starting from -100 to +400 ms around the TMS pulse; for spectral and time/frequency analysis we considered a time window starting from -400 to +400 ms around the TMS pulse. In all the TMS-EEG analysis we considered the electrodes nearby the site of stimulation (i.e. C3, FC1, CP1, and CP5) and in the homologous contralateral site (i.e. C4, FC2, CP2, CP6). Sphericity of data was tested with Mauchly's test; when sphericity was violated (i.e. Mauchly's test < 0.05) the Greenhouse-Geisser correction was used. Pairwise comparisons were correct by the Bonferroni method.

3. RESULTS

3.1 TMS-evoked potentials (TEPs) waveform

Figure 4.1 depicts the grand-average EEG waveform evoked by TMS of M1 in healthy volunteers and HD patients. It is appreciable a well-known pattern of TEPs lasting up to around 200 ms composed by five main peaks: P30, N45, P60, N100 and P180. Such pattern was consistent and visible in almost all the electrodes over the scalp, in particular over the electrodes nearby the site of stimulation (i.e. FC1, C3, and CP1).

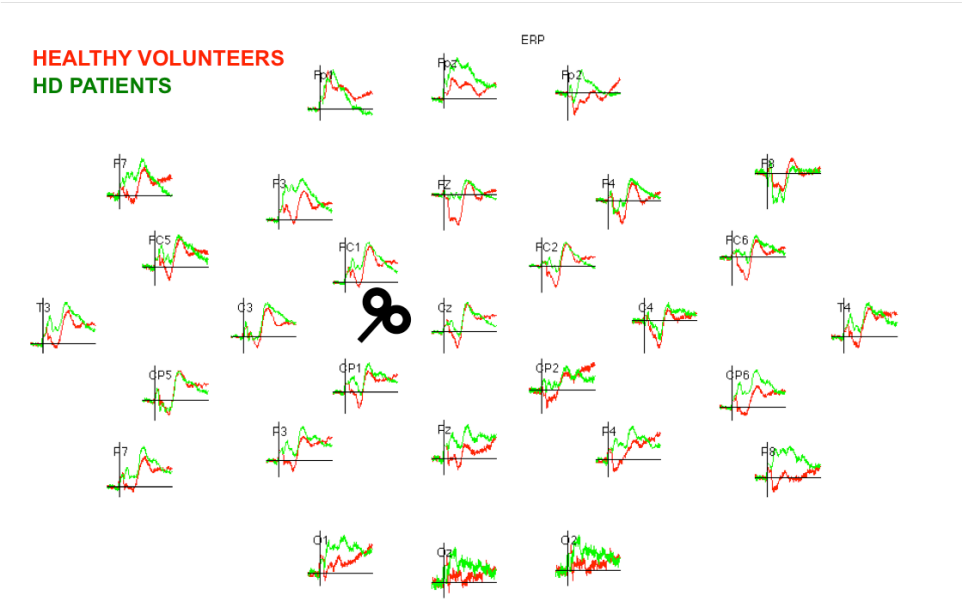

Figure 4.1 Grand-average TEP waveform evoked all over the scalp in healthy volunteers (red line) and HD patients (green line)

The time point-by-time point permutation analysis conducted over the electrodes nearby the M1 hotspot (i.e. site of stimulation) and in the contralateral site revealed the following time windows as significantly different (fig. 4.2):

- *FC1:* from 93 to 106 ms after the TMS pulse
- *Cz:* from 59 to 69 ms and from 90 to 93 ms after the TMS pulse
- *CP1:* from 62 to 96 ms after the TMS pulse
- *FC2:* from 54 to 65 ms and from 88 to 102 ms after the TMS pulse

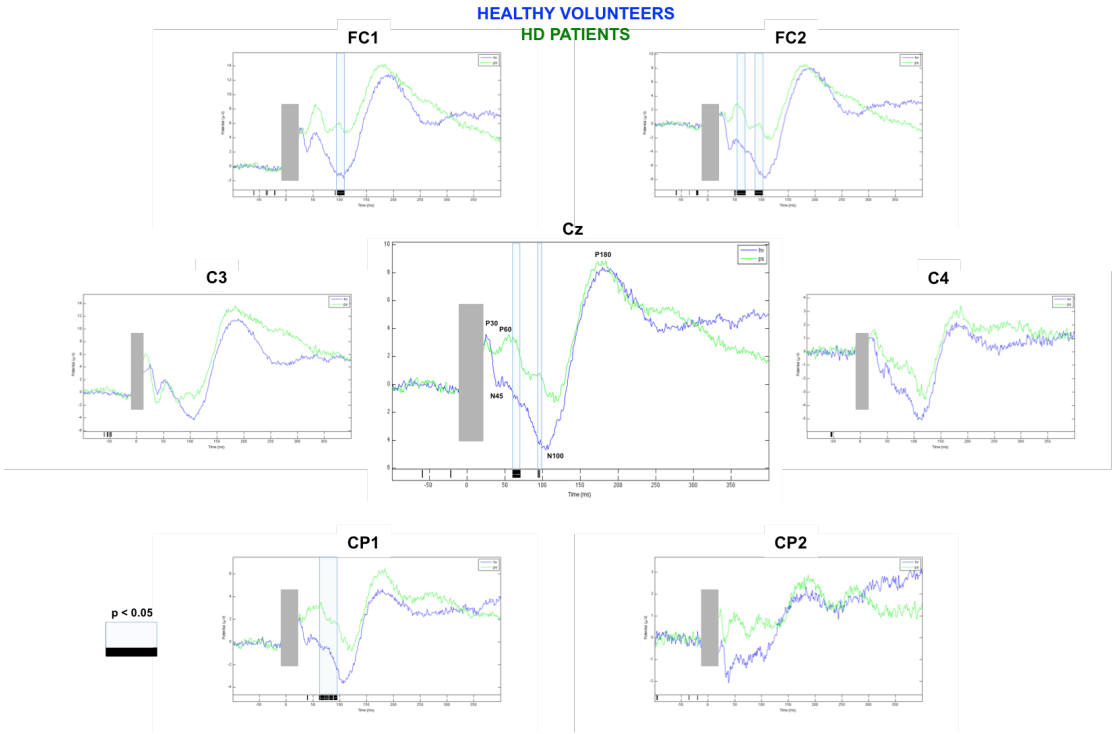

Figure 4.2 Significant time windows in the TEPs waveform evoked in the electrodes nearby the site of stimulation (i.e. APB hotspot over M1) in healthy volunteers (blue line) and HD patients (green line)

The same analysis was conducted by clustering the electrodes of the two ROIs nearby the site of stimulation, the analysis revealed as significantly different the time window of the left ROI starting from 90 ms to 109 ms after the TMS pulse, no difference were detected in the right ROI (fig. 4.3).

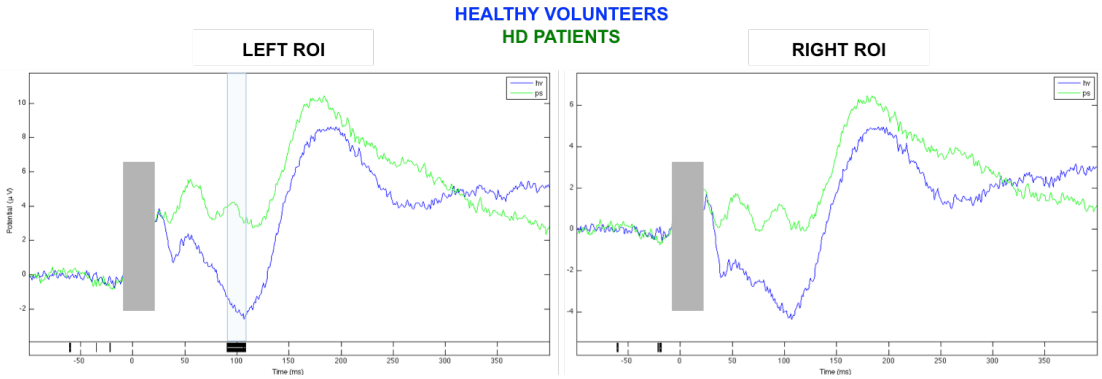

Figure 4.3 Significant time windows in the TEPs waveform evoked in the two ROIs composed by the FC1/FC2, F3/F4, C3/C4 and CP1/CP2 electrodes in stimulated hemisphere (left) and in the contralateral one (right).

3.2 Scalp maps of activity distribution

Following the results on TEPs waveform, we investigated the differences in the mean global activity evoked between 90 and 104 ms after TMS pulse, the topographic maps of this time windows are depicted in fig. 4.4. The following electrodes were detected as significantly different between the two groups: FC1, CP1, FC2, FC6 ($p < 0.05$) and F3, F7, CP6, P8 ($p < 0.02$). From the topographic maps it is observable a general decrease of negativity in HD patients, except from the frontal electrodes.

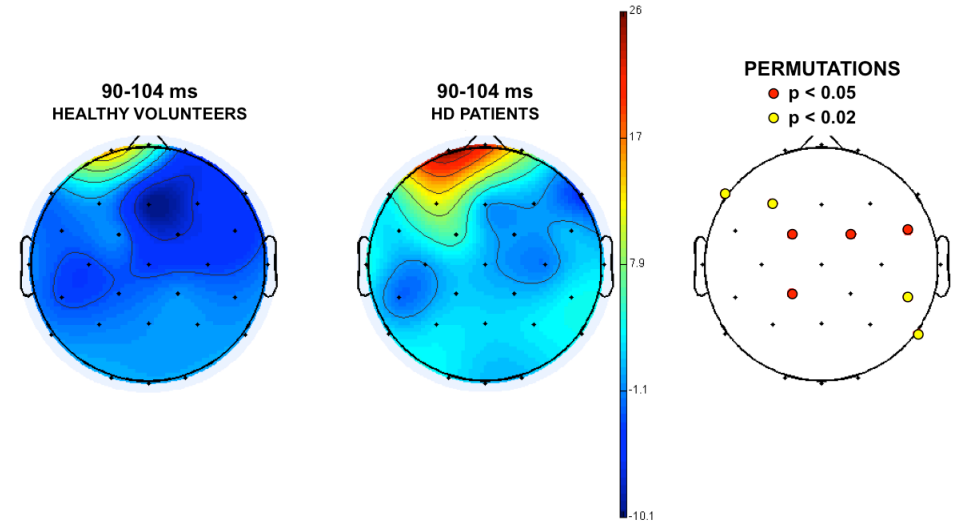

Figure 4.4 Topographic maps of the mean global activity evoked in the time window between 90 and 104 ms after the TMS pulse

3.3 Time/frequency analysis

3.3.1 Event-related spectral perturbation

Event-related spectral perturbation analysis (ERSP) was conducted to assess any change in the oscillatory activity during the entire time window considered. Figure 4.5a depicts the permutation analysis conducted on ERSP to investigate any difference between healthy volunteers and HD patients. Such analysis was conducted in the electrodes nearby the site of stimulation (i.e. FC1, C3 and CP1) and in the homologous contralateral ones (i.e. FC2, C4 and CP2). The analysis revealed significant differences only in the high-frequency beta and gamma range of activity (i.e. 24-40 Hz). Specifically, significant differences were detected over the entire range of frequency in different time points of the baseline activity (i.e. before the

TMS pulse; fig. 4.5a). As regards the post-TMS activity, stronger significant changes were detected over the contralateral hemisphere in particular over the C4 electrode (range 28-40 Hz) between 170 and 210 ms after the TMS pulse. In the stimulated hemisphere, significant differences were detected in the FC1 and C3 electrode in a large range of frequency (24-30 Hz) but only at the end of the considered time window (around 400 ms after the TMS pulse). Significant difference we also detected in the CP1 electrode in a high-frequency range (33-40 Hz) at two specific time windows: around 40 and 100 ms after the TMS pulse (fig. 4.5a).

3.3.2 Inter-trial coherence

Inter-trial coherence analysis (ITC) was conducted to assess the consistency of local phase of the TEPs waveform across all the trials. Figure 4.5b depicts the permutation analysis conducted on ITC to investigate any difference between healthy volunteers and HD patients. Significant changes were detected in the electrode CP1 (range 24-30 Hz), specifically between 50 and 92 ms after the TMS pulse. The same temporal window was detected as significantly different in the three contralateral electrodes (i.e. FC2, C4, and CP2) in a higher range of frequency (30-40 Hz). Other significant differences were detected in the right side after 200 ms from the TMS pulse, in several ranges of frequencies.

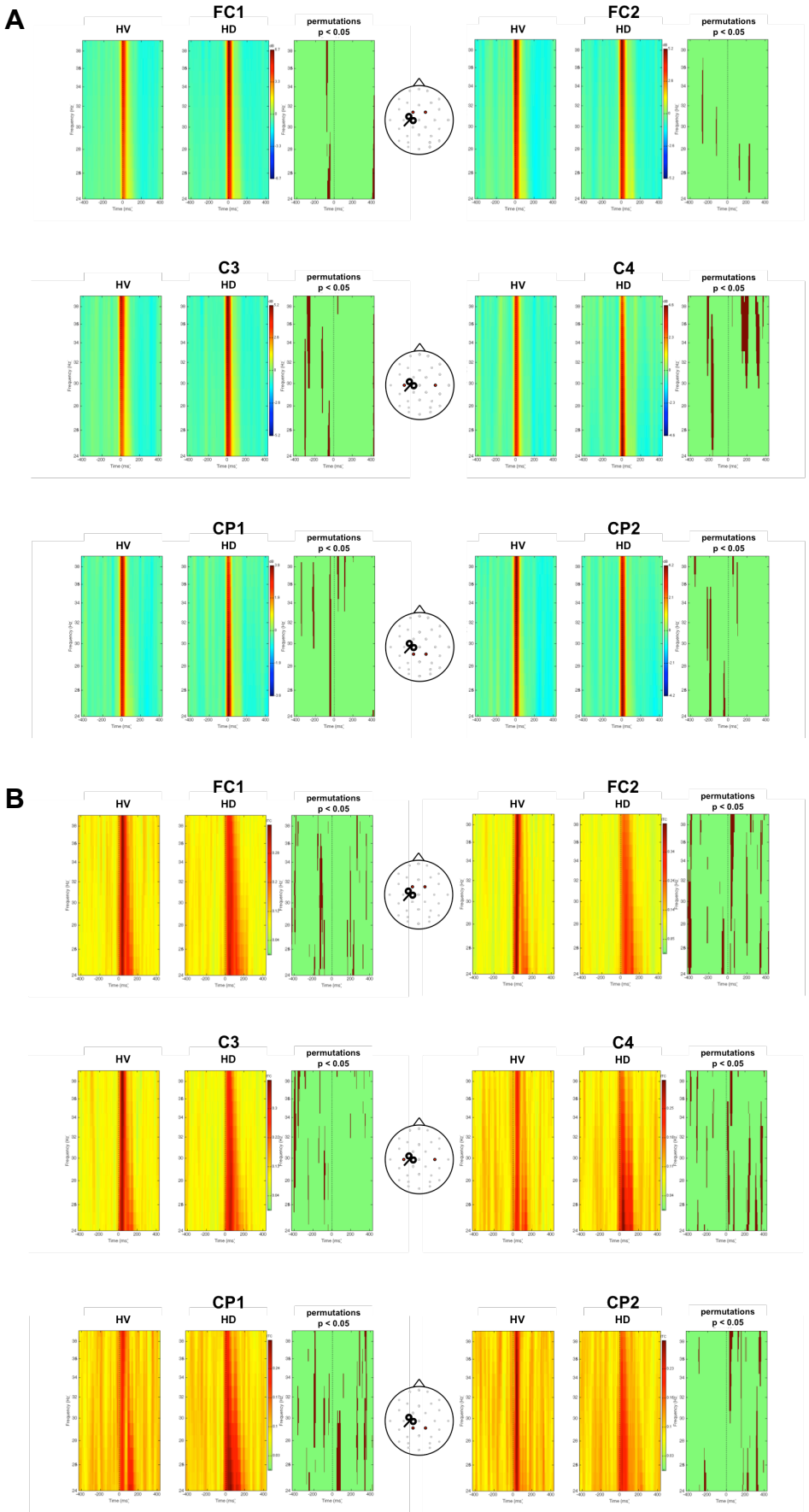

Figure 4.5 Event-related spectral perturbation (a) and Inter-trial coherence (b) analysis conducted in three electrodes nearby the site of stimulation (FC1, C3, CP1) and contralaterally (FC2, C4, CP2)

4. DISCUSSION

The main target of this study was to identify possible electrophysiological markers of Huntington's disease through the simultaneous use of TMS and EEG. As previously stated, the use of TEPs and other TMS-EEG measures for clinical and diagnostic purposes is growing (e.g. Ferrarelli et al., 2008; Helfrich et al., 2013). TEPs have been recently related to the activity of different GABAergic neuronal populations (Ferreri et al., 2011; Rogasch and Fitzgerald, 2013; Premoli et al., 2014), opening new fascinating prospective in their investigation in pathologies with GABA-related deficits.

In the present results we found a specific and significant decrease of the TMS-induced activity between 90 and 109 ms after the TMS pulse (fig. 4.3). Such decrease was prominent in a cluster of electrodes surrounding the site of stimulation, namely the left primary motor cortex. TEPs waveform showed a prominent negativity between 90 and 110 ms after the TMS pulse (fig. 4.1, 4.2, 4.3), that is the TMS-evoked N100, a TEPs that has been recently linked to GABAb-ergic inhibitory processes (Rogasch and Fitzgerald, 2013; Casula et al., 2014; Premoli et al., 2014). HD patients showed an N100 that was about three times lower than the one observed in healthy volunteers. The analysis of the mean activity within this time window showed a significant reduction of the negativity in a large area involving both the hemispheres. Notably, the effect was stronger over the site of stimulation and in lateral and frontal electrodes ($p < 0.02$), however, this later effect is likely to be generated by artefactual activity (muscular, eye blink) (fig. 4.4).

Previous studies found a strong reduction in the TMS-evoked N100 amplitude in different conditions of lower cerebral inhibition related to the activity of GABAergic neurons. For instance, a number of studies using motor behavioural tasks showed a dramatic decrease in N100 amplitude during movement preparation (i.e. a condition of lower cortical inhibition; e.g. Bonnard et al., 2009). Along the same lines, studies using paired-pulse TMS found a significant correlation between the N100 amplitude and the GABAb-ergic EMG measures of CSP and LICI, whose timing coincides with the N100 peak (Daskalakis et al., 2008; Fitzgerald et al., 2008).

Huntington's disease is characterized by a severe and progressive loss of CB1 receptors. Such receptorial degeneration usually precedes the manifestation of the pathology. Notably, CB1 receptors are highly expressed in GABAergic neurons which

constitute about the 95% of the neurons in the striatum, a cerebral area that is highly affected in HD. Stimulation of CB1 receptors results in a decrease of GABA release leading to a reduction of inhibition and, consequently, to an excessive increase in glutamatergic excitability. The observed decrease of N100 might be a consequence of the lower GABAergic inhibition that causes excitoxicity in HD patients, leading to a severe loss of neurons in the striatum. These results might be corroborated by the significant differences in oscillatory activity revealed by the ERSP and ITC analysis in the GABAb-ergic time window (i.e. from 60 ms to about 250 ms after the TMS pulse), although several differences were also revealed in the baselines of the two groups, this is an aspect that deserves further analysis.

5. CONCLUSIONS

Although preliminary, the present results might be of interest for a possible role of the TMS-evoked N100 in the assessment of inhibitory deficits in HD patients. The observed reduction was specific for the N100 time window and was stronger in the site of stimulation, demonstrating that it was related to TMS and not to other confounding factors. A number of neurophysiological, neuroimaging and clinical measures were taken in this project and not reported in the present study. Future studies are needed to look for possible correlations between the observed TMS-EEG results and other measures.

CHAPTER V
STUDY 3 - TMS-EEG ARTIFACTS: A NEW ADAPTIVE ALGORITHM FOR SIGNAL DETRENDING

1. INTRODUCTION

Transcranial magnetic stimulation (TMS) is a technique able to non-invasively stimulate and modulate the excitability of the brain through the electromagnetic induction of an electric field directly in the cortex (Barker et al., 1985). In the last twenty years, the combination of this technique with electroencephalography (EEG) has provided new insights into the investigation of brain dynamics (Ilmoniemi and Kičić, 2010). The EEG is able to record the post-synaptic potentials generated by the neuronal depolarization TMS-evoked providing accurate information on the reactivity of the stimulated area and on its connections over the entire cortex (Ilmoniemi et al., 1997). Besides these advantages, the simultaneous use of TMS-EEG poses several technical issues. Indeed, TMS during EEG results in a number of artifacts of physiological and electrical nature. Three main physiological artifacts are indirectly produced by TMS: (1) auditory artifacts, generated by the sound of the stimulation (Tiitinen et al., 1999); (2) blink artifacts, resulting from a startle response produced by the stimulation (Bruckmann et al., 2012); (3) muscular artifacts, resulting from the stimulation of scalp muscles (Kohronen et al., 2011). A number of methods have been developed to avoid this kind of artifacts, such as the use of a white noise (Massimini et al., 2005); the use of a thickness between the TMS and the scalp (Nikouline et al., 1999) and the re-orientation of the coil (Mutanen et al., 2013). In addition, it has been demonstrated the efficacy of some off-line procedures in removing these artifacts, such as independent component analysis (ICA) (Hernandez-Pavon et al., 2012) and principal component analysis (PCA) (Litvak et al., 2007). TMS artifacts of electrical nature are more complicated to detect and remove from the signal. The voltage induced in the electrodes by the TMS pulse is several orders of magnitude larger than the physiological responses and this

can cause large artifacts in the recording (Virtanen et al., 1999). The first artifact, which is directly produced by the TMS pulse, is a large bipolar artifact of several mV whose length can vary from 5 (Veniero et al., 2009) to 30 ms (Zanon et al., 2010) after the pulse. A subsequent long-lasting artifact has also been reported by a number of studies with the name of "residual artifact" or "long-lasting TMS-artifact" (Komssi et al., 2004; Litvak et al., 2007; Julkunen et al., 2008; Veniero et al., 2009; Zanon et al., 2010; Kohronen et al., 2011; Rogasch et al., 2012; Sekiguchi et al., 2011; Tar Braack et al., 2013). However, only recently this type of artifact has been accurately described by Rogasch and colleagues (2014) and termed "decay artifact" (Rogasch et al., 2014). This artifact is characterized by a slow drift of the signal of a few electrodes (usually the ones underneath the stimulating coil) impeding the correct realignment to the baseline level for tens or hundreds of milliseconds after the TMS pulse (fig. 5.1; Siebner et al., 2009; Ilmoniemi et al., 2010; Rogasch et al., 2012; 2014).

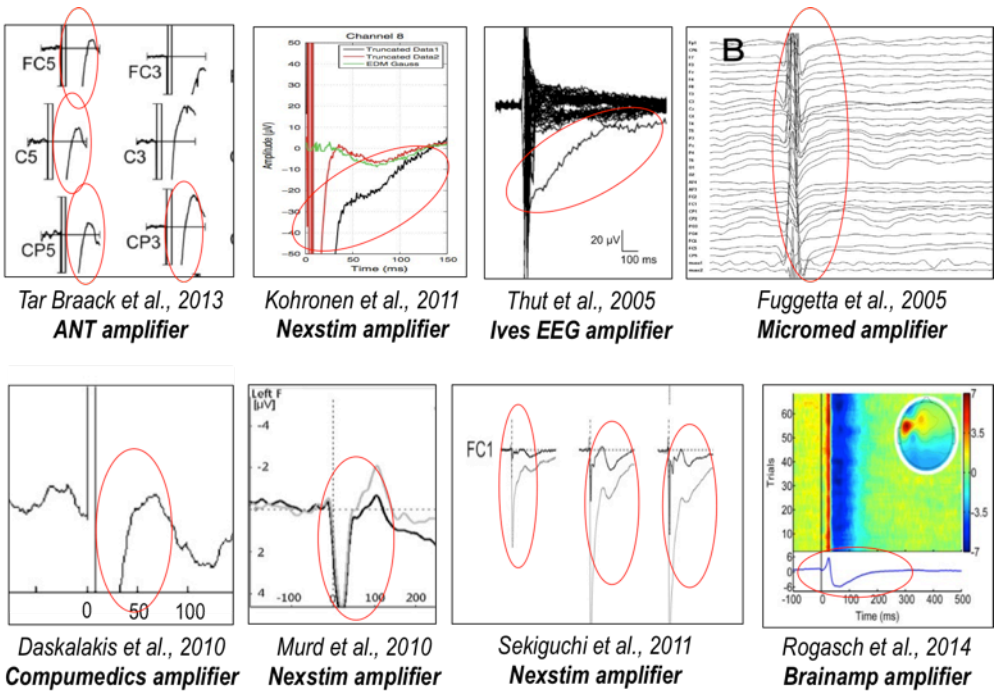

Figure 5.1 Examples of decay artifact recorded with different TMS-compatible EEG amplifiers

The origin of the decay artifact is still a matter of debate: some authors hypothesized that during the TMS pulse some currents can pass through the electrode-electrolyte interface causing a polarization and, consequently, an EEG baseline shift (Siebner et al., 2009; Veniero et al., 2009; Ilmoniemi and Kičić, 2010). Others possible

explanations of the decay artifact have been related to the electromotive forces induced in the electrode wires (Sekiguchi et al., 2011) or to the scalp muscular activity evoked by the stimulation (Rogasch et al., 2014). Importantly, the decay artifact seems not to corrupt the TEPs waveform (Zanon et al., 2010; Rogasch et al., 2014).

Throughout the years, both on-line and off-line strategies have been developed to deal with the electric TMS-induced artifacts. The progressive improvements in the amplifier technology have allowed the removal or the reduction of the TMS pulse-induced artifact during the EEG recording. In 1999, Virtanen and colleagues developed a sample-and-hold EEG system able to block the recording for a few ms preventing large artifacts. In 2003, Thut and colleagues used a slew-rate limited preamplifier to prevent the saturation of the circuits allowing the continuous recording of the signal during TMS. Finally, in 2006, Bonato and colleagues used a TMS-compatible DC amplifier able to work in a large operating range allowing the recording of the TMS-evoked potentials (TEPs) within 10 ms after the TMS. Different off-line strategies of correction have also been developed following two approaches: a "subtraction approach" in which a template artifact generated through a phantom (Bender et al., 2005) or a TMS control condition (Thut et al., 2003) is subtracted from the real data; and a "correction approach" in which the TMS pulse-induced artifact is removed through the use of filtering (Morbidi et al., 2007; Fuertes et al., 2010) or digital correction (Litvak et al., 2007). In addition, several studies have suggested rearrangements of the experimental setting in order to minimize the influence of the TMS-related artifacts (Julkunen et al., 2008; Veniero et al., 2009; Sekiguchi et al., 2011).

Despite these strategies have been successfully applied for the TMS-pulse artifact, their feasibility in removing the decay artifact is problematic for two main reasons: first, the duration of the decay is longer than the time of amplifier disconnection in sample-and-hold systems; second, the high variability in amplitude and latency of the artifact make difficult its off-line removal. In an attempt to solve this problem, some studies interpolated the electrodes that are affected by the artifact (e.g. Bender et al., 2005). However, this poses two main problems: firstly, the electrodes mostly affected by the artifact are the ones nearby the site of stimulation, where also the physiological responses are the strongest, so important information

can be lose after the interpolation; secondly, even the interpolating electrodes surrounding the affected ones usually are at least partially affected by the artifact, making the interpolation problematic or inefficient. Alternatively, two main strategies of correction have been used in literature. Some studies applied a linear detrend function in order to realign the signal on the baseline level (e.g. Van der Werf et al., 2006; Zanon et al., 2010). Other studies used independent component analysis (ICA) to identify and subsequently remove the components related to the decay artifact (e.g. Kohronen et al., 2011; Ter Braack et al., 2013; Rogasch et al., 2014). However, none of these solutions may be considered optimal. The linear detrend fits and subtracts a linear model to the drift assuming that the decay artifact follows a linear trend, which is not always true, especially for the first part of the decay (Litvak et al., 2007). Indeed, in most of the cases the decay artifact follows a non-linear trend, so that the correction with a standard linear detrend might cause an uncompleted removal of the decay or a distortion of the signal. ICA is a computational method for decomposing multivariate signals into additive independent non-gaussian signals, which has been successfully applied to multi-channel EEG data (Onton et al., 2006). Although ICA has been used to correct muscle and blink artifacts (Hamidi et al., 2010; Hernandez-Pavon et al., 2012; Mattavelli et al., 2013), it presents a number of limitations in the correction of the decay artifact. First, the characteristics of the decay artifact are highly variable within and between subjects: the drift can follow a linear or a non-linear trend, the amplitude can vary from a few μV to tens of μV and the length of the baseline shift can last from around 50 to hundreds of ms after the pulse (Rogasch et al., 2014), making its identification with ICA problematic. Second, it cannot be excluded that also physiological responses are partly removed with the rejection of the ICA artifact-related components (Veniero et al., 2013). Third, a standard procedure to identify an ICA component as related to the decay is still lacking and the different criteria applied in literature are rarely specified in papers, making the choice to reject a component too arbitrary and dependent from the experimenter's decision. Fourth, ICA efficiency in identifying components is critically dependent from the number of sources (i.e. electrodes) recorded, as well as from the type of ICA algorithm used, which is also rarely specified in papers.

Starting from these considerations, in the present paper we propose a new adaptive detrend algorithm able to discriminate the different trends of the decay artifact (i.e. linear or non-linear) and to adaptively compute and subtract a different model to the drift. Our target is to test the efficiency and the reliability of this algorithm in correcting the decay artifact produced by TMS. To this aim, we test the efficiency of different solutions by correcting the decay artifact with three ICA procedures and with our algorithm, and then we compared different TMS-EEG measures. To test the effect of different ICAs, we chose to separately run two algorithms of correction already used in TMS-EEG literature (INFOMAX and fastICA) including either 29 and a subselection of 15 electrodes.

2. METHODS

2.1 Participants and procedure

Forty right-handed healthy volunteers (17 males, mean age 25±4 years) were enrolled for the experiment after giving written informed consent. Four participants were subsequently excluded from the study due to excessively noise in their EEG. All participants were tested for TMS exclusion criteria (Rossi et al., 2009). The experimental procedure was approved by the Institutional Review Board of the University of Padua, and was in accordance with the Declaration of Helsinki (Sixth revision, 2008). Each participant underwent a TMS session consisting of 55 single-pulses delivered over the primary motor cortex (M1) during multichannel EEG recordings. During the entire session participants were seated on a comfortable armchair in front of a monitor at 80 cm of distance. They were asked to fixate a white cross (6×6 cm) in the middle of a black screen and to maintain a relaxed position. During TMS participants wore in-ear plugs, which continuously played a white noise that reproduced the specific time-varying frequencies of the TMS click, in order to mask the click and avoid possible auditory ERP responses (Massimini et al., 2005). The intensity of the white noise was adjusted for each subject by increasing the volume (always below 90 dB) until the participant was sure that s/he could no longer hear the click (Paus et al., 2001). To reduce the bone-conducted sound we used an EEG cap with a 4 mm plastic sheet that reduced the transmission

of mechanical vibration produced by the coil (Nikouline et al., 1999; Esser et al., 2006).

2.2 Transcranial magnetic stimulation (TMS)

TMS was carried out using a Magstim R^2 stimulator with a 70mm figure-of-eight coil (Magstim Company Limited, Whitland, UK), which produced a biphasic waveform with a pulse width of ~0.1 ms. The position of the coil on the scalp was functionally defined as the M1 site in which TMS evoked the largest MEPs in the relaxed first dorsal interosseous (FDI) muscle of the right hand. The coil was placed tangentially to the scalp at about 45° angle away from the midline, so that the direction of current flow in the most effective (second) phase was posterolateral-anteromedial. To ensure the same stimulation conditions during the entire experiment, coil positioning and orientation on the optimal hotspot were constantly monitored by means of the Brainsight neuronavigation system (using the ICBM152 template), coupled with a Polaris Vicra infrared camera (NDI, Waterloo, Canada). Stimulation intensity was set at 120% of the resting motor threshold (RMT), defined as the lowest TMS intensity which evoked at least five out of ten MEPs with an amplitude > 50 μV peak-to-peak in the contralateral FDI at rest (Rossini et al., 1994). Single-pulses were delivered with an inter-stimulus interval (ISI) of 4-6 seconds. Surface EMG was acquired from the right FDI muscle via Ag/AgCl electrodes in a belly-tendon montage (Myohandy Matrix Line – Micromed Srl, Mogliano Veneto, Italy); raw signals were sampled at 2.5 kHz and band-pass filtered at 50-1000 Hz. EMG signal was on-line monitored by software Brain-Quick System Plus using epochs of 50 ms.

2.3 Electroencephalographic (EEG) recordings

EEG was recorded using a TMS-compatible AC amplifier (Micromed SD MRI, Micromed Srl., Mogliano Veneto, Italy) designed to work in presence of high external magnetic fields as used in TMS or MRI (Morbidi et al., 2007). The amplifier was optically connected to a PC with software Brain-Quick System Plus through which EEG was on-line monitored, and to a 64-channels customized EEG cap (EasyCap Inc.,

Herrsching, Germany). EEG was continuously recorded from 29 TMS-compatible Ag/AgCl pellet electrodes mounted on the cap according to the 10-20 international system including: Fpz, F7, F3, Fz, F4, F8, FC5, FC1, FC2, FC6, T3, C3, Cz, C4, T4, CP5, CP1, CP2, CP6, T5, P3, Pz, P4, T6, PO3, PO4, O1, Oz, O2. Skin impedance was kept below 5 kΩ. Recordings were referenced to AFz electrode; the ground electrode was placed on POz. EEG signal was bandpass filtered at 0.1-500 Hz and the sampling frequency was 2048 Hz.

2.4 EEG data processing

Off-line analysis was performed with EEGLAB 13.3.2 (Delorme and Makeig, 2004) and Fieldtrip toolbox (Oostenveld et al., 2011), running in a MATLAB environment (Version 7.9.0, MathWorks Inc., Natick, USA). The continuous EEG signal was down-sampled to 1024 Hz and segmented into epochs starting 100 ms before the TMS pulse and ending 500 ms after it. A baseline correction, taken as the interval starting from 100 to 5 ms before the TMS pulse, was applied on all the epochs. Data from -5 ms before the TMS pulse to 20 ms after were removed from each trial to exclude the TMS pulse-induced artifact and then interpolated through the cubic interpolation function of MATLAB (Thut et al., 2011). A 50 Hz notch filter was applied to reduce noise from electrical sources. After this, all the epochs were visually inspected and those excessively noisy were excluded from the analysis (resulting less than 5% for each participant). The identification of artifacts was made using the INFOMAX independent component analysis (ICA) algorithm on EEGLAB (Delorme and Makeig, 2004). We firstly looked for the components reflecting the artifacts unrelated to TMS (i.e. eye blinks, muscle activity). The identified components were visually inspected in terms of scalp distribution, frequency, timing and amplitude and then removed. None of the components related to the decay artifact (Rogasch et al., 2014) were removed at this point. Such artifact was subsequently corrected with four different algorithms, separately for each EEG dataset: (1) an INFOMAX ICA considering all the 29 channels; (1) an INFOMAX ICA with 15 channels (F3, Fz, F4, FC1, FC2, C3, Cz, C4, CP1, CP2, P3, Pz, P4, O1, O2); (3) a fastICA considering all the 29 channels and (4) the adaptive detrend algorithm described in paragraph 1.5. In this way we could investigate the influence of the number of recording sources in the ICA correction

(29 *vs.* 15) and different kinds of ICA algorithm (INFOMAX *vs.* fastICA). For the INFOMAX15 condition, we chose 15 electrodes covering the entire the entire scalp including all the electrodes surrounding the site of stimulation, which was between C3 and FC1. The criteria to define an ICA component as related to the decay artifact were:

- *Waveform*: we considered the components showing a typical decay trend starting from a few ms after the TMS pulse (the first 21 ms were interpolated) to at least 50 ms;
- *Temporal distribution*: we considered the components showing a constant decay trend for at least 75% of the trials;
- *Spatial distribution*: we considered the components distributed over the electrodes that were mainly affected by the stimulation (previously identified by inspecting the raw data)

Components that satisfied all the three criteria were considered related to the decay artifact and then removed. A few examples of such components are presented in fig. 5.3. To verify the reliability of our identification procedure, this was separately performed by two experimenters (EPC and VT) and repeated after three weeks. After all the pre-processing steps each subject had five datasets:

- An EEG dataset of 29 channels corrected with an INFOMAX ICA (INFOMAX29 condition);
- An EEG dataset of 15 channels corrected with an INFOMAX ICA (INFOMAX15 condition);
- An EEG dataset of 29 channels corrected with a fastICA (fastICA condition);
- An EEG dataset of 29 channels corrected with our adaptive detrend algorithm (ALG condition);
- An EEG dataset of 29 channels with no correction of the decay artifact (RAW condition).

2.5 Adaptive detrend algorithm

The algorithm script was developed in a MATLAB environment (Version 7.9.0, MathWorks Inc., Natick, USA). As a first step, for each channel, the average acquired signal in the interval 20-500 ms after TMS was modeled using a regression line:

$$z_{(20-500)}(t) = m \cdot t + q$$

And subsequently using a two-exponential function:

$$z_{(20-500)}t = A1 \cdot \exp(a_1 t) + A2 \cdot \exp(a_2 t)$$

Measurement error was assumed to be additive, uncorrelated, gaussian, zero mean, and with constant variance. The parameters [m, q], of the regression line were estimated by weighted linear least squares while for the two-exponential function the weighted non-linear least squares were used [*A1*, *a1*, *A2*, *a2*]. To make a selection between the two functions in term of model parsimony, the Akaike information criterion (AIC) was used:

$$AIC = Nlog(WRSS) + 2 \cdot P$$

Where *WRSS* is the weighted residual sum of squares (i.e. the weighted sum of the squares of the difference between acquired data and predicted values), P is the number of parameters (i.e. 2 for the regression line, 4 for the two-exponential function) and N is the number of the data points used to fit the functions. The function having the lowest AIC value was selected as the best to describe the decay artifact and used to correct the acquired signal as:

$$z^{correct}_{(20-500)}(t) = z^{acquired}_{(20-500)}(t) - z^{best\ model}_{(20-500)}(t)$$

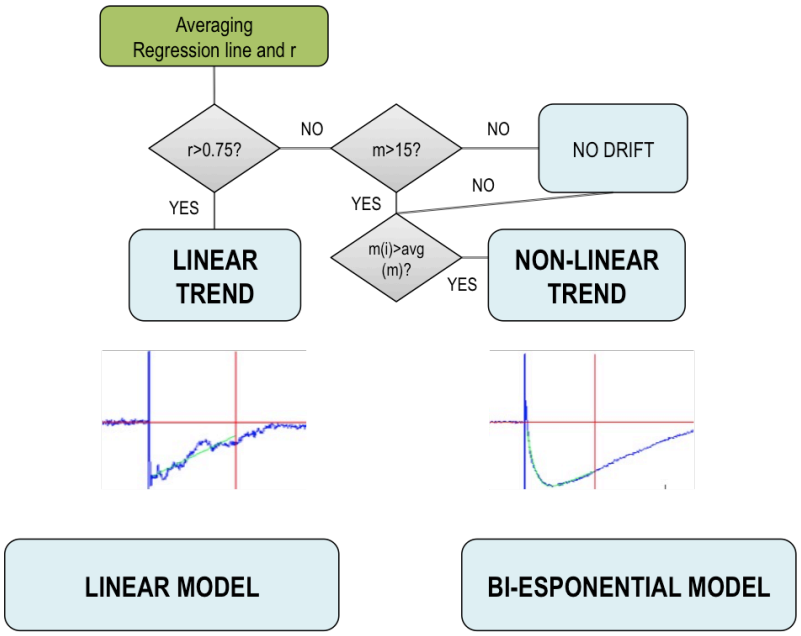

Figure 5.2 Flowchart of the adaptive detrend algorithm (r, regression coefficient; m, slope)

2.6 TMS-EEG data analysis

For the TEPs analysis, all the epochs of each participant were averaged separately for the five conditions. Based on the recent literature (for a review, Ilmoniemi and Kičić, 2010), we chose five time windows to determine the TEPs amplitudes and latencies, computed peak-to-peak in the following intervals: 23-45 ms (positive peak); 30-60 ms (negative peak); 45-70 ms (positive peak); 70-130 ms (negative peak); 130-230 ms (positive peak). The peak-to-peak measure allowed us to compare the relative amplitude and latency of the TEPs among the different conditions, regardless the baseline shift caused by the decay artifact. To assess the total brain activation induced by TMS, we performed a local mean field power analysis (LMFP; Lehmann and Skrandies, 1980; Pellicciari et al., 2013) computed as:

$$MFP(t) = \sqrt{\frac{[\sum_i^k (V_i(t) - V_{mean}(t))^2]}{K}}$$

Where t is time, K the number of channels, V_i the voltage in channel i averaged across subjects and V_{mean} is the mean of the voltage in all the channels. Such measure was computed considering the seven electrodes nearby the site of

stimulation in both the hemispheres: F3/F4, C3/C4, P3/P4, FC1/FC2, CP1/CP2, FC5/FC6, CP5/CP6.

2.7 Statistical analysis

Prior to undergoing ANOVA procedures, normal distribution of EEG data was assessed by means of Shapiro-Wilks' test. Level of significance was set at $\alpha = .05$. Extreme outliers (i.e. 3 standard deviations or more) within individual trials were identified and excluded from the analysis (resulting less than 4% for each participant). To assess whether the artefact correction significantly affected the signal, we separately compared the original signal (i.e. RAW condition) with all the other conditions using a non-parametric, cluster-based permutation statistics conducted at each time point within the considered time window (-100 + 500 ms from the TMS pulse) for each individual electrodes (Maris and Oostenveld, 2007). This method performs a non-parametric statistical test by calculating Monte Carlo estimates of the significance probabilities from the permutation distribution obtained by randomly permuting the two conditions over the condition-specific data for 3000 times. The clusters for permutation analysis were defined as the two (or more) neighbouring electrodes in which the t-value at a given time point exceeded a threshold of $p < 0.05$. Once we found the electrodes and the time windows in which the corrected signals significantly differed from the original (i.e. Monte Carlo p values < 0.05), we compared the TEPs among three conditions: RAW *vs.* ICA correction *vs.* ALG correction by means of a repeated-measures ANOVA with condition (RAW, ICA correction, ALG correction), TEP (P30, N45, P60, N100 and P180) and electrode as factors. We performed three separate ANOVAs for each ICA correction (i.e. INFOMAX 29, INFOMAX 15 and fastICA) comparing the significant time windows in common among the three conditions. Sphericity of data was tested with Mauchly's test; when sphericity was violated (i.e. Mauchly's test < 0.05) the Greenhouse-Geisser correction was used. Pairwise comparisons were correct by the Bonferroni method.

3. RESULTS

3.1 ICA components related to the decay artifact

The identification procedure of the decay-related ICA components was stable and reproducible both within ($p > 0.05$) and between-experimenters ($p > 0.05$). We removed 3±1.3 components in the INFOMAX29 condition; 3±1 in the fastICA condition and 2±0.7 components in the INFOMAX15 condition. All the components removed presented the three criteria explained in paragraph 1.5. Fig. 5.3 represents some examples of the components removed.

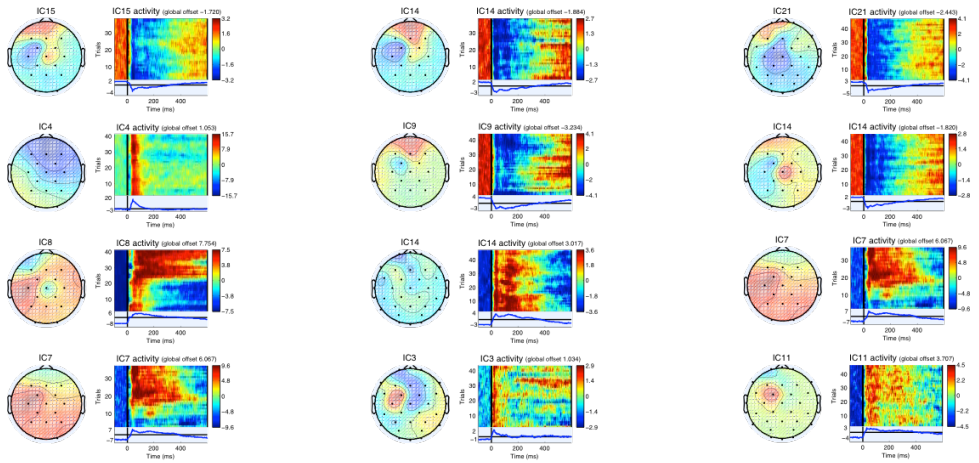

Figure 5.3 Examples of ICA components related to the decay artifact. All the component presented a clear decay waveform in at least 70% of the total number of trial and a dipole in the area of stimulation.

3.2 Decay artifact and voltage distribution scalp maps

Figures 5.4 and 5.5 depict the butterfly chart of the grand-average waveform of the 36 subjects with the topographic voltage distribution at specific time points corresponding to the peaks of EEG activity. A clear decay artifact is observable in the uncorrected data (RAW condition; fig. 5.4): three electrodes (C3, FC1, and CP1) showed a positive decay artifact with maximum amplitude of ~5 (CP1), ~9 (C3) and ~15μV (FC1), lasting for about 400 ms (CP1) or more (FC1, C3). Notably, these electrodes were the closest to the site of stimulation. A strong negative shift of the signal was also appreciable in two electrodes of the hemisphere contralateral to the stimulation (FC2, CP2), although in this case the signal seems to realign to the baseline level at around 150 ms from the TMS pulse. Scalp maps of the voltage distribution (fig. 5.4) showed a clear dipole over the site of stimulation. Specifically, the area around the site of stimulation, comprising the electrodes C3, FC1 and CP1,

showed a sustained positivity lasting for more than 400 ms after the TMS pulse, which represents the decay artifact in these electrodes. The negative shift observed over a few electrodes of the contralateral hemisphere was also observable until 100-150 ms from the TMS pulse. Such dynamic seems to be partially reduced after the INFOMAX29 and fastICA corrections (fig. 5.5a and b). A positive decay was still present at 400 ms over the site of stimulation, in particular to FC1 (fig. 5.5a and b). After the INFOMAX15 correction the FC1 and C3 electrodes were realigned to a standard range of amplitude (from +4 to -6 μV) even if a positive shift from the baseline is still appreciable at 400 ms from the TMS pulse (fig. 5.5c). After the ALG correction (fig. 5.5d) the channels were realigned to a standard range of amplitude (from +4 to -6 μV) no evoked activity was visible from 280 ms after the TMS pulse, as usually reported (Paus et al., 2001; Komssi et al., 2002; Bender et al., 2005; Bonato et al., 2006; Lioumis et al., 2009; Ferreri et al., 2011; Veniero et al., 2013). At 400 ms from the TMS pulse the voltage distribution on the scalp was around 0 μV.

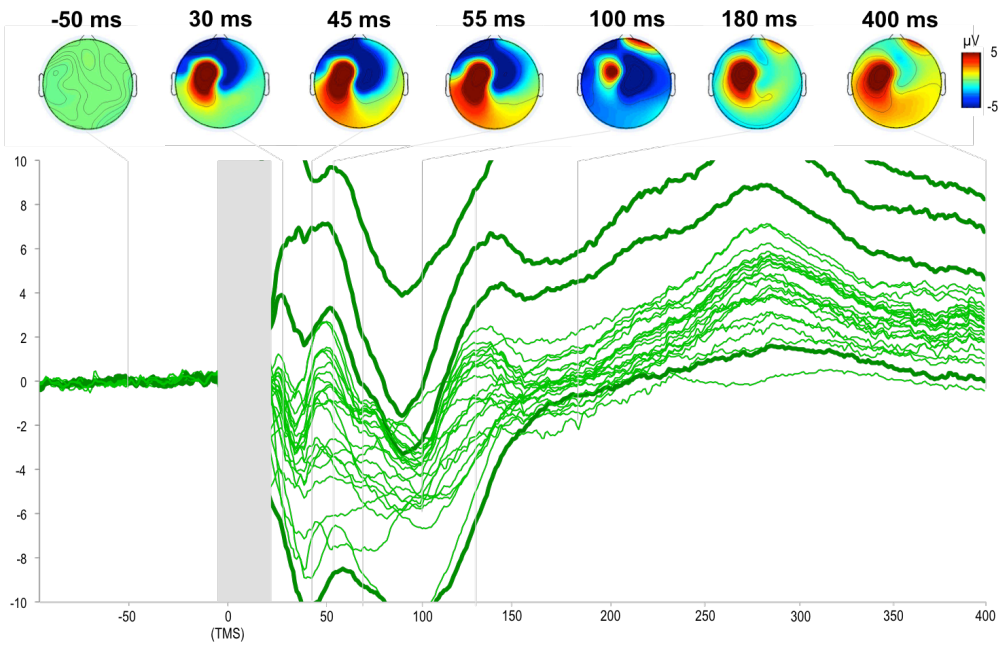

Figure 5.4 Grand-averaged TEP waveform with voltage distribution scalp maps of the RAW condition. Thick lines represent the electrodes showing a clear decay artifact (i.e. from above, FC1, C3, CP1 and FC2)

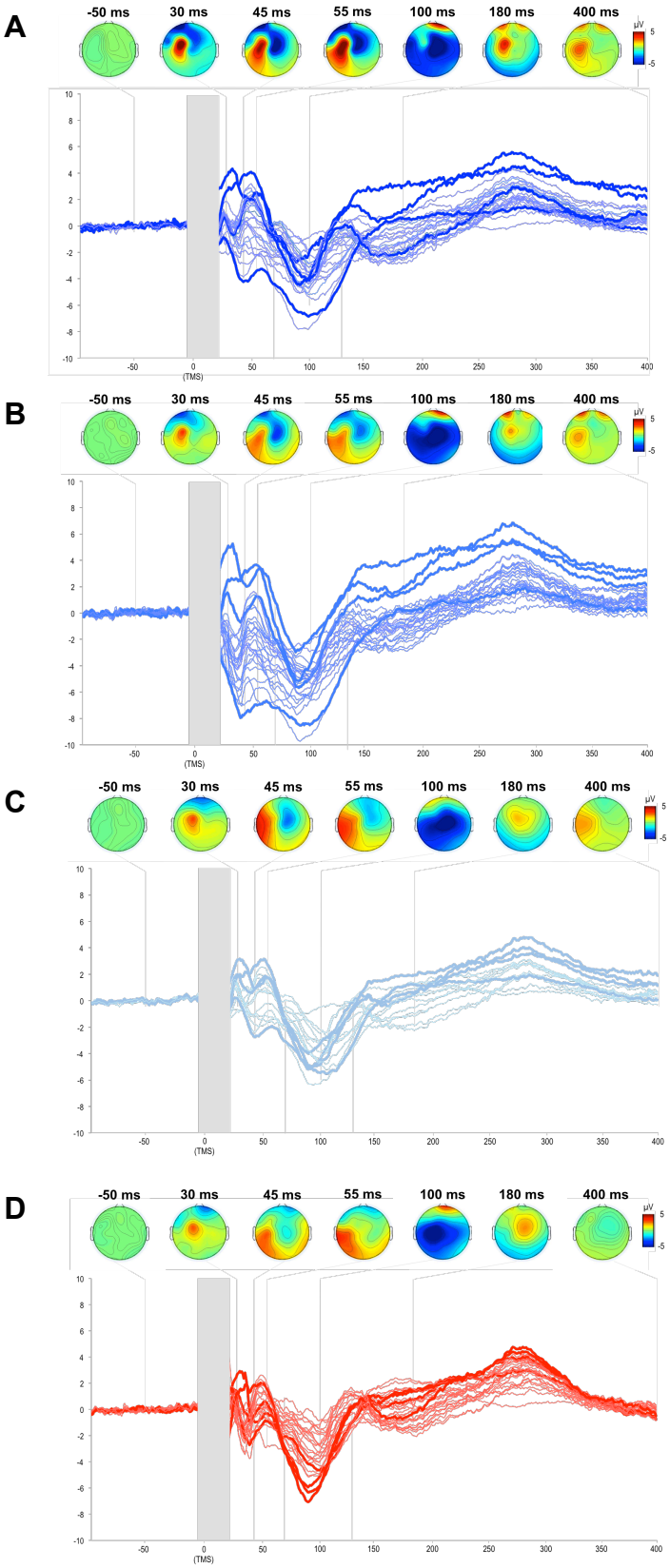

Figure 5.5 Grand-averaged TEP waveform with voltage distribution scalp maps of the INFOMAX29 (a), FASTICA (b), INFOMAX15 (c) and ALG (d) condition. Thick lines represent the electrodes showing a clear decay artifact in the RAW condition (fig. 5.4) (i.e.

3.3 TMS-evoked potentials waveform

Fig. 5.6 depicts the grand-average waveform of the 36 subjects all over the scalp in the RAW, INFOMAX29 and ALG conditions. Single-pulse TMS over M1 evoked a well-known pattern of positive and negative deflections lasting up to 250-280 ms, comprising the following peaks: P30, N45, P55, N100 and P180 (Paus et al., 2001; Komssi et al., 2002; Bender et al., 2005; Bonato et al., 2006; Lioumis et al., 2009; Ferreri et al., 2011; Veniero et al., 2013; Casula et al., 2014; Premoli et al., 2014). Such pattern of response was observable in all the electrodes and it appeared more pronounced nearby the site of stimulation, as previously reported (Paus et al., 2001; Komssi et al., 2002; Bender et al., 2005; Bonato et al., 2006; Lioumis et al., 2009; Ferreri et al., 2011; Veniero et al., 2013; Casula et al., 2014).

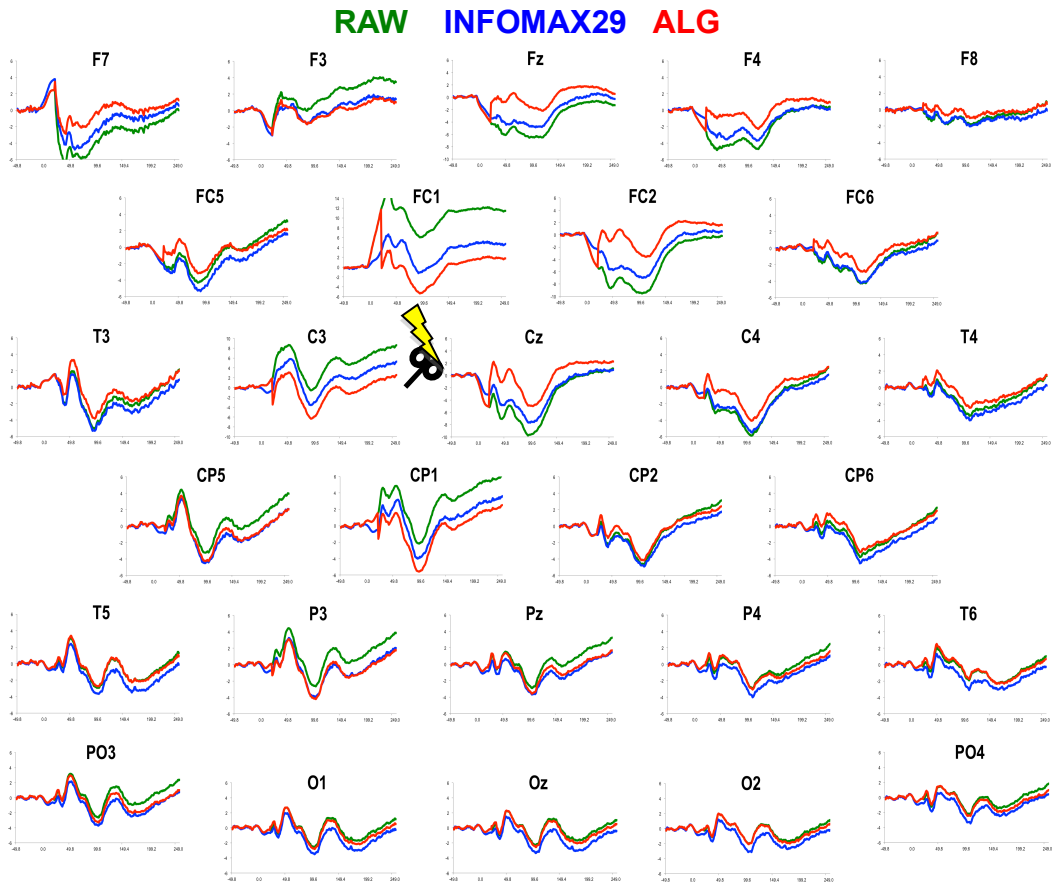

Figure 5.6 Grand-average TEP waveform evoked in each channel in the RAW, INFOMAX29 and ALG condition.

From a visual inspection the TEP waveform did not appear to be corrupted by the different artifact corrections. However, the influence of the decay artifact over the scalp maps of voltage distribution is clear in the RAW signal (fig. 5.4) and, to some extent, after the INFOMAX29 and fastICA corrections (fig. 5.5a and b). After the ALG correction (fig. 5.5d) and, to some extent, the INFOMAX15 (fig. 5.5c) a standard TEPs distribution was observable: the earlier TEPs were distributed over the site of stimulation (P30) and on the contralateral fronto-central regions (N45), whereas the later TEPs had a large distribution over the stimulated hemisphere (P55) and a bilateral distribution over the central (N100) and fronto-central areas (P180), as previously reported (Bonato et al., 2006; Ferreri et al., 2011; Veniero et al., 2013; Premoli et al., 2014). To better characterize the differences in the scalp distribution among the conditions, we also investigated the voltage distribution within the N100 time window (i.e. 70-130 ms after the TMS pulse). This potential, whose origin has been linked to the GABAb-ergic inhibition, shows a typical interhemispheric spread from the stimulated hemisphere, at around 75-80 ms from the stimulation, to the contralateral one at 125-130 ms (Ferreri et al., 2011; Casula et al., 2014; Premoli et al., 2014). Fig. 5.7 depicts the spatiotemporal distribution of the N100 in the different conditions. In the RAW, INFOMAX29 and, to some extent, in the fastICA condition, the maps showed a prominent dipole centered over the site of stimulation which mask the real distribution of the potential. Differently, in the ALG and, to some extent, in the INFOMAX15 condition the N100 distribution showed its typical interhemispheric spread: at 75-80 ms after the TMS pulse the N100 was localized over the site of stimulation; progressively, it spread around the site of stimulation (90-100 ms) and over central areas (100-110 ms); at 120-130 ms the negativity was mainly distributed over the contralateral hemisphere.

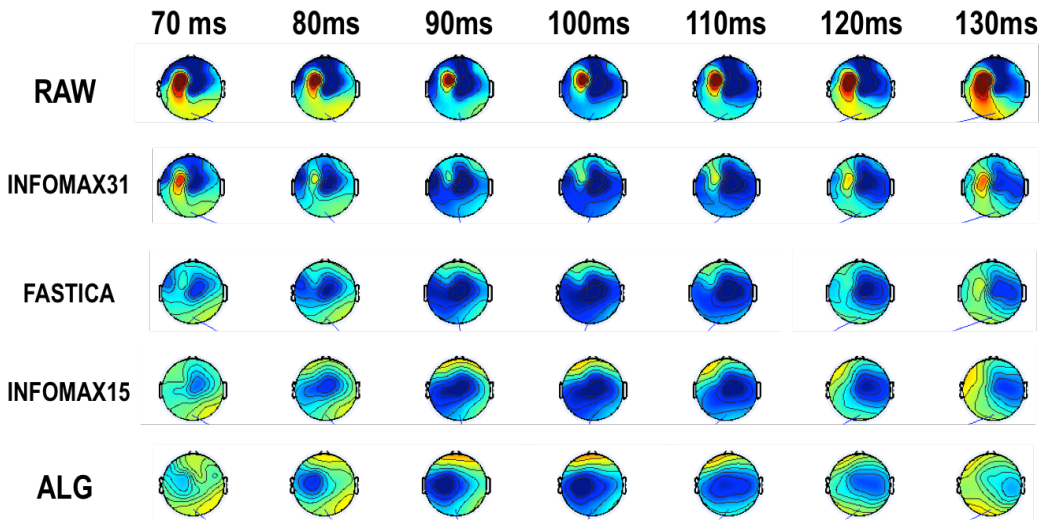

Figure 5.7 Voltage distribution scalp maps in the TMS-evoked N100 time window. In the INFOMAX15 and ALG condition it is clearly visible the characteristic interhemispheric spread.

3.4 TMS-evoked potentials (TEPs) amplitude and latency

To assess "where" (i.e. in which electrode) and "when" (i.e. in which temporal window) the artifact corrections significantly affected the signal, we applied a cluster-based permutation analysis (explained in paragraph 2.7 of the methods section) comparing the uncorrected RAW data with the corrected data (i.e. INFOMAX29, INFOMAX15, fastICA and ALG). The analysis revealed that TEPs showed significant differences in amplitude across conditions in the following time windows (all Monte Carlo ps < 0.05; fig. 5.8):

- RAW *vs.* INFOMAX29: 21-250 ms in FC1; 21-60 ms and 67-250 ms in CP1
- RAW *vs.* INFOMAX15: 21-250 ms in FC1, C3, CP1 and FC2
- RAW *vs.* fastICA: 21-250 ms in FC1, C3 and CP1
- RAW *vs.* ALG: 21-250 ms in FC1, C3, CP1 and FC2

To assess "how much" the artifact corrections affected the TEPs we compared the peak-to-peak amplitude and latency of the components within the temporal window detected as significant, by means of repeated-measures ANOVA. We performed three analyses comparing the different ICA corrections with the ALG correction and the RAW uncorrected data.

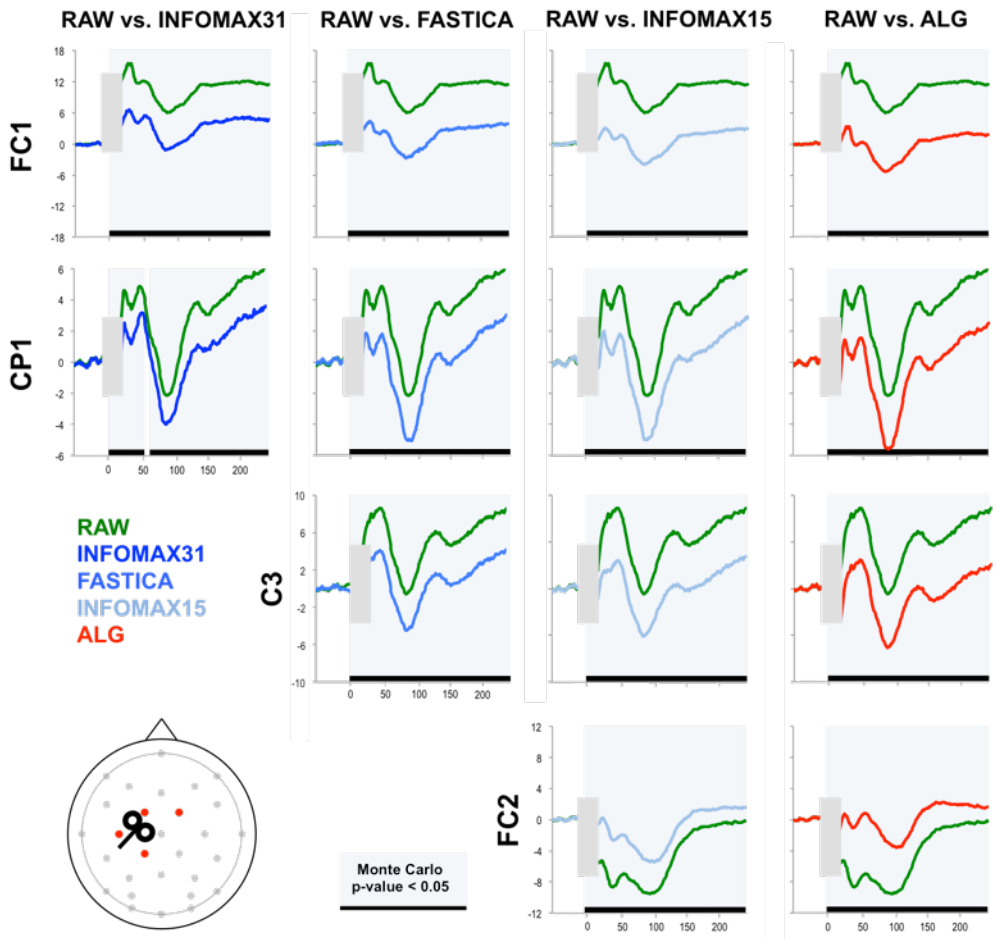

Figure 5.8 Time point by time point analysis of the significant differences between RAW and the other signal corrections conditions.

3.4.1 Analysis 1: RAW vs. INFOMAX29 vs. ALG

In this analysis we performed a 3×4×2 repeated-measures ANOVA with condition (RAW *vs.* INFOMAX29 *vs.* ALG), TEP (P30/N45, N45/P55, P55/N100, N100/P180) and electrode (FC1, CP1) as within-subjects factors. The analysis of TEP amplitude revealed a significant condition×TEP×electrode interaction [$F(2.9,104.9) = 8.55$, $p < 0.001$]. In the FC1 electrode, post-hoc analysis of the interaction revealed a significantly higher amplitude of three TEPs (N45/P55, P55/N100, N100/P180) in the INFOMAX29 condition compared to the RAW (N45/P55: 2.412±0.54 μV, $p < 0.001$; P55/N100: 1.959±0.69 μV, $p = 0.022$; N100/P180: 1.731±0.69 μV, $p = 0.05$), two of these components (N45/P55 and P55/N100) were also significantly higher in the INFOMAX29 condition compared to the ALG (N45/P55: 2.566±0.58 μV, $p < 0.001$; P55/N100: 2.717±0.68 μV, $p = 0.001$) (fig. 5.9). In the CP1 electrode, post-hoc

analysis of the interaction revealed a significantly higher amplitude of the N45/P55 component in the INFOMAX29 condition compared to the RAW (1.071±0.43 μV, p = 0.05) and to the ALG condition (1.080±0.43 μV, p = 0.05) (fig. 5.9). No TEP differences were detected between the ALG and the RAW condition in any of the electrodes (all ps > 0.05). No effects on TEP latencies were detected across conditions (all ps > 0.05; fig. 5.10).

3.4.2 Analysis 2: RAW vs. FASTICA vs. ALG

In this analysis we performed a 3×4×3 repeated-measures ANOVA with condition (RAW *vs.* fastICA *vs.* ALG), TEP (P30/N45, N45/P55, P55/N100, N100/P180) and electrode (FC1, C3, CP1) as within-subjects factors. The analysis on the TEPs amplitude revealed a significant condition×TEP×electrode interaction [$F(4.6,163.1) = 9.54$, $p < 0.001$]. In the FC1 electrode, post-hoc analysis of the interaction revealed a significantly lower amplitude of the P30/N45 component in the fastICA condition compared to the RAW (2.380±0.49 μV, p < 0.001) and to the ALG condition (1.804±0.47 μV, p = 0.001) (fig. 5.9). In the C3 electrode, post-hoc analysis of the interaction revealed a significantly lower amplitude of the P55/N100 component in the fastICA condition compared to the RAW (1.231±0.48 μV, p = 0.047) and to the ALG condition (1.324±0.45 μV, p = 0.017); a significant lower amplitude of the N100/P180 component in the fastICA condition compared to the RAW condition was also revealed (1.282±0.31 μV, p = 0.001) (fig. 5.9). In the CP1 electrode, post-hoc analysis of the interaction revealed a significantly lower amplitude of the N100/P180 component in the fastICA condition compared to the RAW condition (0.722±0.28 μV, p = 0.045) (fig. 7c). Again, no TEP differences were detected between the ALG and the RAW condition in any of the electrodes (all ps > 0.05). No effects on the TEP latencies were detected (all ps > 0.05; fig. 5.10).

3.4.3 Analysis 3: RAW vs. INFOMAX15 vs. ALG

In this analysis we performed a 3×4×4 repeated-measures ANOVA with condition (RAW *vs.* INFOMAX29 *vs.* ALG), TEP (P30/N45, N45/P55, P55/N100, N100/P180)

and electrode (FC1, C3, CP1, FC2) as within-subjects factors. The analysis on TEP amplitude revealed a significant condition×TEP×electrode interaction [$F(5.3,186.5) = 11.37$, $p < 0.001$]. In the FC1 electrode, post-hoc analysis of the interaction revealed a significantly lower amplitude of the P30/N45 component in the INFOMAX15 condition compared to the RAW (3.525±0.59 μV, $p < 0.001$) and to the ALG condition (2.95±0.6 μV, $p < 0.001$) (fig. 8a). In the C3 electrode, post-hoc analysis of the interaction revealed a significantly lower amplitude of the N100/P180 component in the INFOMAX15 condition compared to the RAW condition (1.357±0.46 μV, $p = 0.018$; fig. 5.9). In the CP1 electrode, post-hoc analysis of the interaction revealed a significantly lower amplitude of the N100/P180 component in the INFOMAX15 condition compared to the RAW condition (1.007±0.39 μV, $p = 0.042$; fig. 5.9) In the FC2 electrode, post-hoc analysis of the interaction revealed a significantly lower amplitude of the N45/P55 component in the INFOMAX15 condition compared to the RAW (1.331±0.45 μV, $p = 0.017$) and to the ALG condition (1.3±0.42 μV, $p = 0.011$). A difference was also detected in the P60/N100 component which was significantly lower in the ALG condition compared to the RAW (1.341±0.27 μV, $p < 0.001$) and in the N100/P180 component which was significantly lower in the INFOMAX15 (2.289±0.49 μV, $p < 0.001$) and in the ALG condition (3.624±0.59 μV, $p < 0.001$) compared to the RAW (fig. 5.9). The analysis on TEPs latency revealed a significant condition×TEP×electrode interaction [$F(6.1,213.2) = 7.68$, $p < 0.001$]. Significant differences were revealed in the latency of all the TEPs of the FC2 electrode (fig. 5.10). The P30/N45 component showed a peak-to-peak latency significantly later in the INFOMAX15 condition compared to the RAW (3.339±1.07 ms, $p = 0.012$) and to the ALG condition (6.072±1.07 ms, $p = 0.012$); the N45/P60 peak-to-peak latency was significantly earlier in the INFOMAX15 condition compared to the RAW condition (2.733±0.92 ms, $p = 0.016$); the P60/N100 component was significantly later in the ALG condition compared to the RAW (9.325±2.25 ms, $p = 0.001$); the N100/P180 was significantly earlier in the ALG condition compared to the RAW (16.042±3.78 ms, $p < 0.001$) and to the INFOMAX15 condition (11.972±4.19 ms, $p = 0.022$).

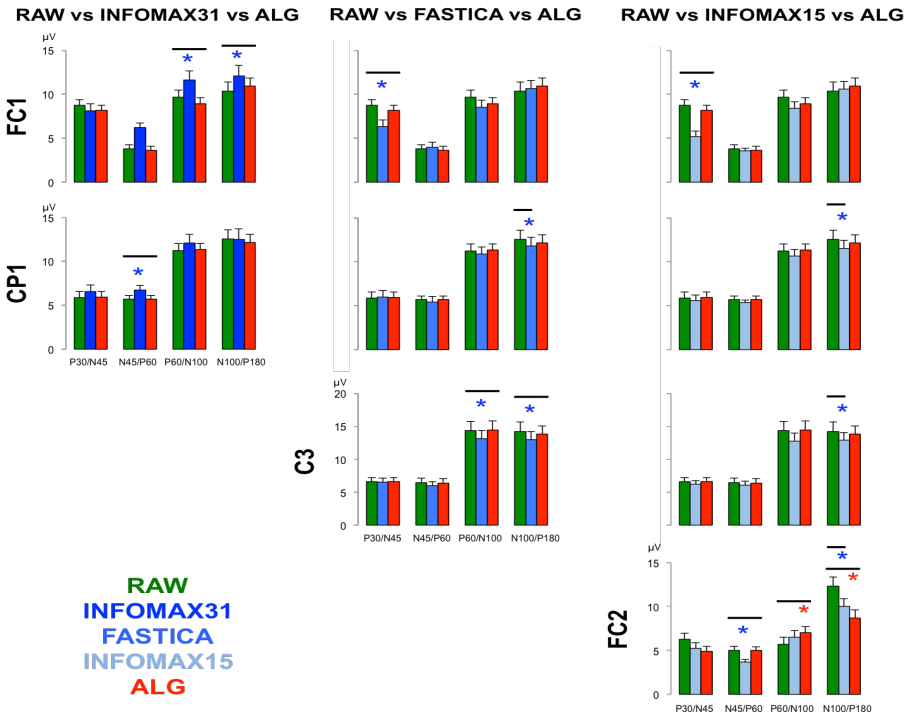

Figure 5.9 TEP peak-to-peak amplitudes in the electrode's time windows revealed as significant by the Monte Carlo analysis.

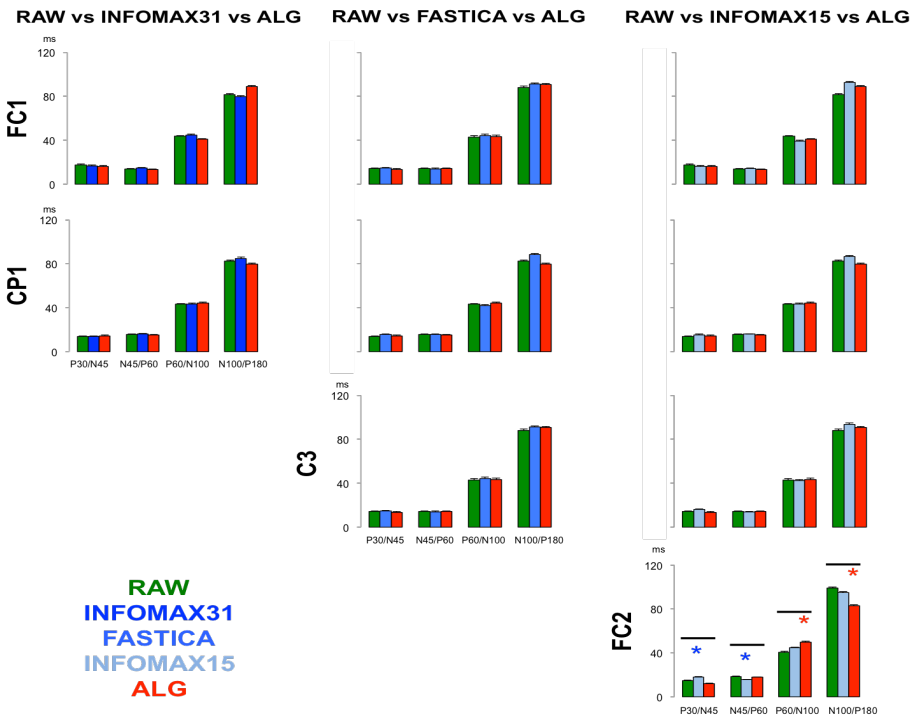

Figure 5.10 TEP peak-to-peak latency in the electrode's time windows revealed as significant by the Monte Carlo analysis.

3.5 Local mean field power (LMFP)

Fig. 5.10 depicts the LMFP evoked by TMS over left M1 in the RAW, INFOMAX29, fastICA, INFOMAX15 and ALG conditions. Four peaks are observable (P1, P2, P3 and P4). The latencies of the four peaks were very similar among all the conditions and corresponded to the mean latencies of four TEPs: P30 (RAW and ALG: 36.1 ms, INFOMAX29: 32.1 ms, fastICA: 34.1 ms); P55 (RAW and INFOMAX29: 54.7 ms, fastICA: 53.7ms, ALG: 50.7 ms); N100 (RAW: 105.5 ms; INFOMAX29: 103.5 ms; fastICA: 102.5 ms; ALG: 97.5 ms) and P180 (RAW: 173.8 ms; INFOMAX29: 162.1 ms; fastICA 173.8 ms; ALG: 176.7 ms). The N45 component, mainly distributed on the hemisphere controlateral to the stimulation (Bonato et al., 2006; Ferreri et al., 2011; Premoli et al., 2014), was not represented in the left LMFP. The mean amplitudes of the four LMFP were highly different especially in the first 80 ms after the TMS pulse (RAW: 4.593±0.7 μV; INFOMAX29: 2.444±0.38 μV; fastICA: 1.35±0.33 μV; ALG: 1.004±0.3 μV). Among the four peaks the P1, representing the P30, was the highest in all the conditions except in the ALG, such peak was particularly large in the RAW-LMFP where it reached the amplitude of 5.914 μV at 36.1 ms. Differently, in the ALG condition the highest peak was the P3 representing the N100 (1.678 μV at 95.7 ms). None of the LMFP realigned to the baseline level at 250 ms (RAW: 3.219 μV; INFOMAX29: 1.575 μV; fastICA: 1.107 μV) except for the ALG-LMFP, which reached the value of 0.377 μV (fig. 5.10). On the right side the LMFP showed three main peaks (P1, P2, and P3) in all the conditions; the fourth peak (P4) was mainly visible only in the ALG condition (fig. 5.10). Again, the latencies of the four peaks were very similar among the conditions and corresponded to the mean latencies of the TEPs: P30 (RAW: 27.3 ms; INFOMAX29: 28.3 ms; fastICA: 26.3 ms; ALG: 26.3 ms); N45 (RAW, ALG, fastICA: 46.8 ms; INFOMAX29: 47.8 ms); N100 (RAW: 77.1 ms; INFOMAX29: 76.1 ms; fastICA: 91.8 ms; ALG: 91.8 ms) and P180 (INFOMAX29and fastICA: 172.8 ms; ALG: 164 ms). Notably, a clear P4 was not observable in the RAW condition. The P60 component, mainly distributed on the side ipsilateral to the stimulation (Bonato et al., 2006; Ferreri et al., 2011; Premoli et al., 2014), was not represented in the right LMFP. The mean amplitudes of the four GMFP were highly different especially in the first 150 ms after the TMS pulse (RAW: 2.281±0.57 μV; INFOMAX29: 1.277±0.43 μV; fastICA: 1.171±0.37 μV; ALG: 0.685±0.2 μV). The relative peak amplitudes were also different among the conditions: in the RAW,

INFOMAX29 and fastICA conditions the highest peak was the P2 (RAW: 3.25 μV at 46.8 ms; INFOMAX29: 2.01 μV at 47.8 ms; fastICA: 1.79 μV at 46.8 ms); in the ALG condition the peak amplitudes were more homogeneous, the P4 was the highest: (1.244 μV at 164 ms). Again, none of the LMFP realigned to the baseline level at 250 ms (RAW: 3.145 μV; INFOMAX29: 1.588 μV; fastICA: 1.129 μV) except for the ALG-LMFP, which reached the value of 0.534 μV (fig. 5.10). Figure 5.10 depicts the LMFP computed in five electrodes in both the hemispheres (F3/F4, C3/C4, P3/P4, FC1/FC2, CP1/CP2) for three conditions: RAW, INFOMAX15 and ALG. Four peaks are observable in the left LMFP (P1, P2, P3, P4) whose latencies were compatible with the mean latencies of four TEPs: P30 (RAW: 33.2 ms; INFOMAX15: 34.2 ms; ALG 36.1 ms); P55 (RAW: 61.5 ms, INFOMAX15: 50.7ms, ALG: 50.7 ms); N100 (RAW: 105.5 ms; INFOMAX15: 96.6 ms; ALG: 95.7 ms) and P180 (RAW: 165 ms; INFOMAX15: 163 ms; ALG: 164 ms). Again, the N45 component was not represented in the left LMFP. After the TMS pulse (i.e. at 20 ms), the mean amplitude of the RAW-LMFP was higher (3.892±0.61 μV) compared to the INFOMAX15 and to the ALG conditions, which were very similar to each other (0.94±0.35 μV; 0.91±0.42 μV, respectively). Among the four peaks, the P1 was the highest for the RAW condition (5.859 μV at 33.2 ms), whereas in the INFOMAX15 and in the ALG the relative TEP amplitudes were more similar, the P3 was the highest in both the LMFPs (1.781 μV at 96.6 ms; 1.939 μV at 95.7 ms, respectively). Also in this case, the RAW-LMFP still had a large amplitude at 250 ms (3.360 μV) whereas the LMFP in the INFOMAX 15 and in the ALG condition seemed to realign to the baseline level (0.768 and 0.649 μV, respectively; fig. 5.10). In the right hemisphere, the LMFP presented four main peaks (P1, P2, P3, P4) whose latencies were compatible with the mean latencies of four TEPs: P30 (RAW: 27.3 ms; INFOMAX15: 26.5 ms; ALG 27.3 ms); N45 (RAW: 47.8 ms, INFOMAX15: 47.8 ms, ALG: 47.8 ms); N100 (RAW: 81 ms; INFOMAX15: 90.8 ms; ALG: 99.6 ms) and P180 (RAW: 164 ms; INFOMAX15: 177.7 ms; ALG: 164 ms). As in the 29 channels-LMFP, a clear P4 was not visible in the RAW condition, the mean LMFP amplitude in this condition was higher compared to the RAW and INFOMAX15 conditions, especially in the first 150 ms after the TMS pulse (RAW: 1.853±0.94 μV; INFOMAX15: 0.823±0.29 μV; ALG: 0.745±0.27 μV). The highest peak was different in three conditions: for the RAW condition the P2 was the more pronounced (3.46 μV at 47.8 ms), in the INFOMAX15 was the P3 (1.439 μV at 90.8

ms) and in the ALG was the P4 (1.247 μV at 165 ms). Again, the RAW-LMFP still had a large amplitude at 250 ms (1.410 μV) whereas the LMFP in the INFOMAX 15 and in the ALG condition seemed to realign to the baseline level (0.524 μV and 0.650 μV, respectively; fig. 5.10).

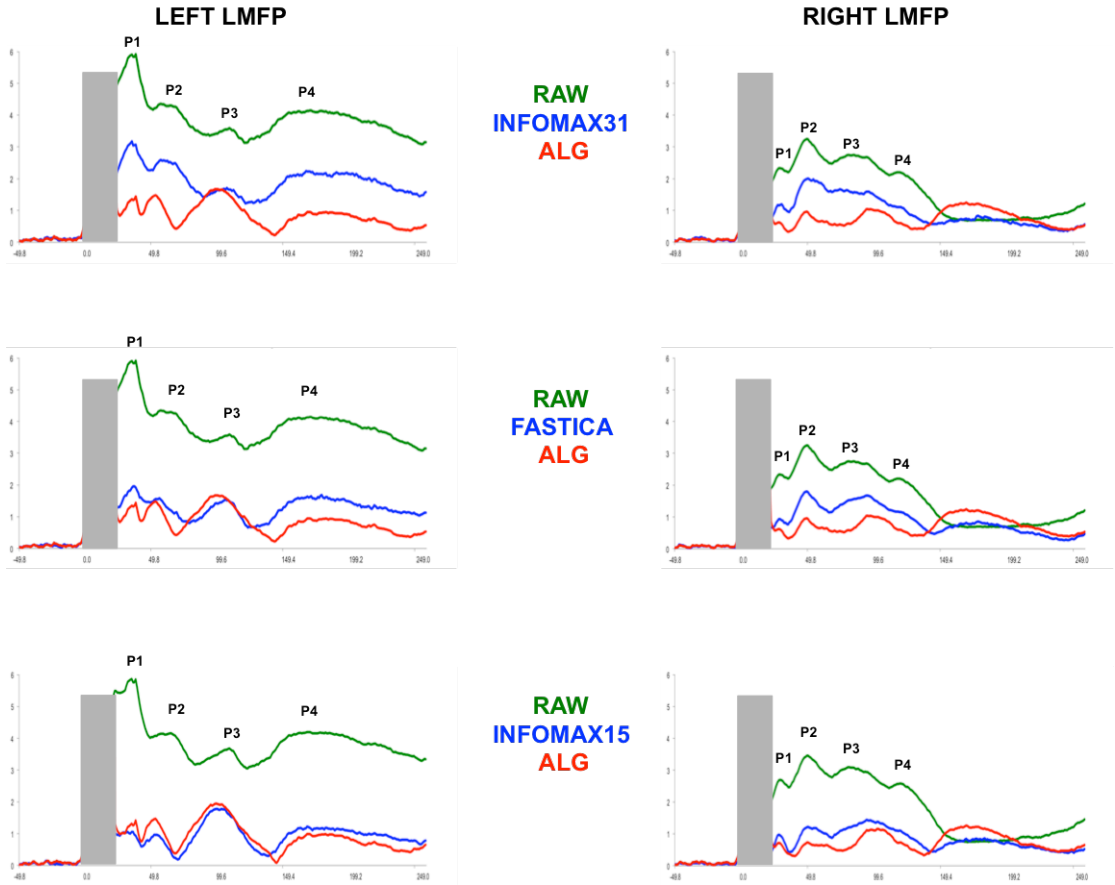

Figure 5.10 Local mean field power (LMFP) of the two hemispheres in the RAW, INFOMAX29, FASTICA, INFOMAX15 and ALG conditions.

4. DISCUSSION

The aims of the present study were: (1) to characterize the impact of the decay artifact on different TMS-EEG measures; (2) to assess and analyze the impact of the standard ICA correction of the decay artifact on the physiological responses to TMS (i.e. TEPs); (3) to propose a new method to correct the decay artifact that goes beyond the intrinsic limitations of ICA.

4.1 The problem of identifying and correcting the decay artifact

A first problem of the decay artifact is its relatively unknown and unclarified nature. Investigating the origin of this artifact was not the main point of the present study, even if this can be useful in order to avoid its occurrence. For instance, it has been reported that keeping the impendence level at very low values (i.e. 5 kΩ) during EEG recording strongly reduce the occurrence and the impact of long-lasting TMS-induced artifacts (Ilmoniemi and Kičić, 2010), that is what we observed in our study. However, keeping a very low impedance level it may not be always possible because of several factors related to the experimental participant (e.g. when testing patients or children) or to the experimental conditions (e.g. time, cap). Although this is a problem in TMS-EEG experiments, a very few published papers tried to characterize the decay artifact and its impact in the EEG signal (fig. 5.1). Indeed, this artifact has been reported by a number of studies (Komssi et al., 2004; Litvak et al., 2007; Julkunen et al., 2008; Veniero et al., 2009; Zanon et al., 2010; Kohronen et al., 2011; Rogasch et al., 2012; Sekiguchi et al., 2011; Tar Braack et al., 2013) under the term "long-lasting artifact" or "residual artifact" but its characteristic and, especially, its impact on TMS-EEG measures have not been assessed so far. Rogasch and colleagues (2014) were the first to term this artifact as "decay artifact" due to its characteristic shape that is clearly visible also on the ICA components related to the decay (fig. 5.2). Indeed, as demonstrated in this study, the accurate identification of the ICA components related to the decay is stable and reproducible.

The impact of the decay artefact on the TMS-induced physiological responses is still a relatively unknown topic in literature. One reason that account for this lack is that its correction with ICA or other procedures (e.g. linear detrend, interpolation) is relatively easy and efficient, although not optimal, as we demonstrated in this

study (see paragraph 4.2 of this discussion). A second reason lies in the fact that the decay artefact seems not to corrupt the TEP waveform, as previously reported (Zanon et al., 2010; Rogasch et al., 2014). However, in the present study we showed the impact of the decay in specific TMS-EEG measures such as voltage distribution scalp maps (fig. 5.4) and the LMFP (fig. 5.10). In the maps, the strong baseline shift of the decay artefact caused a distortion of the topographic distribution producing a clear dipole over the site of stimulation for more than 400 ms after the TMS pulse that masked the real distribution of the TEPs. Specifically, a prominent positive shift of the FC1, C3 and CP1 electrode as well as a negative shift of the FC2 electrode, is clearly evident in the scalp maps. Notably, these electrodes were the closest to the stimulating coil (fig. 5.4). The same pattern can be observed in the voltage distribution scalp maps within the N100 temporal window (fig. 5.7). In the left LMFP, the decay artefact had an impact both in the global power, showing an abnormal high amplitude that did not realign to the baseline level (i.e. 0 μV) after the TEPs evocation (i.e. 250 ms); and in the relative peak amplitude, in which the P1 (corresponding to the P30, a peak with a relatively low amplitude compared to the other TEPs) showed the highest amplitude, whereas the P3 (corresponding to the N100, the TEP with the highest amplitude, as assessed in the TEPs analysis) had the lowest. In the right LMFP, the decay produced an abnormal high amplitude of the P2 (corresponding to the N45, the TEP with the lowest amplitude, as assessed in the TEPs analysis), whereas the P4 (corresponding to the highest P180) showed the lowest amplitude.

4.2 The impact of ICA correction in TMS-EEG measures

The second aim of this study was to investigate the efficiency of ICA in the correction of the decay artifact. Currently, ICA is the most common solution for this purpose; however, as largely discussed in the introduction of this study, it presents a number of intrinsic limitations. A first critical point is that the criteria of identification and removal of the ICA components artifact-related, are rarely specified, making such procedure too arbitrary and dependent from the experimenter's decisions. Furthermore, it is also rarely specified which ICA algorithm is used for the analysis. Another critical point is that ICA may also affect the physiological responses evoked

by TMS (Kohronen et al., 2011; Ter Braack et al., 2013; Rogasch et al., 2014). Nevertheless, a clear investigation of the impact of ICA on physiological responses has never been published yet.

The grand-averaged response in the INFOMAX29 and FASTICA conditions (fig. 5.5a, b) showed a positive shift (especially in FC1 electrode) that affected the TEPs distribution, as assessed by the scalp maps. Notably, such positive shift lasted for more than 400 ms. It must be taken in consideration that in our study we identified (and subsequently removed) only the components that were clearly related to the decay artifact (i.e. that presented the three criteria explained in section 3.4) which were in average 3±1 for both the INFOMAX29 and FASTICA conditions. It cannot be excluded that the rejection of further components could have produced a better removal of the decay artifact, however this poses two main problems: firstly, the difficulty to establish some clear criteria to identify the decay ICA components, making their selection too arbitrary; secondly, a stronger modification of the TEPs measures and morphology due to an greater number of components removed.

In this regard, results on TEPs analysis showed a significant corruption of TEPs amplitude in the INFOMAX29 and FASTICA conditions compared to the original RAW signal (fig. 5.9). Specifically, INFOMAX29 produced higher amplitude in 3 out of the 8 TEPs analyzed, whereas FASTICA produced lower amplitude in4 out of the 12 TEP analyzed. The differences in the algorithms used might account for this discrepancy. Importantly, in none of the TEPs analyzed the ALG correction produced a significant difference compared to the original RAW signal. When the INFOMAX15 correction was used, a significant amplitude reduction was produced in 5 out of the 16 TEPs analyzed. Notably, in this analysis also the ALG correction produced a significant increase of the P60/N100 component and a significant decrease of the N100/P180 component in the FC2 electrode (discussed in section 5.3).

The LMFP in the INFOMAX29 and FASTICA conditions (fig. 5.10) confirmed that the correction of the decay artifact was not optimal. Indeed, the mean activity showed abnormal higher amplitude that does not realign to the baseline level after 250 ms from the TMS pulse. Furthermore, as in the RAW condition, it is clear that the relative amplitude of the peaks is, at least partially, corrupted: firstly, in the left LMFP, the first peak (P1, corresponding to the P30) presented the highest

amplitude, that is a distortion caused by the decay artifact shift; secondly, the third peak (P3), is the lowest, although it represents the N100 peak, which was the highest, as revealed in the TEPs waveform (fig. 5.5). Similarly, in the right LMFP, the second peak (P2, corresponding to the N45), showed the highest relatively amplitude, as a consequence of a decay distortion.

4.3 Decay correction with the proposed adaptive detrend

The third and main aim of the study was to propose a new efficient method to correct the decay artifact. Our purpose was to develop an algorithm able to discriminate the different trends of the decay algorithm (linear and nonlinear) but whose efficiency did not depend on the experimenter's choices and on the number of electrodes, which are two main limits of ICA.

The grand-averaged TEPs waveform after the ALG correction (fig. 5.5d) showed a well-known pattern of TEPs whose distribution, as revealed by the scalp maps, are in line with the TEPs distribution reported in literature, namely: a P30 focused in the site of stimulation; an N45 controlateral to the site of stimulation; a P60 distributed in the stimulated hemisphere; an N100 over the central areas of both hemispheres; and a P180 over the bilateral fronto-central areas (Ferreri et al., 2011; Premoli et al., 2014). Looking at the N100 spreading dynamics, depicted in the scalp maps within the N100 temporal window (fig. 5.7), the N100 followed a well-known interhemispheric spread: initially it was distributed over the site of stimulation (75-90 ms) and then it spread over central and contralateral sites (95-120 ms). Such pattern was visible only after the INFOMAX15 and ALG correction.

The analysis on TEPs amplitude and latency, did not reported any difference between the ALG and the original RAW condition for 34 out of the 36 TEPs analyzed. A significant corruption was reported for the P60/N100 and N100/P180 component in the FC2 electrode in which the ALG correction produced an increase in the P60/N100 and a decrease in the N100/P180, both in amplitude and in latency, compared to the RAW and to the INFOMAX15 condition. However, this difference can be due to the strong negative shift presented in the RAW condition in which the signal showed a smaller N100 probably due to a sort of "floor effect", and a higher

P180 due to the attempt of the signal to realign to the baseline level (fig. 5.8). In this view, the difference between the two conditions might be artefactual.

The LMFP after ALG condition presented two main feature different from the INFOMAX29 and the FASTICA condition (fig. 5.10): first, after 250 ms the signal tend to realign to the baseline level; second, the relative amplitude of the four peaks is correctly reported with a prominent peak 3 in the left hemisphere, corresponding to the highest N100, as depicted in the TEPs waveform; and a prominent peak 4 in the right hemisphere, corresponding to the P180 which was the highest peak in the hemisphere contralateral to the stimulation (fig. 5.10)

5. CONCLUSIONS

The main contribute of this study is the proposal of a new adaptive algorithm for the correction of the decay artifact induced by TMS during EEG. We showed the strong impact of this artifact on different TMS-EEG measures, and we also demonstrated the limits of the common solutions proposed in literature, that is the use of ICA. Our results showed that the proposed algorithm is able to correct the decay artifact with a standard procedure that it does not have the intrinsic limitations of ICA. Interestingly, we observed that when a subselection of electrodes is considered for ICA, specifically the electrodes where the artifact is stronger, the identification and the correction of such artifact seems to be more effective, as revealed by the better results provided with the INFOMAX15 correction, compared to the INFOMAX29 and FASTICA. This is an interesting result that might be considered when ICA is used for specific artifacts. In conclusion, we demonstrated that the proposed adaptive detrend algorithm is a reliable solution for the correction of the TMS-evoked decay artifact, especially considering that, contrary to ICA, (1) it is not dependent from the number of recording channels; (2) it does not affect the physiological responses and (3) it is completely independent from the experimenter's choices

GENERAL CONCLUSIONS

The combined use of TMS and EEG is currently one of the most promising approaches in the investigation of human brain functioning. EEG and TMS represent two complementary techniques whose combined use is likely to be more widespread in the future. In the chapter I and II of this thesis, the high potential of this integrative trend has been stressed, as shown by the large number of studies discussed. In particular, the investigation of plasticity mechanisms in healthy and pathological brain seems to be particularly promising with TMS-EEG. In chapter III there is an example of TMS-EEG application in the investigation of plasticity mechanism in healthy volunteers (study 1). The results of this study provided insights into the inhibitory mechanisms of the 1-Hz rTMS, a neuromodulatory protocol which is commonly used for clinic purposes. In chapter IV there is an example of TMS-EEG application in the investigation of abnormal brain dynamics in pathological brain (study 2). In this study we reported some preliminary results on TEPs markers of inhibitory deficits that characterize Huntington's disease. Besides the fascinating perspectives opened by the TMS-EEG approach, several technical problems have limited the advancement in some application fields. Therefore, there is the need of studies aimed to solve such technical problems. An example of this research is provided in chapter V (study 3). In this study we developed a solution for an EEG artefact resulting from the electromagnetic TMS stimulation and we demonstrated the feasibility of the proposed algorithm comparing it with other commons solutions in literature.

REFERENCES

Aguirre GK (2003) *Functional imaging in behavioral neurology and cognitive neuropsychology*. In Feinberg TE, Farah MJ *Behavioral Neurology and Cognitive Neuropsychology,* 35–46, McGraw-Hill

Amassian VE, Stewart M, Quirk GJ, Rosenthal JL (1987) *Physiological basis of motor effects of a transient stimulus to cerebral cortex*. Neurosurgery 20, 74-93

Amassian VE, Cracco RQ, Maccabee PJ, Cracco JB (1992) *Cerebello-frontal cortical projections in humans studied with the magnetic coil*. Electroencephalography and Clinical Neurophysiology, 85:265–272

Antal A, Kincses TZ, Nitsche MA, Bartfai O, Demmer I, Sommer M, et al., (2002) *Pulse configuration dependent effects of repetitive transcranial magnetic stimulation on visual perception*. Neuroreport, 13:1-5

Arai N, Okabe S, Furubayashi T, Terao Y, Yuasa K, Ugawa Y (2005) Comparison between short train, monophasic and biphasic repetitive transcranial magnetic stimulation (rTMS) of the human motor cortex. Clinical Neurophysiology, 116:605-613

Ashbridge E, Walsh V, Cowey A (1997) Temporal aspects of visual search studied by transcranial magnetic stimulation. Neuropsychologia, 35:1121-1131

Aurora SK, Ahmad BK, Welch KMA, Bhardhwaj P, Ramadan NM (1998) Transcranial magnetic stimulation confirms hyperexcitability of occipital cortex in migraine. Neurology, 50:1111-1114

Barker AT (1991) *An introduction to the basic principles of magnetic nerve stimulation.* Journal of Clinical Neurophysiology 8:26-37

Barker AT, Jalinous R, Freeston IL (1985) *Non-invasive magnetic stimulation of human motor cortex*. Lancet, 1:1106–1107

Bastiaansen MC, Böcker KBE, Cluitmans PJM, Brunia CH (1999) *Event-related desynchronization related to the anticipation of a stimulus providing knowledge of results.* Clinical Neurophysiology, 110:250-260

Bender S, Basseler K, Sebastian I, Resch F, Kammer T, Oelkers-Ax R, et al. (2005) *Transcranial Magnetic Stimulation Evokes Giant Inhibitory Potentials in Children*. Annals of Neurology, 58:58-67

Berg P e Scherg M (1994) A *multiple source approach to the correction of eye artifacts*. Electroencephalography and Clinical Neurophysiology, 90:229–241

Bestmann S, Baudewig J, Frahm J (2003) *On the synchronization of trans- cranial magnetic stimulation and functional echo-planar imaging*. Journal of Magnetic Resonance Imaging, 17:309-31

Bestmann S, Baudewig J, Siebner HR, Rothwell JC, Frahm J (2004) *Functional MRI of the immediate impact of transcranial magnetic stimulation on cortical and subcortical motor circuits*. European Journal of Neuroscience, 19:1950-1962

Bikmullina R, Kičić D, Carlson S, Nikulin VV (2009) *Electrophysiological correlates of short-latency afferent inhibition: a combined EEG and TMS study.* Experimental Brain Research, 194:517-526

Bisiacchi PS, Cona G, Schiff S, Basso D (2011) *Modulation of a fronto-parietal network in event-based prospective memory: an rTMS study*. Neuropsychologia, 49:2225-2232

Bohning DE, Pecheny AP, Epstein CM, Speer AM, Vincent DJ, Dannels W, George M (1997) *Mapping transcranial magnetic stimulation (TMS) fields in vivo with MRI*. Neuroreport, 8:2535-2538

Bonato C, Miniussi C, Rossini PM (2006) *Transcranial magnetic stimulation and cortical evoked potentials: a TMS/EEG coregistration study*. Clinical Neurophysiology, 117:1699-1707

Bonnard M, Spieser L, Meziane HB, De Graaf JB, Pailhous J (2009) *Prior intention can locally tune inhibitory processes in the primary motor cortex: direct evidence from combined TMS-EEG.* European Journal of Neuroscience, 30:913-932

Boorman ED, O'Shea J, Sebastian C, Rushworth MF, Johansen-Berg H (2007) *Individual differences in white-matter microstructure reflect variation in functional connectivity during choice.* Current Biology, 17:1426-1431

Boroojerdi B, Battaglia F, Muellbacher W, Cohen LG (2001) *Mechanisms influencing stimulus-response properties of the human corticospinal system.* Clinical Neurophysiology, 112:931-937

Boroojerdi B, Topper R, Foltys H, Meincke U (1999) *Transcallosal inhibition and motor conduction studies in patients with schizophrenia using transcranial magnetic stimulation.* British Journal of Psychiatry, 175:375-379

Brasil-Neto JP, Cohen LG, Panizza M, Nilsson J, Roth BJ, Hallett M (1992) *Optimal focal transcranial magnetic activation of the human motor cortex: effects of coil orientation, shape of the induced current pulse, and stimulus intensity*. Journal of Clinical Neurophysiology, 9:132–136

Brignani D, Manganotti P, Rossini PM, Miniussi C (2008) *Modulation of Cortical Oscillatory Activity During Transcranial Magnetic Stimulation*. Human Brain Mapping, 29:603-612

Bruckmann S, Hauk D, Roessner V, Resch F, Freitag CM, Kammer T et al. (2012) *Cortical inhibition in attention deficit hyperactivity disorder: new insights from the electroencephalographic response to transcranial magnetic stimulation.* Brain, 135:2215-2230

Bungert A, Chambers CD, Phillips M, Evans CJ (2012) *Reducing image artefacts in concurrent TMS/fMRI by passive shimming*. Neuroimage, 59:2167-2174

Cappa SF, Sandrini M, Rossini PM, Sosta K, Miniussi C (2002) *The role of the left frontal lobe in action naming: rTMS evidence*. Neurology, 59:720–723

Caramia MD, Palmieri MG, Giacomini P, Iani C, Dally L, Silvestrini M (2000) *Ipsilateral activation of the unaffected motor cortex in patients with hemiparetic stroke*. Clinical Neurophysiology 111, 1990-1996.

Casula EP, Tarantino V, Basso D, Bisiacchi PS (2013) *Transcranial magnetic stimulation and neuroimaging coregistration.* INTECH Open Access Publisher, 2013

Casula EP, Tarantino V, Basso D, Arcara G, Marino G, Toffolo GM, Rothwell JC, Bisiacchi PS (2014) *Low-frequency rTMS inhibitory effects in the primary motor cortex: insights from TMS-evoked potentials.* Neuroimage, 98:225-232

Chen R (2000) *Studies of human motor physiology with transcranial magnetic stimulation.* Muscle and Nerve Supplement 9, S26-32

Chen R, Classen J, Gerloff C, Celnik P, Wassermann EM, Hallett M, Cohen LG (1997) *Depression of motor cortex excitability by low-frequency transcranial magnetic stimulation*. Neurology, 48:1398-1403

Chen R, Tam A, Bütefisch C, Corwell B, Ziemann U, Rothwell JC et al. (1998) *Intracortical inhibition and facilitation in different representations of the human motor cortex*. Journal of Neurophysiology 80:2870-2881

Chen R, Lozano AM, Ashby P (1999) *Mechanism of the silent period following transcranial magnetic stimulation evidence from epidural recordings*. Experimental Brain Research, 128:539-542

Chen R, Yung D, Li JY (2003) *Organization of ipsilateral excitatory and inhibitory pathways in the human motor cortex.* Journal of Neurophysiology 89:1256-1264

Chiang TC, Vaithianathan T, Leung T, Lavidor M, Walsh V, Delpy DT (2007) *Elevated haemoglobin levels in the motor cortex following 1 Hz transcranial magnetic stimulation: a preliminary study*. Experimental Brain Research, 181:555-560

Civardi C, Cantello R, Asselman P, Rothwell JC (2001) *Transcranial magnetic stimulation can be used to test connections to primary motor areas from frontal and medial cortex in humans.* NeuroImage 14:1444-1453

Cohen LG, Roth BJ, Nilsson J, Dang N, Panizza M, Bandinelli S (1990) *Effects of coil design on delivery of focal magnetic stimulation: technical considerations*. Electroencephalography and Clinical Neurophysiology, 75:350-357

Cohen D, Cuffin BN (1991) *Developing a more focal magnetic stimulator. Part I: Some basic principles.* Journal of Clinical Neurophysiology 8:102-111

Cohen LG, Celnik P, Pascual-Leone A, Corwell B, Falz L, Dambrosia J et al. (1997) *Functional relevance of cross-modal plasticity in blind humans*. Nature, 389:180–183

Cohen E, Bernardo M, Masana J, Arrufat FJ, Navarro V, Valls-Solé, et al. (1999) *Repetitive transcranial magnetic stimulation in the treatment of chronic negative schizophrenia: a pilot study.* Journal of Neurology, Neurosurgery and Psychiatry, 67:129-130

Correa A, Cona G, Arbula S, Vallesi A, Bisiacchi PS (2014) *Neural dissociation of automatic and controlled temporal preparation by transcranial magnetic stimulation.* Neuropsychologia, 65:131-136

Corthout E, Barker AT, Cowey A (2001) *Transcranial magnetic stimulation. Which part of the current waveform causes the stimulation?*. Experimental Brain Research, 141:128-132

Cowey A and Walsh V (2000) *Magnetically induced phosphenes in sighted, blind and blindisighted observers.* Neuroreport, 11:3269-3273

Cracco RQ, Amassian VE, Maccabee PJ, Cracco JB (1989) *Comparison of human transcallosal responses evoked by magnetic coil and electrical stimulation*. Electroencephalography and Clinical Neurophysiology, 74:417–424

Daskalakis ZJ, Farzan F, Barr MS, Maller JJ, Chen R, Fitzgerald PB (2008) *Long-interval cortical inhibition from the dorsolateral prefrontal cortex: a TMS-EEG study.* Neuropsychopharmacology, 33:2860-2869

Daskalakis ZJ, Möller B, Christensen BK, Fitzgerald PB, Gunraj C, Chen R (2006) *The effects of repetitive transcranial magnetic stimulation on cortical inhibition in healthy human subjects*. Experimental brain research, 174:403-412.

Davare M, Rothwell JC, Lemon RN (2010) Causal Connectivity between the Human Anterior Intraparietal Area and Premotor Cortex during Grasp. Current Biology, 26:176-181

Davey NJ, Hazel CS, Wells E, Maskill DW, Gordana S, Ellaway PH, Frankel HL (1998) Responses of thenar muscles to transcranial magnetic stimulation of the motor cortex in patients with incomplete spinal cord injury. Journal of Neurology, Neurosurgery and Psychiatry, 65:80-87

Davies CH, Davies SN, Collingridge GL (1990) Paired-pulse depression of monosynaptic GABA-mediated inhibitory post- synaptic responses in rat hippocampus. Journal of Physiology, 424:513–531

Deisz RA (1999) GABA(B) receptor-mediated effects in human and rat neocortical neurones in vitro. Neuropharmacology, 38:1755–1766

Delorme A, Makeig S (2004) *EEGLAB: an open source toolbox for analysis of single-trial EEG dynamics including independent component analysis*. Journal of Neuroscience Methods, 134:9-21

Di Lazzaro V, Oliviero A, Mazzone P, Insola A, Pilato F, Saturno E, Accurso A, Tonali P, Rothwell JC (2001a) *Comparison of descending volleys evoked by monophasic and biphasic magnetic stimulation of the motor cortex in conscious humans*. Experimental Brain Research 141: 121-127

Eichhammer P, Johann M, Kharraz A, Binder H, Pittrow D, Wodarz N, Hajak G (2003) High-frequency repetitive transcranial magnetic stimulation decreases cigarette smoking. Journal of Clinical Psychiatry 64:951-953

Epstein CM (1998) Transcranial magnetic stimulation: language function. Journal of Clinical Neurophysiology, 15:325-332

Eriksen BA and Eriksen CW (1974) *Effects of noise letters upon the identification of a target letter in nonsearch task*. Perception & Psychophysics, 16:143-149

Esser SK, Huber R, Massimini M, Peterson MJ, Ferrarelli F, Tononi G (2006) *A direct demonstration of cortical LTP in humans: a combined TMS/EEG study.* Brain Research Bulletin, 69:86-94

Farzan F, Barr MS, Levinson AJ, Chen R, Wong W, Fitzgerald PB, et al. (2010) *Reliability of long-interval cortical inhibition in healthy human subjects: a TMS-EEG study.* Journal of Neurophysiology, 104:1339-1346

Ferbert A, Priori A, Rothwell JC, Day BL, Colebatch JG, Marsden CD (1992) *Interhemispheric Inhibition of the Human Motor Cortex.* Journal of Physiology, 453:525-546

Ferreri F, Pasqualetti P, Maatta S, Ponzo D, Ferrarelli F, Tononi G, Mervaala E, Miniussi C, Rossini PM (2011) Human brain connectivity during single and paired pulse transcranial magnetic stimulation. Neuroimage, 54:90–102

Fitzgerald PB, Fountain S, Daskalakis ZJ (2006) A comprehensive review of the effects of rTMS on motor cortical excitability and inhibition. Clinical Neurophysiology, 117:2584-2596

Fitzgerald PB, Daskalakis ZJ, Hoy K, Farzan F, Upton DJ, Cooper NR, et al. (2008) *Cortical inhibition in motor and non-motor regions: a combined TMS-EEG study*. Clinical EEG and Neuroscience, 39:112-117

Fregni F, Boggio PS, Valle AC, Rocha RR, Duarte J, Ferreira MJ, et al. (2006) *A sham-controlled trial of a 5-day course of repetitive transcranial magnetic stimulation of the unaffected hemisphere in stroke patients.* Stroke, 37:2115-2122

Fuhr P, Agostino R, Hallett M (1991) *Spinal motor neuron excitability during the silent period after cortical stimulation.* Electroencephalography and Clinical Neurophysiology, 81:257-262

Greenberg BD, Ziemann U, Harmon A, Murphy DL, Wassermann EM (1998) *Decreased neuronal inhibition in cerebral cortex in obsessive-compulsive disorder on transcranial magnetic stimulation.* Lancet, 352:881-882

Hamada M, Galea JM, Di Lazzaro V, Mazzone P, Ziemann U, Rothwell JC (2014) Two distinct interneuron circuits in human motor cortex are linked to different subsets of physiological and behavioural plasticity. Journal of Neuroscience, 34: 12837-12849

Hamidi M, Slagter HA, Tononi G, Postle BR (2010) Brain responses evoked by high-frequency repetitive transcranial magnetic stimulation: An event-related potential study. Brain Stimulation, 3:2–14

Hamzei F, Liepert J, Dettmers C, Weiller C, Rijntjes M (2006) *Two Different Reorganization Patterns After Rehabilitative Therapy: An Exploratory Study with fMRI and TMS.* Neuroimage 31:710-720

Hanajima R, Ugawa Y, Machii K, Mochizuki H, Terao Y, Enomoto H, et al. (2001) *Interhemispheric facilitation of the hand motor area in humans*. Journal of Physiology, 531:849–859

Hasan A, Galea JM, Casula EP, Falkai P, Bestmann S, Rothwell JC (2012) Muscle and timing-specific functional connectivity between the dorsolateral prefrontal cortex and the primary motor cortex. Journal of Cognitive Neuroscience, 25:558-570

Helfrich C, Pierau SS, Freitag CM, Roeper J, Ziemann U, Bender S (2013) *Monitoring cortical excitability during repetitive transcranial magnetic stimulation in children with ADHD: a single-blind, sham-controlled TMS-EEG study.* Plos One, 7:e50073

Helfrich RF, Schneider TR, Rach S, Trautmann-Lengsfeld SA, Engel AK, Herrmann CS (2014) Entrainment of brain oscillations by transcranial alternating current stimulation. Current Biology, 24:333-339

Herrmann CS, Rach S, Neuling T, Strüber (2013) Transcranial alternating current stimulation: a review of the underlying mechanisms and modulation of cognitive processes. Frontiers in Human Neuroscience, 7

Huang Y-Z, Edwards MJ, Rounis E, Bhatia KP, Rothwell JC (2005) *Theta Burst Stimulation of the Human Motor Cortex*. Neuron, 45:201-206

Huang Y-Z, Chen RS, Rothwell JC, Wen HY (2007*) The after-effect of human theta burst stimulation is NMDA receptor dependent.* Clinical Neurophysiology, 118:1028–1032

Ilmoniemi RJ, Virtanen J, Ruohonen J, Karhu J, Aronen HJ, Näätänen R, et al. (1997) *Neuronal responses to magnetic stimulation reveal cortical reactivity and connectivity*. Neuroreport, 8:3537-3540

Ilmoniemi RJ e Kičić D (2010) *Methodology for Combined TMS and EEG.* Brain Topography, 22:233-248

Inghilleri M, Conte A, Curra A, Frasca V, Lorenzano C, Berardelli A (2004) Ovarian hormones and cortical excitability. An rTMS study in humans. Clinical Neurophysiology, 115:1063-1068

Iramina K, Maeno T, Nohaka Y, Ueno S (2003) *Measurement of evoked electroencephalography induced by transcranial magnetic stimulation*. Journal of Applied Physics, 93:6718–6720

Ives JR, Rotenberg A, Poma R, Thut G, Pascual-Leone A (2006) *Electroencephalographic recording during transcranial magnetic stimulation in humans and animals*. Clinical Neurophysiology, 117:1870–1875

Johnson JS, Hamidi M, Postle BR (2010) *Using EEG to explore how rTMS produces its effects on behaviour.* Brain Topography, 22:281-293

Julkunen P, Pääkkönen A, Hukkanen T, Könönen M, Tiihonen P, Vanhatalo S, Karhu J (2008) *Efficient reduction of stimulus artifact in TMS–EEG by epithelial short-circuiting by mini-punctures*. Clinical Neurophysiology, 119:475–481

Kähkönen S, Kesäniemi M, Nikouline VV, Karhu J, Ollikainen M, Holi M, et al. (2001) *Ethanol modulates cortical activity: direct evidence with combined TMS and EEG*. NeuroImage, 14:322–328

Kähkönen S, Komssi S, Wilenius J, Ilmoniemi RJ (2005a) *Prefrontal TMS produces smaller EEG responses than motor-cortex TMS: implications for rTMS treatment in depression*. Psychopharmacology, 181:16–20

Käkhönen S, Komssi S, Ilmoniemi RJ (2005b) Prefrontal transcranial magnetic stimulation produces intensity-dependent EEG responses in humans. Neuroimage, 24: 955-960

Kähkönen S, Wilenius J (2007) *Effects of alcohol on TMS-evoked N100 responses*. Journal of Neuroscience Methods, 166:104-108

Kammer T, Beck S, Thielscher A, Laubis-Hermann U, Topka H (2001) *Motor thresholds in humans: a transcranial magnetic stimulation study comparing different pulse waveforms, current directions and stimulator types.* Clinical Neurophysiology, 112:250-258

Kandel ER and Spencer WA (1961) Excitation and inhibition of single pyramidal cells during hippocampal seizure. Experimental Neurology, 4:162-179

Kiers L, Cros D, Chiappa KH, Fang J (1993) *Variability of motor potentials evoked by transcranial magnetic stimulation.* Electroencephalography and Clinical Neurophysiology, 89:415-423

Kimiskidis VK, Papagiannopoulos S, Kazis DA, Vasiliadis G, Oikonomidi A, Sotirakoglou K, et al. (2008) *Silent period (SP) to transcranial magnetic stimulation: the EEG substrate. Brain Stimulation 1. A*bstracts from 3rd international conference on transcranial magnetic stimulation and direct current stimulation, 315-316

Kirschen MP, Davis-Ratner MS, Jerde TE, Schraedley-Desmond P, Desmond JE (2006) Enhancement of phonological memory following transcranial magnetic stimulation (TMS). Behavioural Neurology, 17:187-194

Kleim JA, Chan S, Pringle E, Schallert K, Procaccio V, Jimenez R, Cramer SC (2006) BDNF val66met polymorphism is associated with modified experience-dependent plasticity in human motor cortex. Nature, 9:735-737

Klimesch W, Sauseng P, Gerloff C (2003) *Enhancing cognitive performance with repetitive transcranial magnetic stimulation at human individual alpha frequency*. European Journal of Neuroscience, 17:1129–1133

Knops A, Nuerk HC, Sparing R, Foltys H, Willmes K (2006) On the functional role of human parietal cortex in number processing: how gender mediates the impact of a 'virtual lesion' induced by rTMS. Neuropsychologia 44, 2270-2283

Koch G, Ponzo V, Di Lorenzo F, Caltagirone C, Veniero D (2013) Hebbian and anti-hebbian spike-timing-dependent plasticity of human cortico- cortical connections. Journal of Neuroscience, 33:9725-9733

Koch G, Franca M, Del Olmo MF, Cheeran B, Milton R, Alvarez Sauco M, et al. (2006) *Time course of functional connectivity between dorsal premotor and contralateral motor cortex during movement selection.* Journal of Neuroscience, 26:7452-7459

Kohler S, Paus T, Buckner RL, Milner B (2004) Effects of left inferior pre- frontal stimulation on episodic memory formation: a two-stage fMRI-rTMS study. Journal of Cognitive Neuroscience, 16:178-188.

Komssi S, Aronen HJ, Huttunen J, Kesäniemi M, Soinne L, Nikouline VV, et al. (2002) *Ipsi- and contralateral EEG reactions to transcranial magnetic stimulation*. Clinical Neurophysiology, 113:175–184

Komssi S, Kähkönen S, Ilmoniemi RJ (2004) *The effect of stimulus intensity on brain responses evoked by transcranial magnetic stimulation*. Human Brain Mapping, 21:154–164

Komssi S and Kähkönen S (2006) *The novelty value of the combined use of electroencephalography and transcranial magnetic stimulation for neuroscience research*. Brain Research Reviews, 52:183-192

Korhonen RJ, Hernandez-Pavon JC, Metsomaa J, Mäki H, Ilmoniemi RJ, Sarvas J (2011) Removal of large muscle artifacts from transcranial magnetic stimulation-evoked EEG by independent component analysis. Medical & Biological Engineering & Computing, 49:397-407

Kozel FA, Nahas Z, deBrux C, Molloy M, Lorberbaum JP, Bohning D, et al. (2000) *How coil–cortex distance relates to age, motor threshold, and antidepressant response to repetitive transcranial magnetic stimulation*. Journal of Neuropsychiatry and Clinical Neurosciences, 12:376-384

Kraus KH, Gugino LD, Levy WJ, Cadwell J, Roth BJ (1993) *The use of a cap-shaped coil for transcranial magnetic stimulation of the motor cortex.* Journal of Clinical Neurophysiology, 10:353-362

Kujirai T, Caramia MD, Rothwell JC, Day BL, Thompson PD, Ferbert A, et al. (1993) *Cortico-cortical inhibition in human motor cortex.* Journal of Physiology, 471:501-519

Kuo MF, Paulus W, Nitsche MA (2008) Boosting focally-induced brain plasticity by dopamine. Cerebral Cortex, 18, 648-651

Kuwabara S, Cappelen-Smith C, Lin CS, Mogyoros I, Burke D (2002) Effects of voluntary activity on the excitability of motor axons in the peroneal nerve. Muscle Nerve, 25:176-184

Lang N, Harms J, Weyh T, Lemon RN, Paulus W, Rothwell JC, et al. (2006) *Stimulus intensity and coil characteristics influence the efficacy of rTMS to suppress cortical excitability*. Clinical Neurophysiology, 117:2292-2301

Lee L, Siebner HR, Rowe JB, Rizzo V, Rothwell JC, Frackowiak RSJ, et al. (2003b) *Acute remapping within the motor system induced by low-frequency repetitive transcranial magnetic stimulation*. Journal of Neuroscience, 23:5308-5318

Lee SH, Kim W, Chung YC, Jung KH, Bahk WM, Jun TY, et al. (2005) *A double blind study showing that two weeks of daily repetitive TMS over the left or right temporoparietal cortex reduces symptoms in patients with schizophrenia who are having treatment-refractory auditory hallucinations.* Neuroscience Letters, 376:177-181

Lehmann D and Skrandies W (1980) *Reference-free identification of components of checkerboard-evoked multichannel potential fields.* Electroencephalography and Clinical Neurophysiology, 48: 609-621

Lewald J, Foltys H, Töpper R (2002) Role of the posterior parietal cortex in spatial hearing. Journal of Neuroscience, 22:RC207

Li X, Large CH, Ricci R, Taylor JJ, Nahas Z, Bohning DE, et al. (2011) *Using Interleaved Transcranial Magnetic Stimulation/Functional Magnetic Resonance Imaging (fMRI) and Dynamic Causal Modeling to Understand the Discrete Circuit Specific Changes of Medications: Lamotrigine and Valproic Acid Changes in Motor or Prefrontal Effective Connectivity.* Psychiatry Research, 194:141-148

Li X, Nahas Z, Kozel FA, Anderson B, Bohning DE, George MS (2004) *Acute left prefrontal transcranial magnetic stimulation in depressed patients is associated with immediately increased activity in prefrontal cortical as well as subcortical regions*. Biological Psychiatry, 55:882-890

Liepert J, Schwenkreis P, Tegenthoff M, Malin JP (1997) The glutamate antagonist riluzole suppresses intracortical facilitation. Journal of neural transmission, 104:1207-1214

Lioumis P, Kičić D, Savolainen P, Mäkelä JP, Kähkönen S (2009) *Reproducibility of TMS-Evoked EEG Responses*. Human Brain Mapping, 30:1387-1396

Litvak V, Komssi S, Scherg M, Hoechstetter K, Classen J, Zaaroor M, et al. (2007) *Artifact correction and source analysis of early electroencephalographic responses evoked by transcranial magnetic stimulation over primary motor cortex.* Neuroimage, 37:56–70

Luber B, Kinnunen LH, et al. (2006) *Facilitation of performance in a working memory task with rTMS stimulation of the precuneus: frequency- and time-dependent effects. Brain Research,* 1128:120-129

Luber B, Kinnunen LH, Rakitin BC, Ellsasser R, Stern Y, Lisanby SH (2007) Facilitation of performance in a working memory task with rTMS stimulation of the precuneus: frequency- and time-dependent effects. Brain Research, 1128:120-129

Maeda F, Keenan JP, Tormos JM, Topka H, Pascual-Leone A (2000) *Modulation of corticospinal excitability by repetitive transcranial magnetic stimulation*. Clinical Neurophysiology, 111:800-805

Massimini M, Ferrarelli F, Huber R, Esser SK, Singh H, Tononi G (2005) *Breakdown of cortical effective connectivity during sleep*. Science, 309:2228–2232

Mattavelli G, Rosanova M, Casali AG, Papagno C, Romero LJ (2013) *Top-down interference and cortical responsiveness in face processing: A TMS-EEG study.* NeuroImage, 76:24-32

McConnell KA, Nahas Z, Shastri A, Lorberbaum JP, Kozel FA, Bohning DE, George MS (2001) *The transcranial magnetic stimulation motor threshold depends on the distance from coil to underlying cortex: a replication in healthy adults comparing two methods of assessing the distance to cortex*. Biological Psychiatry, 49:454–459

McDonnell MN, Orekhov Y, Ziemann U (2006) *The role of GABA(B) receptors in intracortical inhibition in the human motor cortex.* Experimental Brain Research, 173:86-93

Mills KR, Boniface SJ, Schubert M (1992) *Magnetic brain stimulation with a double coil: the importance of coil orientation*. Electroencephalography and Clinical Neurophysiology, 85:17–21

Mills KR, Nithi KA (1997) Corticomotor threshold is reduced in early sporadic amyotrophic lateral sclerosis. Muscle Nerve, 20:1137–41

Mills KR (1999) *Magnetic brain stimulation: a review after 10 years experience.* Electroencephalography and Clinical Neurophysiology 49(Suppl):239-244.

Miniussi C, Ruzzoli M, Walsh V (2010) *The mechanism of transcranial magnetic stimulation in cognition*. Cortex, 46:128-130

Miniussi C, Thut G (2010) *Combining TMS and EEG Offers New Prospects in Cognitive Neuroscience*. Brain Topography, 22:249-256

Mochizuki H, Furubayashi T, Hanajima R, Terao Y, Mizuno Y, Okabe S, et al. (2007) *Hemoglobin concentration changes in the contralateral hemisphere during and after theta burst stimulation of the human sensorimotor cortices*. Experimental Brain Research, 180:667-675

Mochizuki H, Ugawa Y, Terao Y, Sakai KL (2006) *Cortical hemoglobin concentration changes under the coil induced by single-pulse TMS in humans: a simultaneous recording with near-infrared spectroscopy.* Experimental Brain Research, 169:302–310

Moll GH, Heinrich H, Trott G-E, Wirth S, Rothenberger A (2000) Deficient intracortical inhibition in drug-naive children with attention-deficit hyperactivity disorder is enhanced by methylphenidate. Neuroscience Letters, 284:121-125

Moll GH, Heinrich H, Rothenberger A (2003) Methylphenidate and intracortical excitability: opposite effects in healthy subjects and attention-deficit hyperactivity disorder. Acta Psychiatrica Scandinavica, 107:69-72

Morbidi F, Garulli A, Prattichizzo D, Rizzo C, Manganotti P, Rossi S (2007) *Off-line removal of TMS-induced artifacts on human electroencephalography by Kalman filter.* Journal of Neuroscience Methods, 162:293-302

Mottaghy FM, Hungs M, Brugmann M, Sparing R, Boroojerdi B, Foltys H, Huber W, Topper R (1999) *Facilitation of picture naming after repetitive transcranial magnetic stimulation.* Neurology, 53:1806-1812

Mottaghy FM, Keller CE, Gangitano M, Ly J, Thall M, Parker JA et al. (2002) *Correlation of cerebral blood flow and treatment effects of repetitive transcranial magnetic stimulation in depressed patients.* Psychiatry Research, 115:1-14.

Mottaghy FM, Krause BJ, Kemna LJ, Töpper R, Tellmann L, Beu M, Pascual-Leone A, Müller-Gärtner HW (2000) Modulation of the neuronal circuitry subserving working memory in healthy human subjects by repetitive transcranial magnetic stimulation. Neuroscience Letters, 280:167-170

Mull BR and Seyal M (2001) Transcranial magnetic stimulation of left prefrontal cortex impairs working memory. Clinical Neurophysiology, 112:1672-1675

Münchau A,Bloem BR, Irlbacher M, Trimble MR, Rothwell JC (2002) Functional Connectivity of Human Premotor and Motor Cortex Explored with Repetitive Transcranial Magnetic Stimulation. Journal of Neuroscience, 22:554-561

Mutanen T, Mäki H, Ilmoniemi RJ (2013) T*he effect of stimulus parameters on TMS-EEG muscle artifacts*. Brain Stimulation, 6:371-376

Näätänen R, Picton T (1987) *The N1 wave of the human electric and magnetic response to sound: a review and an analysis of the component structure.* Psychophysiology, 24:375-425

Nadeau SE, McCoy KJ, Crucian GP, Greer RA, Rossi F, Bowers D et al. (2002) *Cerebral blood flow changes in depressed patients after treatment with repetitive transcranial magnetic stimulation: evidence of individual variability*. Neuropsychiatry, Neuropsychology and Behavioral Neurology, 15:159-175

Nahas Z, McConnell K, Collins S, Molloy M, Oliver NC, Risch SC, Christie S, Arana GW, George MS (1999) *Could left prefrontal rTMS modify negative symptoms and attention in Schizophrenia?* Biological Psychiatry, 45:1s-147s

Niehaus L, Meyer B-U, Weyh T (2000) *Influence of pulse configuration and direction of coil current on excitatory effects of magnetic motor cortex and nerve stimulation.* Clinical Neurophysiology, 111:75-80

Nikouline V, Ruohonen J, Ilmoniemi RJ (1999) *The role of the coil click in TMS assessed with simultaneous EEG.* Clinical Neurophysiology, 110:1325-1328

Nikulin VV, Kičić D, Kähkönen S, Ilmoniemi RJ (2003) *Modulation of electroencephalographic responses to transcranial magnetic stimulation: evidence for changes in cortical excitability related to movement*. European Journal of Neuroscience, 18:1206-1212

Nikulin VV, Kičić D, Kähkönen S, Ilmoniemi RJ (2003) *Modulation of electroencephalographic responses to transcranial magnetic stimulation: evidence for changes in cortical excitability related to movement*. European Journal of Neuroscience, 18:1206-1212

Noguchi Y, Watanabe E, Sakai KL (2003) *An event-related optical topography study of cortical activation induced by single-pulse transcranial magnetic stimulation*. Neuroimage, 19:156-162

Okamoto M, Dan H, Sakamoto K, Takeo K, Shimizu K, Kohno S et al. (2004) *Three-dimensional probabilistic anatomical cranio-cerebral correlation via the international 10–20 system oriented for transcranial functional brain mapping*. NeuroImage, 21:99-111

Oliviero A, Di Lazzaro V, Piazza O, Profice P, Pennisi MA, Della Corte F, et al. (1999) *Cerebral blood flow and metabolic changes produced by repetitive magnetic brain stimulation*. Journal of Neurology, 246:1164-1168

Pascual-Leone A, Gates JR, Dhuna A (1991) Induction of speech arrest and counting errors with rapid rate transcranial magnetic stimulation. Neurology, 41:697-702

Pascual-Leone A, Cohen LG, Brasil-Neto JP, Hallett M (1994) *Non-invasive differentiation of motor cortical representation of hand muscles by mapping of optimal current directions*. Electroencephalography and Clinical Neurophysiology, 93:42–48

Pascual-Leone A, Tormos JM, Keenan J, Tarazona F, Cañete C, Català MD (1998) *Study and Modulation of Human Cortical Excitability With Transcranial Magnetic Stimulation.* Journal of Clinical Neurophysiology, 15:333-343

Paus T, Jech R, Thompson CJ, Comeau R, Peters T, Evans AC (1997) *Transcranial magnetic stimulation during positron emission tomography: a new method for studying connectivity of the human cerebral cortex*. Journal of Neuroscience, 17:3178-3184

Paus T, Castro-Alamancos MA, Petrides M (2001) *Cortico-cortical connectivity of the human mid-dorsolateral frontal cortex and its modulation by repetitive transcranial magnetic stimulation*. European Journal of Neuroscience, 14:1405-1411

Pellicciari MC, Brignani D, Miniussi C (2013) *Excitability modulation of the motor system induced by transcranial direct current stimulation: a multimodal approach.* Neuroimage, 8:569-580

Perez MA, Tanaka S, Wise SP, Sadato N, Tanabe HC, Willingham DT, Cohen LG (2007) Neural substrates of intermanual transfer of a newly acquired motor skill. Current Biology, 17:1896-1902

Peterchev AV, Murphy DL, Lisanby SH (2010) Repetitive transcranial magnetic stimulation with controllable pulse (cTMS). 32nd Annual International Conference of the IEEE EMBS, 2922-2926

Peterchev AV, Goetz SM, Westin GG, Luber B, Lisanby SH (2013) Pulse width dependence of motor threshold and input–output curve characterized with controllable pulse parameter transcranial magnetic stimulation. Clinical Neurophysiology, 124:1364-1372

Pobric G, Jefferies E, Ralph MA (2010) Amodal semantic representations depend on both anterior temporal lobes: Evidence from repetitive transcranial magnetic stimulation. Neuropsychologia, 48:1336-1342

Poldrack RA (2005) Can cognitive processes be inferred from neuroimaging data?. Trends in Cognitive Sciences, 10:59-63

Ponton CW, Vasama JP, Tremblay K, Khosla D, Kwong B, Don M (2001) *Plasticity in the adult human central auditory system: evidence from late-onset profound unilateral deafness.* Hearing Research, 154:32-44

Premoli I, Castellanos N, Rivolta D, Belardinelli P, Bajo R, Zipser C, Espenhahn S, Heidegger T, Müller-Dahlhaus F, Ziemann U (2014) TMS-EEG Signatures of GABAergic Neurotransmission in the Human Cortex. Journal of Neuroscience, 34:5603-5612

Raichle ME (1998) *Behind the scenes of functional brain imaging: a historical and physiological perspective*. Proceedings of the National Academy of Sciences of the United States, 95:765–772

Ridding MC, Rothwell JC (2007) *Is there a future for therapeutic use of transcranial magnetic stimulation?* Nature Reviews Neuroscience, 8:559-567

Rogasch NC and Fitzgerald PB (2012) Assessing cortical network properties using TMS-EEG. Human Brain Mapping, 34:1652-1669

Rogasch NC, Daskalakis ZJ, Fitzgerald PB (2013) Mechanisms underlying long-interval cortical inhibition in the human motor cortex: a TMS-EEG study. Journal of Neurophysiology, 109:89-98

Rogasch NC, Thomson RG, Farzan F, Fitzgibbon BM, Bailey NW, Hernandez-Pavon JC, Daskalakis ZJ, Fitzgerald PB (2014). Removing artefacts from TMS-EEG recordings using independent component analysis: Importance for assessing prefrontal and motor cortex network properties. Neuroimage, 101:425-439

Romei V, Brodbeck V, Michel C, Amedi A, Pascual-Leone A, Thut G (2008) *Spontaneous fluctuations in posterior alpha-Band EEG activity reflect variability in excitability of human visual areas*. Cerebral Cortex, 18:2010–2018

Rossi S, Hallett M, Rossini PM, Pascual-Leone A, The safety of TMS Consensus Group (2009) *Safety, ethical considerations, and application guidelines for the use of transcranial magnetic stimulation in clinical practice and research.* Clinical Neurophysiology, 120:2008-2039

Rossini PM, Barker AT, Berardelli A, Caramia MD, Caruso G, Cracco RQ, et al. (1994) *Non-invasive electrical and magnetic stimulation of the brain, spinal cord and roots—basic principles and procedures for routine clinical application*. Electroencephalography and Clinical Neurophysiology, 91:79–92

Rossini PM, Rossi S (1998) Clinical applications of motor evoked potentials. Electroencephalography and Clinical Neurophysiology, 106:180-194

Rossini D, Magri L, Lucca A, Giordani S, Smeraldi E, Zanardi R. (2005) *Does rTMS hasten the response to escitalopram, sertraline, or venlafaxine in patients with major depressive disorder? A double-blind, randomized, sham-controlled trial.* Journal of Clinical Psychiatry, 66:1569-1575.

Roth BJ, Pascual-Leone A, Cohen LG, Hallett M (1992) *The heating of metal electrodes during rapid-rate magnetic stimulation: a possible safety hazard*. Electroencephalography and Clinical Neurophysiology, 85:116–123

Roth Y, Zangen A, Hallett M (2002*) A coil design for transcranial magnetic stimulation of deep brain regions*. Journal of Clinical Neurophysiology, 19:361–370

Rothwell JC (2010) *Using transcranial magnetic stimulation methods to probe connectivity between motor areas of the brain*, Human Movement Science, 30:906-915

Rudiak D e Marg E (1994) *Finding the depth of magnetic brain stimulation: a re-evaluation*. Electroencephalography and Clinical Neurophysiology, 93:358–371

Rumi DO, Gattaz WF, Rigonatti SP, Rosa MA, Fregni F, Rosa MO et al. (2005) *Transcranial magnetic stimulation accelerates the antidepressant effect of amitriptyline in severe depression: a double-blind placebo-controlled study.* Biological Psychiatry 57:162-166.

Sach M, Winkler G, Glauche V, Liepert J, Heimbach B, Koch MA, et al. (2003) *Diffusion tensor MRI of early upper motor neuron involvement in amyotrophic lateral sclerosis.* Brain, 127:340-350

Sack AT and Linden EJD (2003) *Combining transcranial magnetic stimulation and functional imaging in cognitive brain research: possibilities and limitations.* Brain Research Reviews, 43:41-56

Sack AT, Kohler A, Bestmann S, Linden DEJ, Dechent P, Goebel R, et al. (2007) *Imaging the brain activity changes underlying impaired visuospatial judgments: simultaneous fMRI, TMS, and behavioural studies.* Cerebral Cortex, 17:2841-2852

Sadato N, Pascual-Leone A, Grafman J, Ibañez V, Deiber MP, Dold G, Hallett M (1996) *Activation of the primary visual cortex by Braille reading in blind subjects.* Nature, 380:526-528

Sandrini M, Umiltà CA, Rusconi E (2011) The use of transcranial magnetic stimulation in cognitive neuroscience: A new synthesis of methodological issues. Neuroscience and Behavioural Reviews, 35:516-536

Sauseng P, Klimesch W, Gerloff C, Hummel FC (2009) Spontaneous locally restricted EEG alpha activity determines cortical excitability in the motor cortex. Neuropsychology, 47:284-288

Schall JD, Morel A, King DJ, Bullier J (1995) Topography of visual cortex connections with frontal eye field in macaque: convergence and segregation of processing streams. Journal of Neuroscience, 15:4464-4487

Sekiguchi H, Takeuchi S, Kadota H, Kohno Y, Nakajima Y (2011) TMS-induced artifacts on EEG can be reduced by rearrangement of the electrode's lead wire before recording. Clinical Neurophysiology, 122:984-990

Shimizu T, Hosaki A, Hino T, Sato M, Komori T, Hirai S, et al. (2002) *Motor cortical disinhibition in the unaffected hemisphere after unilateral cortical stroke*. Brain 125, 1896-1907

Siebner HR, Tormos JM, Ceballos-Baumann AO, Auer C, Catala MD, Conrad B, et al. (1999) *Low-frequency repetitive transcranial magnetic stimulation of the motor cortex in writer's cramp*. Neurology, 52:529–537

Siebner HR, Bergmann TO, Bestmann S, Massimini M, Johansen-Berg H, Mochizuki H, et al. (2009) *Consensus paper: Combining transcranial magnetic stimulation with neuroimaging.* Brain Stimulation, 2:58-80

Silvanto J, Muggleton NG, Cowey A, Walsh V (2007) *Neural activation state determines behavioral susceptibility to modified theta burst transcranial magnetic stimulation*. European Journal of Neuroscience, 26:523-528

Sommer M, Lang N, Tergau F, Paulus W (2002) *Neuronal tissue polarization induced by repetitive transcranial magnetic stimulation?.*, 13:809–811

Sommer M, Aràanzazu A, Rummel M, Speck S, Lang N, Tings T, et al. (2006) *Half sine, monophasic and biphasic transcranial magnetic stimulation of the human motor cortex.* Clinical Neurophysiology, 117:838-844

Sommer M, D'Ostilio K, Ciocca M, Hannah R, Hammond P, Goetz S, Rothwell JC (2014) TMS can selectively activate and condition two different sets of excitatory synaptic inputs to corticospinal neurons in humans. SFN society for Neuroscience 2014

Sparing R, Hesse MD, Fink GR (2010) Neuronavig NeuroReport ation for transcranial magnetic stimulation (TMS): Where we are and where we are going. Cortex, 46:118-120

Speer AM, Benson BE, Kimbrell TK, Wassermann EM, Willis MW, Herscovitch P, et al. (2009) Opposite Effects of High and Low Frequency rTMS on Mood in Depressed Patients: Relationship to Baseline Cerebral Activity on PET. Journal of Affective Disorders, 115:386-394

Speer AM, Kimbrell TA, Wassermann EM, Repella JD, Willis MW, Herscovitch P, et al. (2000) Opposite effects of high and low frequency rTMS on regional brain activity in depressed patients. Biological Psychiatry, 48:1133-1141

Starck J, Rimpiläinen I, Pyykkö I, Toppila E (1999) The noise level in magnetic stimulation. Scandinavian Audiology, 25:223-226

Stefan K, Kunesch E, Cohen LG, Benecke R, Classen J (2000) Induction of plasticity in the human motor cortex by paired associative stimulation. Brain, 123:572-584

Stefan K, Wycislo M, Classen J (2004) Modulation of associative human motor cortical plasticity by attention. Journal of Neurophysiology, 92:66-72

Stewart LM, Battelli L, Walsh V, Cowey A (1999) Motion perception and perceptual learning studied by magnetic stimulation. Electroencephalography and Clinical Neurophysiology, 51:334-350

Steward LM, Walsh V, Rothwell JC (2001) Motor and phosphene thresholds: a transcranial magnetic stimulation correlational study. Neuropsychologia, 39:415-419

Stokes MG, Chambers CD, Gould IC, Henderson TR, Janko NE, Allen NB, Mattingley JB (2005) Simple metric for scaling motor threshold based on scalp–cortex distance: application to studies using transcranial magnetic stimulation. Journal of Neurophysiology, 94:4520–4527

Strafella AP, Ko JH, Grant J, Fraraccio M, Monchi O (2005) Corticostriatal functional interactions in Parkinson's disease: a rTMS/[11C]raclopride PET study. European Journal of Neuroscience, 22:2946-2952

Tallgreen P, Vanhatalo S, Kaila K, Voipio J (2005) Evaluation of commercially available electrodes and gels for recording of slow EEG potentials. Clinical Neurophysiology, 116:799-806

Tamás G, Lorincz A, Simon A, Szabadics J (2003) Identified sources and targets of slow inhibition in the neocortex. Science, 21:1902-1905

Taylor PC, Nobre AC, Rushworth MFS (2007) *Subsecond changes in top down control exerted by human medial frontal cortex during conflict and action selection: a combined transcranial magnetic stimulation electroencephalography study*. Journal of Neuroscience, 27:11343–11353

Taylor PCJ, Nobre AC, Rushworth MFS (2006) *FEF TMS Affects Visual Cortical Activity*. Cerebral Cortex, 17:391-399

Tegenthoff M, Ragert P, Pleger B, Schwenkreis P, Förster AF, Nicolas V, et al. (2005) I*mprovement of tactile discrimination performance and enlargement of cortical somatosensory maps after 5 Hz rTMS.* PLoS Biology, 3:e362

Ter Braack EM, De Vos CC, Van Putten MJ (2013) *Masking the auditory evoked potential in TMS-EEG: a comparison of various methods.* Brain Topography, 1-9

Terao Y, Ugawa Y, Suzuki M, Sakai K, Hanajima R, Gemba-Shimuzu K, et al. (1997) *Shortening of simple reaction time by peripheral electrical and submotor-threshold magnetic cortical stimulation*. Experimental Brain Research, 115:541-545

Thielscher A e Kammer T (2004) *Electric field properties of two commercial figure-8 coils in TMS: calculation of focality and efficiency.* Clinical Neurophysiology, 115:1697-1708

Thut G e Miniussi C (2009) *New insights into rhythmic activity from TMS-EEG studies.* Trends in Cognitive Sciences, 13:182-189

Thut G e Pascual-Leone A (2010) *A Review of Combined TMS-EEG Studies to Characterize Lasting Effects of Repetitive TMS and Assess Their Usefulness in Cognitive and Clinical Neuroscience*. Brain Topography, 22:219-232

Thut G, Ives JR, Kampmann F, Pastor MA, Pascual-Leone A (2005) *A new device and protocol for combining TMS and online recordings of EEG and evoked potentials*. Journal of Neuroscience Methods, 141:207–217

Thut G, Northoff G, Ives JR, Kamitani Y, Pfennig A, Kampmann F et al. (2003) *Effects of single-pulse transcranial magnetic stimulation (TMS) on functional brain activity: a combined event-related TMS and evoked potential study*. Clinical Neurophysiology, 114:2071-2080

Thut G, Veniero D, Romei V, Miniussi C, Schyns P, Gross J (2011) Rhythmic TMS causes local entrainment of natural oscillatory signatures. Current Biology, 21:1176-1185

Tiitinen H, Virtanen J, Ilmoniemi RJ, Kamppuri J, Ollikainen M, Ruohonen J, et al. (1999) *Separation of contamination caused by coil clicks from responses elicited by transcranial magnetic stimulation*. Clinical Neurophysiology, 110:982-985

Tings T, Lang N, Tergau F, Paulus W, Sommer M (2005) *Orientation-specific fast rTMS maximizes corticospinal inhibition and facilitation*. Experimental Brain Research, 164:323-33

Ueno S, Tashiro T, Harada K (1998) Localised stimulation of neural tissues in the brain by means of a paired configuration of time-varying magnetic fields. Journal of Applied Physiology, 64:5862-5864

Ugawa Y, Uesaka Y, Terao Y, Hanajima R, Kanazawa I (1995) Annals of Neurology 37:703-713.

Van Der Werf YD, Paus T (2006) The neural response to transcranial magnetic stimulation of the human motor cortex. I. Intracortical and cortico-cortical contributions. Experimental Brain Research, 175:231-245

Veniero D, Bortoletto M, Miniussi C (2009) TMS-EEG co-registration: On TMS-induced artefact. Clinical Neurophysiology, 120:1392-1399

Veniero D, Ponzo P, Koch G (2013) Paired associative stimulation enforces the communication between interconnected areas. The Journal of Neuroscience, 33:13773-13783

Vernet M, Bashir S, Yoo W-K, Perez JM, Najib U, Pascual-Leone A (2013) Insights on the neural basis of motor plasticity induced by theta burst stimulation from TMS–EEG. European Journal of Neuroscience, 37:598-606

Virtanen J, Ruohonen J, Naatanen R, Ilmoniemi RJ (1999) *Instrumentation for the measurement of electric brain responses to transcranial magnetic stimulation*. Medical and Biological Engineering and Computing, 37:322–326

Walsh V e Cowey A (2000) *Transcranial magnetic stimulation and cognitive neuroscience.* Nature Reviews Neuroscience, 1:73-79

Walsh V, Ellison A, Battelli L, Cowey A (1998) *Task-specific impairments and enhancements induced by magnetic stimulation of human visual area V5*. Proceedings of the Royal Society B: Biological Sciences, 265:537–543

Wassermann EM (1998) *Risk and safety of repetitive transcranial magnetic stimulation: report and suggested guidelines from the International Workshop on the Safety of Repetitive Transcranial Magnetic Stimulation,* Electroencephalography and Clinical Neurophysiology, 108:1-16

Weiskopf N, Josephs O, Ruff CC, Blankenburg F, Featherstone E, Thomas A, et al. (2009) *Image artifacts in concurrent transcranial magnetic stimulation (TMS) and fMRI caused by leakage currents: Modeling and compensation*. Journal of Magnetic Resonance Imaging, 29:1211-1217

Werhahn KJ, Kunesch E, Noachtar S, Benecke R, Classen J (1999) *Differential effects on motorcortical inhibition induced by blockade of GABA uptake in humans.* Journal of Physiology, 517:591-597

Wolters A, Sandbrink F, Schlottmann A, *et al*. (2003) *A temporally asymmetric Hebbian rule governing plasticity in the human motor cortex.* Journal of Neurophysiology 89:2339-2345.

Ziemann U, Lönnecker S, Steinhoff BJ, Paulus W (1996a) *Effects of antiepileptic drugs on motor cortex excitability in humans: A transcranial magnetic stimulation study.* Annals of Neurology, 40:367-378

Ziemann U, Lönnecker S, Steinhoff BJ, Paulus W (1996b) *The effect of lorazepam on the motor cortical excitability in man.* Experimental Brain Research 109:127-135